NUREG/CR-2331
BNL-NUREG-51454
VOL. 4, NO. 3

SAFETY RESEARCH PROGRAMS SPONSORED BY OFFICE OF NUCLEAR REGULATORY RESEARCH

QUARTERLY PROGRESS REPORT
JULY 1 — SEPTEMBER 30, 1984

Date Published — February 1985

DEPARTMENT OF NUCLEAR ENERGY, BROOKHAVEN NATIONAL LABORATORY
UPTON, NEW YORK 11973

Prepared for the U.S. Nuclear Regulatory Commission
Office of Nuclear Regulatory Research
Contract No. DE-AC02-76CH00016

NUREG/CR-2331
BNL-NUREG-51454
VOL. 4, NO. 3
AN, R-1,4,5,7,8, RD

SAFETY RESEARCH PROGRAMS SPONSORED BY OFFICE OF NUCLEAR REGULATORY RESEARCH

QUARTERLY PROGRESS REPORT
JULY 1 — SEPTEMBER 30, 1984

Herbert J.C. Kouts, Department Chairman
Walter Y. Kato, Deputy Chairman

Principal Investigators:

R.A. Bari
R.J. Cerbone
C.J. Czajkowski
T. Ginsberg
G.A. Greene
J.G. Guppy
R.E. Hall
W.J. Luckas, Jr.
J.N. O'Brien
W.T. Pratt
M. Reich
P. Saha
C. Sastre
J.H. Taylor
J.R. Weeks
W. Wulff
D. van Rooyen

Compiled by: Allen J. Weiss

Manuscript Completed December 1984

DEPARTMENT OF NUCLEAR ENERGY
BROOKHAVEN NATIONAL LABORATORY, ASSOCIATED UNIVERSITIES, INC.
UPTON, NEW YORK 11973

Prepared for the
OFFICE OF NUCLEAR REGULATORY RESEARCH
U.S. NUCLEAR REGULATORY COMMISSION
CONTRACT NO. DE-AC02-76CH00016
FIN NOS. A-3014,-3015,-3016,-3024,-3041,-3208,-3215,-3219,
-3226,-3227,-3257,-3261,-3266,-3268,-3270,-3271,-3275

NOTICE

Available from
GPO Sales Program
Division of Technical Information and Document Control
U.S. Nuclear Regulatory Commission
Washington, D.C. 20555
and
National Technical Information Service
Springfield, Virginia 22161

FOREWORD

The Advanced and Water Reactor Safety Research Programs Quarterly Progress Reports have been combined and are included in this report entitled, "Safety Research Programs Sponsored by the Office of Nuclear Regulatory Research - Quarterly Progress Report." This progress report will describe current activities and technical progress in the programs at Brookhaven National Laboratory sponsored by the Division of Accident Evaluation, Division of Engineering Technology, and Division of Risk Analysis and Operations of the U. S. Nuclear Regulatory Commission, Office of Nuclear Regulatory Research.

The projects reported are the following: High Temperature Reactor Research, SSC Development, Validation and Application, Generic Balance of Plant Modeling, Thermal-Hydraulic Reactor Safety Experiments, Development of Plant Analyzer, Code Assessment and Application (Transient and LOCA Analyses), Thermal Reactor Code Development (RAMONA-3B), Calculational Quality Assurance in Support of PTS; Stress Corrosion Cracking of PWR Steam Generator Tubing, Probability Based Load Combinations for Design of Category I Structures, Identification of Age Related Failure Modes; Analysis of Human Error Data for Nuclear Power Plant Safety Related Events, Human Factors Aspects of Safety/Safeguards Interactions, Emergency Action Levels, and Protective Action Decisionmaking. The previous reports have covered the period October 1, 1976 through June 30, 1984.

TABLE OF CONTENTS

	Page
FOREWORD	iii
FIGURES	viii
TABLES	xi
I. DIVISION OF ACCIDENT EVALUATION	1
SUMMARY	1
1. High Temperature Reactor Research	7
1.1 Graphite and Ceramics	7
1.2 Fission Product Transport	13
1.3 Analytical	18
References	24
2. SSC Development, Validation and Application	25
2.1 SSC-L Code	25
2.2 SSC-S Code	34
References	34
Publications	36
3. Generic Balance of Plant Modeling	37
3.1 Balance of Plant Models	37
3.2 MINET Code Improvements	37
3.3 MINET Standard Input Decks	38
3.4 MINET Validations and Applications	39
3.5 User Support	41
Reference	42
Publications	42
4. Thermal-Hydraulic Reactor Safety Experiments	43
4.1 Core Debris Thermal-Hydraulic Phenomenology: Ex-Vessel Debris Quenching	43
4.2 Core Debris Thermal-Hydraulic Phenomenology: In-Vessel Debris Quenching	43
4.3 Core-Concrete Heat Transfer Studies: Coolant Layer Heat Transfer	45

TABLE OF CONTENTS (Cont'd.)

		Page
5.	Development of Plant Analyzer	47
	5.1 Introduction	47
	5.2 Assessment of Existing Training Simulators	47
	5.3 Acquisition of Special-Purpose Peripheral Processor and Ancillary Equipment	48
	5.4 Model Implementation on AD10 Processor and Developmental Assessment	48
	5.5 Further Model Improvements	50
	5.6 Simulation for Emergency Procedure Guidelines	53
	5.7 Future Plans	64
	References	64
6.	Code Assessment and Application (Transient and LOCA Analyses)	66
	6.1 Code Implementation and Assessment	66
	6.2 Code Application	67
7.	Thermal Reactor Code Development (RAMONA-3B)	68
	7.1 RAMONA-3B Improvement	68
	7.2 RAMONA-3B User Support	70
	7.3 Nuclear Cross Sections for Browns Ferry Cycle 5	71
	References	71
8.	Calculational Quality Assurance in Support of PTS	72
	8.1 Assessment of RELAP5 Thermal-Hydraulic Analysis of PTS Transients of H. B. Robinson Unit 2	72
	References	77
II.	DIVISION OF ENGINEERING TECHNOLOGY	87
	SUMMARY	87
9.	Stress Corrosion Cracking of PWR Steam Generator Tubing	89
	9.1 Constant Load	89
	9.2 CERT	89
	9.3 Dents	89
	9.4 U-Bends	89
	9.5 Future Work	89
10.	Probability Based Load Combinations for Design of Category I Structures	90
	10.1 Load Combination Criteria for Design of Concrete Containments	90
	10.2 Reliability Analysis of Frame Structures with Shear Walls	90
	10.3 Design and Construction Errors	90

TABLE OF CONTENTS (Cont'd.)

Page

11. Identification of Age Related Failure Modes. 92
11.1 Electric Motors 92
11.2 Battery Chargers and Inverters. 93

III. DIVISION OF RISK ANALYSIS AND OPERATIONS 95

SUMMARY. 95

12. Analysis of Human Error Data for Nuclear Power Plant Safety Related Events 97
12.1 Success Likelihood Index Method (SLIM) Development. 97
12.2 Multiple Sequential Failure Model Development and Testing . . 98
12.3 PRA Human Reliability Data. 99
References 100

13. Human Factors Aspects of Safety/Safeguards Interactions 101

14. Emergency Action Levels. 102

15. Protective Action Decisionmaking 103
15.1 Background. 103
15.2 Project Objectives. 103
15.3 Technical Approach. 104
15.4 Project Status. 104

FIGURES

		Page
1.1.1	Oxidation Rates of 2020 Graphite at 850°C in 500 ppm H_2O/5000 ppm H_2/He.	11
1.1.2	Oxidation Rates of PGX Graphite at 850° in 500 ppm H_2O/5000 ppm H_2/He.	12
1.1.3	Silver Plate-Out as a Function of Distance From the Susceptor for Run #70884	14
1.1.4	Silver Plate-Out as a Function of Distance From the Susceptor for Run #81484	15
1.1.5	Silver Plate-Out as a Function of Distance From the Susceptor for RUN #51884	16
1.1.6	Silver Plate-Out as a Function of Distance From the Susceptor for RUN #92884	17
1.3.1	Containment Building Temperatures and Pressures During Unrestricted Core Heatup Accidents	19
1.3.2	Containment Building Temperatures and Pressures During Unrestricted Core Heatup Accidents	20
1.3.3	Transient Response for Typical Modular Pebble Bed Reactor to Loss of Forced Circulation With Depressurization Accident.	22
2.1	Core Average and Vessel Outlet Coolant Temperature for LOHS Event.	29
2.2	IHX Inlet and Outlet Coolant Temperatures for LOHS Event	29
2.3	Primary Loop Flow Rate for LOHS Event.	30
2.4	Seven-Assembly Cluster Model for Inter-Assembly Heat Transfer.	31
2.5	Sample Output for Extended SSC Graphics Capability	35
3.1	MINET Deck BF3 Modules	40
4.1	Transient Temperature History of a Particle Thermocouple Being Quenced in a Saturated Pool of Water	44

FIGURES (Cont'd.)

		Page
4.2	Instantaneous Volumetric Heat Flux as a Function of Particle Superheat.	45
5.1	Flow Schematic and Control Blocks for BWR Simulation	49
5.2	Boron Reactivity and Boron Concentration for MSIV-Induced ATWS . .	51
5.3	Fission Power and System Pressure for MSIV-Induced ATWS with Boron Injection.	51
5.4	Results for Case 1	55
5.5	Results for Case 1	56
5.6	Results for Case 2	58
5.7	Results for Case 2	59
5.8	Results for Case 3	60
5.9	Results for Case 3	61
5.10	Results for Case 4	62
5.11	Results for Case 4	63
8.1	Transient 1: Liquid Temperature in the Downcomer	78
8.2	Transient 1: Loop A Liquid Temperature	78
8.3	Transient 1: Loop B Liquid Temperature	79
8.4	Transient 1: Loop C Liquid Temperature	79
8.5	Transient 1: Cold Leg Liquid Temperatures.	80
8.6	Transient 1: Primary and Secondary Pressure.	80
8.7	Transient 4: Liquid Temperature in the Downcomer	81
8.8	Transient 4: Normalized Pressurizer Level.	81
8.9	Transient 4: Downcomer Pressure.	82
8.10	Transient 6: Downcomer and Hot Leg Liquid Temperature.	82

FIGURES (Cont'd.)

		Page
8.11	Transient 6: Liquid Temperature in the Downcomer	83
8.12	Transient 6: Normalized Pressurizer Level.	83
8.13	Transient 6: Downcomer Pressure.	84
8.14	Transient 8: Downcomer and Hot Leg Liquid Temperature.	84
8.15	Transient 8: Liquid Temperature in the Downcomer	85
8.16	Transient 8: Downcomer Pressure.	85

TABLES

		Page
1.1.1	The Estimated Densities for the Oxidized Sample No. 3.	8
1.1.2	The Estimated Moduli of Elasticity, E (GPa), for the Oxidized Sample No. 3.	9
1.1.3	Oxidation Rates for 2020, PGX and TS-1621 Graphites at 850°C With 30 ppm H_2O/5000 ppm H_2 (Balance He).	10

I. DIVISION OF ACCIDENT EVALUATION

SUMMARY

High Temperature Reactor Research

The No. 3 medium sized 2020 graphite sample was taken to Oak Ridge National Laboratory for nondestructive measurements after it added 50 hours of oxidation time (total oxidation time, 6286 hours) through oxidation rate runs. On this sample, eddy current responses were measured at different positions of the sample to see the density changes on the surface. Elastic moduli were estimated by ultrasonic wave velocity measurements. The results are comparable to those from the previous testings of the other three samples.

The oxidation rate runs with larger size (15.24 cm x 5.97 cm x 5.72 cm) 2020 and PGX graphites are completed, and the testings with TS-1621 are in progress. The results suggest that it may be dangerous to extrapolate the short-term experimental results to the long-term reactor condition.

Four integrated fission product transport experimental runs have been completed. The results show that silver fission product aerosols do form and are transported to the environment when the temperature gradient is large enough and flow rate is high enough. Presently, we are attempting to quantify this information by monitoring the temperature gradient throughout the experimental run.

In previous work the water ingress into the core cavity from degrading PCRV concrete during unrestricted core heatup accidents had been analyzed. In this quarter, the effects of chemically bound water were included in the analysis. It was found that the water ingress into the core cavity increased about proportional to the increase in total initial water in the concrete.

A model analyzing the containment building temperatures and pressure during Unrestricted Core Heatup Accidents was added to our ATMOS code. Results show that the previously used temperature history estimates were valid. However, with the reduced water ingress rates indicated by the above work, anticipated containment building failure times are significantly extended.

An application of our THATCH code to modular pebble bed reactor accidents was made, using data representative of concepts currently considered in the DOE program. Since several of the dimensions and material descriptions are not finalized at this time, various assumptions had to be made. The typical results are in general agreement with those reported in the DOE program. The sensitivity of input assumptions on the essential results, and the effects on the confinement building atmosphere will be investigated next.

SSC Development, Validation and Application

The Super System Code (SSC) Development, Validation and Application Program encompasses a series of three computer codes; (1) SSC-L for system transients in loop-type liquid metal-cooled reactors (LMRs); (2) SSC-P for system transients in pool-type LMRs and (3) SSC-S for long term shutdown transients. In addition to these code development and application efforts, validation of these codes is an ongoing task.

The long-term case to study the efficacy of pipe radiation losses as a heat sink during losss-of-heat-sink accidents in a loop-type LMR plant has been completed. SSC was modified to include pipe radiation losses and was used to simulate such an LOHS in an LMR plant. In order to enhance these losses, the pipes were assumed to be insulated by rock wool, a material whose thermal conductivity increases with increasing temperature. A transient was simulated for a total of eight days, during which the coolant temperatures peaked well below saturation conditions and then declined steadily. The coolant flow rate in the loop remained positive throughout the transient.

The development and coding of the inter-assembly heat transfer model was completed during this quarter. The model is written for a cluster of assemblies composed of a central assembly, which transfers heat with one ring of adjacent neignbors. Debugging and validation of the model are being conducted.

An enhanced computer graphics output capability has been developed. This extended capability is ultimately intended for an interactive version of SSC, but can be used now to provide "snapshots" of certain plant conditions during a transient. Work on providing improved capabilities for permitting large timesteps during long-term transients is progressing well.

Generic Balance of Plant Modeling

The Generic Balance of Plant (BOP) Modeling Program deals with the development of safety analysis tools for system simulation of nuclear power plants. It provides for the developent and validation of models to represent and link together BOP components (e.g., steam generator components, feedwater heaters, turbine/generator, condensers) that are generic to all types of nuclear power plants. This system transient analysis package is designated MINET to reflect the generality of the models and methods, which are based on a momentum integral network method. The code is to be fast-running and capable of operating as a self-standing code or to be easily interfaced to other system codes.

Version 1 of MINET has been upgraded to improve on several system modeling capabilities. This intermediate version is designated 1A. Code enhancements currently in progress include a trapped cover gas option, improved plot support software and additional input processor error testing. Major model development for the control system representation and for the rotor module is continuing.

The RAMONA/MINET composite code (to provide an improved SASA capability for BWRs) is undergoing extensive testing and input deck improvement. Current efforts have been focused on proper representation of the feedwater line, including the high pressure coolant injection (HPCI) and the reactor core isolation cooling (RCIC) systems.

During this reporting period, a workshop on the MINET code was conducted. The response from particlpants was quite positive. They provided some useful immediate feedback concerning several user related enhancements. Also, two organizations are planning to obtain the MINET code.

Thermal-Hydraulic Reactor Safety Experiments

The top-flood debris bed quench experiments with beds of 1-mm steel particles were repeated, and the results show that heat balances are accurate to within 5-10%. The final reduction of the debris bed quench data gathered to date was ocmpleted. A final report is in preparation.

The core-debris heat transfer facility was modified to allow the debris bed height to be doubled. To measure the instantaneous rate of heat loss experienced by the solid particles during the quenching process, special thermocouple probes, with the thermocouple junction inside the particle (3.18-mm stainless steel sphere), were fabricated and tested.

Analysis of the compiled R11/liquid metal and H_2O/liquid metal liquid-liquid film boiling data continued. The R11 data demonstrate stable film boiling, increasing with gas superficial velocity in a linear fashion. The H_2O data exhibit unstable film boiling, almost invariably resulting in pool-geometry steam explosions when boiling on liquid metal melts.

Development of Plant Analyzer

The LWR Plant Analyzer Program is being conducted to develop an engineering plant analyzer capable of performing accurate, real-time and faster than real-time simulations of plant transients and Small-Break Loss of Coolant Accidents (SBLOCAs) in LWR power plants. The first program phase was carried out earlier to establish the feasibility of achieving faster than real-time simulations and faster than mainframe, general-purpose computer (CDC-7600) simulations through the use of modern, interactive, high-speed, special-purpose minicomputers, which are specifically designed for interactive time-critical systems simulations. It has been successfully demonstrated that special-purpose minicomputers can compete with, and outperform, mainframe computers in reactor simulations. The current program phase is being carried out to provide a complete BWR simulation capability, including on-line, multicolor graphic display of safety-related parameters.

The plant analyzer program is directed primarily toward reactor safety analyses, but it is also useful for on-line plant monitoring and accident diagnosis, for accident mitigation, further for developing operator training programs and for assessing and improving existing and future training simulators. Major assets of the simulator under development are its low cost, unsurpassed convenience of operation and high speed of simulation. Major achievements of the program are summarized below.

Existing training simulator capabilities and limitations regarding their representation of the Nuclear Steam Supply System have been assessed previously. Simulators reviewed at the time have been found to be limited to steady-state simulations and to restricted quasi-steady transients within the range of normal operating conditions.

A special-purpose, high-speed peripheral processor had been selected for the plant analyzer, which is specifically designed for efficient systems simulations at real-time or faster computing speeds. The processor is the AD10 from Applied Dynamics International (ADI) of Ann Arbor, Michigan. A PDP-11/34 Minicomputer serves as the host computer to program and control the AD10 peripheral processor. Both the host computer and the peripheral processor have been operating at BNL since March 15, 1982.

A four-equation model for nonequilibrium, nonhomogeneous two-phase flow in a typical BWR/4 had been implemented on the AD10 processor. It is called HIPA-BWR/4 for High-Speed Interactive Plant Analysis of a BWR/4 power plant. The implementation of HIPA-BWR/4 had been carried out in the high-level language MPS10 of the AD10.

It had been demonstrated during the last quarter of 1982 that the AD10 special-purpose peripheral processor can produce accurate simulations of a BWR design base transient at computing speeds up to 10 times faster than real-time and 110 times faster than the CDC-7600 mainframe computer carrying out the same simulation.

After the successful completion of the feasibility demonstration, work has continued to expand the simulation capability to simulating the dynamics of the entire nuclear steam supply system as well as the entire balance of plant (steam lines, turbines, condensers and feedwater trains).

Models have been developed and implemented for point neutron kinetics with seven feedback mechanisms and seven automatic scram trip initiations, for thermal conduction in fuel elements, for steam line dynamics capable of simulating acoustical effects from sudden valve actions, for turbines, condensers, feedwater preheaters and feedwater pumps and for emergency cooling systems.

The software systems of both the PDP-11/34 host computer and the AD10 special-purpose peripheral processor have been upgraded to achieve greater computing speed and a larger number of analog input/output channels. Two AD10s are coupled via a direct bus-to-bus interface to compute in parallel.

Models had been developed and implemented for the feedwater controller, the pressure regulator and the recirculation flow controller. Twenty-eight parameters for initiating control systems and valve failures and for selecting set points can be changed on-line from a 32-channel control panel. Sixteen dedicated analog output lines are provided for the simultaneous display of 15 selected parameters versus time. All input-output channels are addressed approximately 200 times per second.

All program modules have been combined into the HIPA-BWR/4 code. The entire BWR power plant simulation, including the nuclear steam supply system, the steam lines with all valves, the turbines, condensers, feedwater preheater and pumps, and the control and plant protection systems, has been executed. Fifteen selected parameters can be stored simultaneously in the IBM Personal Computer and then displayed as functions of time in labelled diagrams. A silent movie has been produced to show how the plant analyzer is operated and how it responds to on-line analog signals.

During the first reporting period of 1984, we presented the comparison of plant analyzer results with published results from GE for 10 different ATWS events as a part of developmental assessment. The assessment showed that the plant analyzer is capable of simulating ATWS. The plant analyzer has been generalized to simulate any BWR-4 power plant in response to input data changes from the keyboard. A draft report has been completed to document the plant analyzer.

During the previous reporting period, we continued the developmental assessment of the plant analyzer by comparisons against GE, TRAC-BD1, RELAP-5, and RAMONA-3B. The results showed that the plant analyzer is capable of realistically simulating a large class of plant transients efficiently at very low cost.

During the current reporting period, we implemented the capability of simulating flow reversal, continued the implementation of the level tracking model with the drift flux model, and demonstrated successfully the simulation of boron injection and the subsequent cessation of fission power. Several transients have been simulated to demonstrated the plant response to manual depressurization and HPCI flow reduction during an ATWS event in order to assess the efficacy of proposed emergency procedure guidelines. The results indicated that the fission power can be reduced without boron injection and core uncovery, by lowering the pressure and by lowering the coolant level in the downcomer and thereby reducing the core flow rate.

The previously distributed draft report documenting the BWR plant analyzer has been updated as a final report [Wulff, Cheng, Lekach and Mallen, 1984] and submitted for printing.

The interest in the Plant Analyzer Development Program continues to be high, both in domestic and foreign institutions. Four presentations with demonstrations were given at BNL to foreign and domestic visitors, and two invited papers have been submitted for publication during the current reporting

period. Discussions were held at Singer-Link, Silver Spring, MD, on possible cooperation and exchange of information related to nuclear power plant simulations.

Code Assessment and Application (Transient and LOCA Analyses)

The TRAC-BD1/MOD1 (Version 22) code has been successfuliy implemented on the BNL CDC-7600 computer. Significant progress has been made in developing a TRAC-BD1/MOD1 input deck for simulating the BWR Full Integral Simulation Test (FIST) facility.

In addition, the thermal-hydraulic program of the BWR stability analysis code, NUFREQ-NP, developed at Rensselaer Polytechnic Institute has been implemented on the BNL CDC-7600 computer. However, the neutronic program will require significant modification for implementation on the BNL CDC-7600 computer.

Thermal Reactor Code Development (RAMONA-3B)

Several improvements and corrections have been made to the RAMONA-3B code. They are: (1) implementation of the Feedwater Control System, (2) some improvements for reverse flow situations, (3) modifications to restart capabilities, and (4) time step corrections.

A BNL/INEL/NRC meeting was held at BNL in order to resolve discrepancies between the TRAC-BD1/MOD1 calculations using 1-D neutron kinetics and the Peach Bottom 2 Turbine Trip Test 3 results.

Generation of 3-D neutronic cross sections for the Browns Ferry Cycle 5 reactor core has been completed. This task was performed under joint sponsorship of this and another NRC program (FIN A-3273, Application of RAMONA to BWR ATWS).

Calculational Quality Assurance in Support of PTS

The quantitative in-depth review of the RELAP5/MOD1.6 claculations and extrapolations of four transients for the H. B. Robinson-2 PTS study has been completed. The calculations performed at INEL seem to be reasonable. However, there are uncertainties due to the pressurizer model, structure stored energy and multidimensionality of some of the transients. Two additional transients are also being reviewed in-depth using the simple method developed at BNL.

1. High Temperature Reactor Research

1.1 Graphite and Ceramics (B. S. Lee, J. H. Heiser, III, and D. R. Wales)

1.1.1 Nondestructive Measurements

The No. 3 medium sized 2020 graphite sample was taken to the Oak Ridge National Laboratory for nondestructive measurements after it added 50 hours of oxidation time (total oxidation time, 6286 hours for No. 3 sample) through oxidation rate runs. On this sample, eddy current responses were measured at different positions of the sample to see the density changes on the surface. Elastic moduli were estimated by ultrasonic wave velocity measurements.

1.1.1.1 Eddy Current Measurements

The eddy current responses were measured on the No. 3 medium sized 2020 graphite sample that had been oxidized for 260 days. The measured values were converted to densities using the relationship between eddy current response and density developed by C. R. Kennedy of Oak Ridge National Laboratory. Table 1.1.1 shows the surface densities of the top, bottom, and sides of the sample.

1.1.1.2 Sonic Testings

Ultrasonic wave velocity measurement methods utilizing longitudinal and shear waves were used to estimate the elastic moduli of the oxidized 2020 graphite sample No. 3 in the axial direction and the results are shown in Table 1.1.2.

Due to the severely oxidized portions on the side of the sample, the ultrasonic wave velicities could not be measured in the radial direction.

These values will be compared with those which will be generated with a destructive method.

1.1.2 Oxidation Kinetics Measurements

The oxidation rate runs with larger size (15.24 cm x 5.97 cm x 5.72 cm) 2020 and PGX graphites are completed, and the testings with TS-1621 are in progress. The oxidation rates were measured as a function of time in the helium impurities loop (HIL) at 850°C with the initial gas composition of 500 ppm H_2O/5000 ppm H_2/balance He. With the gas purifying system disconnected, the levels of CO and CO_2 were monitored by infrared monitors. The H_2 level was monitored by a gas chromotograph. The H_2O level was maintained at 500 ppm with a water dew point meter. The rate run duration depends on the reactivity of the graphite, and for 2020 graphite, it ranged between 1 and 3 hours for each run. After each rate run, the gas purifying system is connected, and the levels for H_2O and H_2 are maintained at 500 ppm and 5000 ppm until the next rate run.

Table 1.1.1

The Estimated Densities for the Oxidized Sample No. 3.

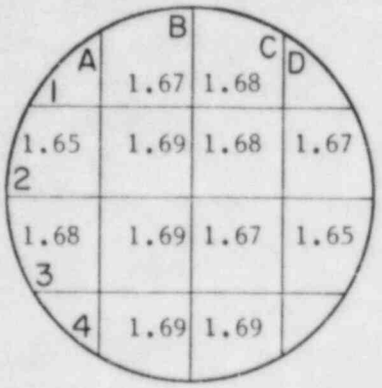

TOP

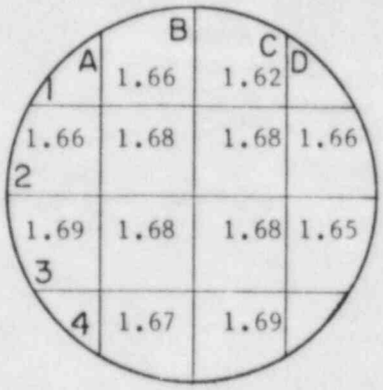

BOTTOM

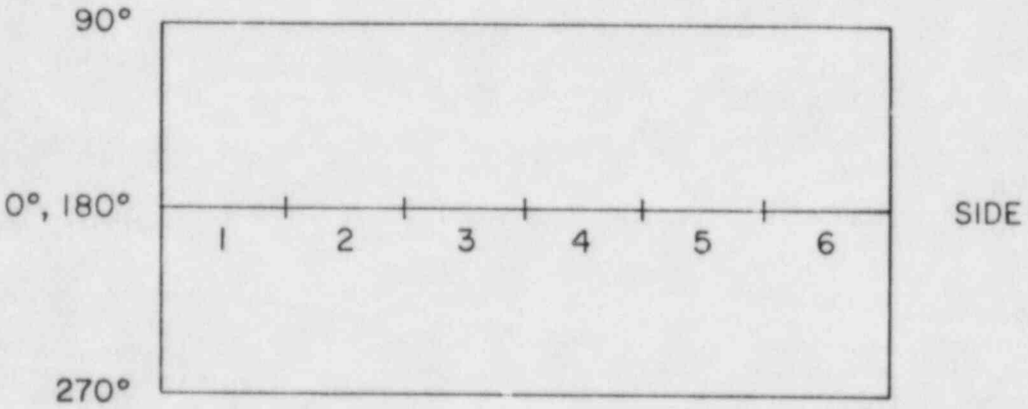

Position \ Angle	0	90	180	270
1	NR*	1.37	1.66	1.39
2	NR	1.22	1.65	1.20
3	NR	1.43	1.66	1.20
4	NR	1.35	1.67	1.46
5	NR	1.46	1.65	1.53
6	NR	1.60	1.65	1.55

*No reading

Table 1.1.2
The Estimated Moduli of Elasticity, E (GPa), for the Oxidized Sample No. 3

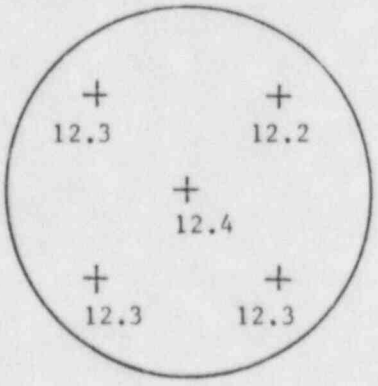

The oxidation rate run results are shown in Table 1.1.3 and Figures 1.1.1 and 1.1.2. For 2020 graphite, the initial rate was 278 ppm ($CO + CO_2$)/hr, which is equivalent to 2.26×10^{-7}g (graphite loss)/cm^2 min. The oxidation rate decreased to 239 ppm ($CO + CO_2$)/hr after 50 hours of accumulated oxidation time, which was followed by a slow increase to ~290 ppm ($CO + CO_2$)/hr. As shown in Figure 1.1.1, the oxidation rate stayed nearly constant for up to 450 hours. The initial rate decrease was also observed in our previous short term oxidation rate runs with small size 2020 samples (diameter: 1.27cm) (B. S. Lee, 1983). However, the long term (~9 month) oxidation experiment showed a continuous increase of oxidation rate of 2020 graphite (B. S. Lee, 1984). Thus, these three sets of experiments clearly show the dangers of extrapolating the short term experimental results to the long term (~40 years) reactor conditions.

Table 1.1.3

Oxidation Rates for 2020, PGX and TS-1621 Graphites at 850°C with 500 ppm H_2O/5000 ppm H_2 (balance He)

Graphite	Oxidation Rate (ppm ($CO+CO_2$)/hr)		
	Initial Rate	After 50 hrs	After 440 hrs
2020	278	239	262
PGX	673	1273	3746
TS-1621	451	340	358 (after 170 hrs)

PGX graphite showed an increase in oxidation rate for up to 360 hours and a constant rate at ~4000 ppm ($CO + CO_2$)/hr until the end of the rate run (640 hours). As shown in Table 1.1.1, PGX showed much higher rates than 2020 for the equivalent duration time. However, this comparison is somewhat exaggerated because of the different oxidation surface area for the two different grades of graphites. After the same period of oxidation, the more active graphite develops larger surface area by opening up more pores, which results in a higher oxidation rate. Thus, the accurate comparison of the oxidation rates requires the information about the surface area increase as a function of burnoff. In the near future, the existing information on surface area will be reviewed for this purpose.

TS-1621 graphite showed an initial oxidation rate which was between those of 2020 and PGX graphites.

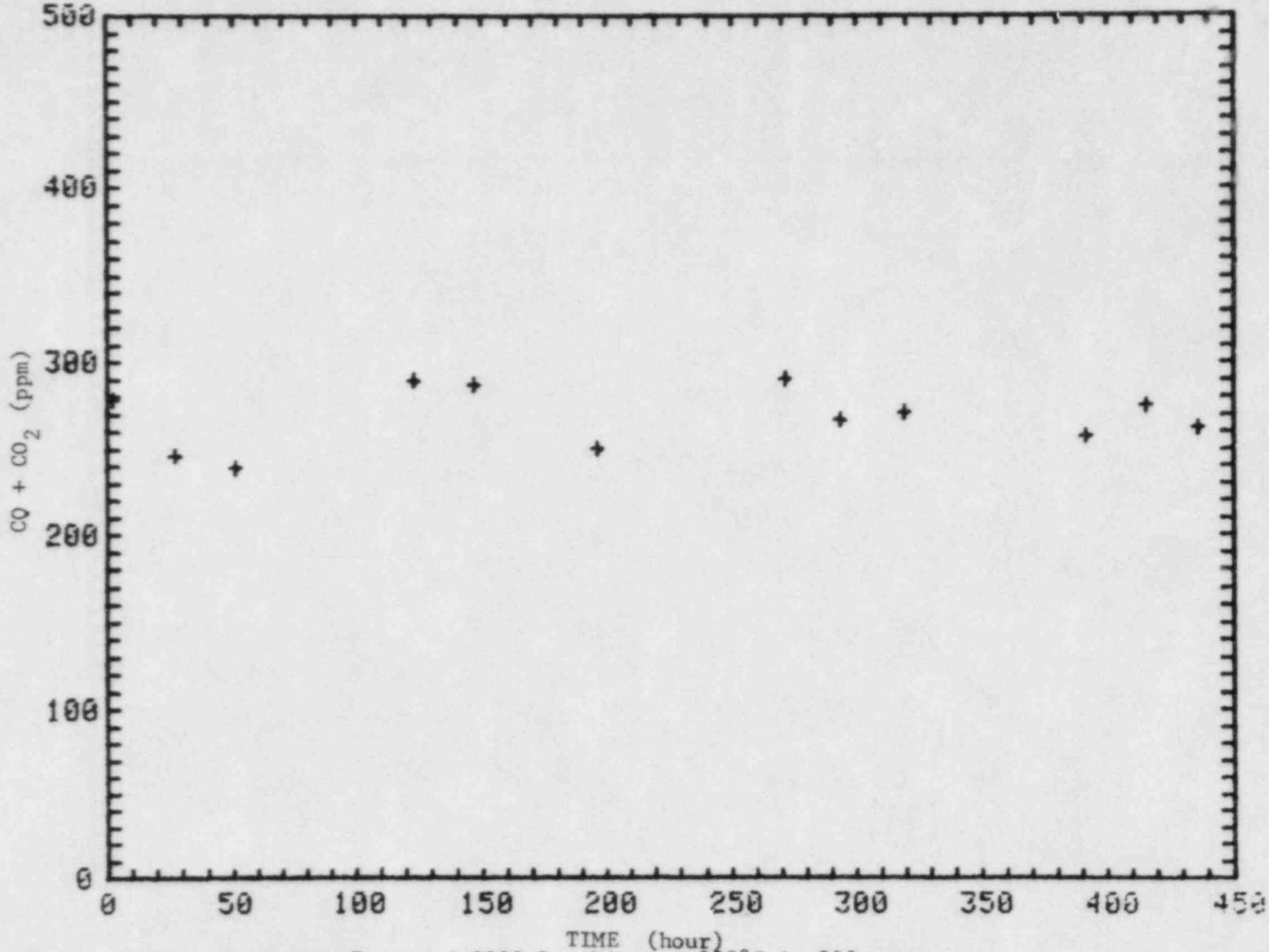

Figure 1.1.1 Oxidation Rates of 2020 Graphite at 850°C in 500 ppm H_2O/5000 ppm H_2/He.

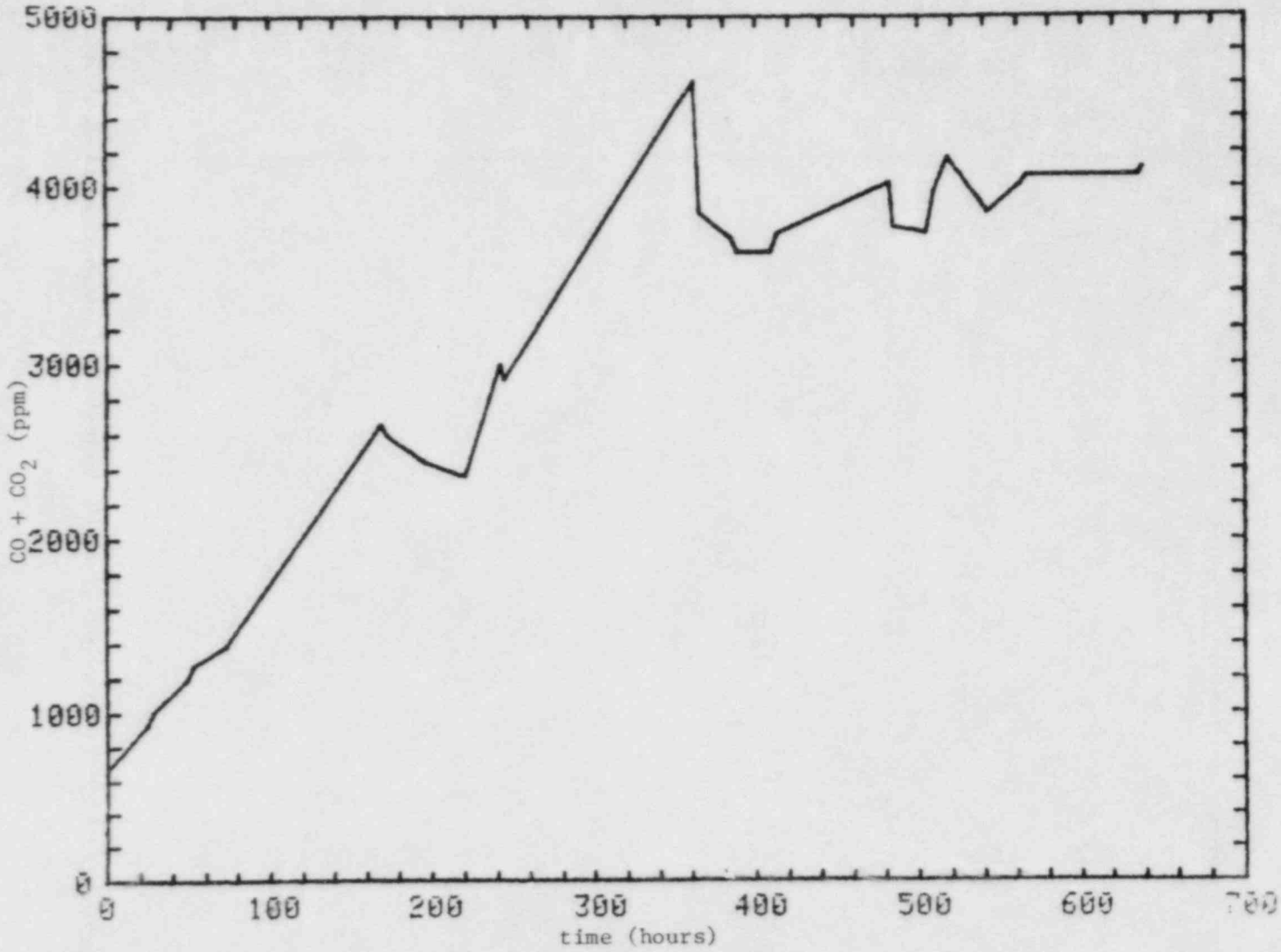

Figure 1.1.2 Oxidation Rates of PGX Graphite at 850°C in 500 ppm H_2O/5000 ppm H_2/He.

1.2 Fission Product Transport (B. S. Lee, J. H. Heiser, III, and C. C. Finfrock)

During the last quarter, three integrated fission product transport (IFPT) experimental runs incorporating silver were conducted. An earlier run at 1500°C with a flow rate of 7.3 cm/sec (Run #51884) was reported in the previous progress report. In this period, all four chimneys and filters were analyzed for silver.

Since we have no means of controlling the temperature gradient in the chimney at the present time, we have used two different sized IFPT systems to generate different temperature gradients.

Since no silver was detected with an EDAX on the filter of the Run #51884, two more experimental runs were conducted in the small IFPT system which generates larger temperature gradient in the chimney.

Runs #70884 and #81484 (small IFPT) were at 1400°C and 1480°C, loaded with 12g and 9g of silver, and had He flow rates of 0.1 and 25 cm/sec, respectively. In run #70884 (12 hrs) no silver was collected on the filter while 46.8 mg of silver plated on the chimney wall. Run #81484 (8 hrs) had 10.8 mg of silver (as aerosols) reached the filter with 38.6 mg plating out on the chimney.

In order to determine the silver distribution, the chimneys were cross-sectioned at 2.54 cm intervals and leached for 24 hours with 35% nitric acid. Atomic absorption spectrophotometry analysis was used to measure the amount of silver plated-out as a function of distance from the susceptor. The results from runs #70884 and #81484 are shown in Figures 1.1.3 and 1.1.4 as histograms.

Another run at 1500°C with the large IFPT system loaded with 24 g of silver was conducted with a coolant flow rate of 19.7 cm/sec for 7 hours. In this run, 0.47 mg of silver reached the filter as aerosols and 291 mg of silver plated out on the chimney. The same analytical method as described above was used for the analysis. The chimney and the filter from the earlier run, run #51884, were also analyzed. The amount of silver on the filter was below the detectability limit, and the amount of silver plated out on the chimney was 189 mg. These results are shown in Figures 1.1.5 and 1.1.6.

The results so far showed that silver fission product aerosols do form and are transported to the environment when the temperature gradient is large enough and flow rate is high enough. Presently, we are attempting to quantify this information by monitoring the temperature gradient throughout the experimental run.

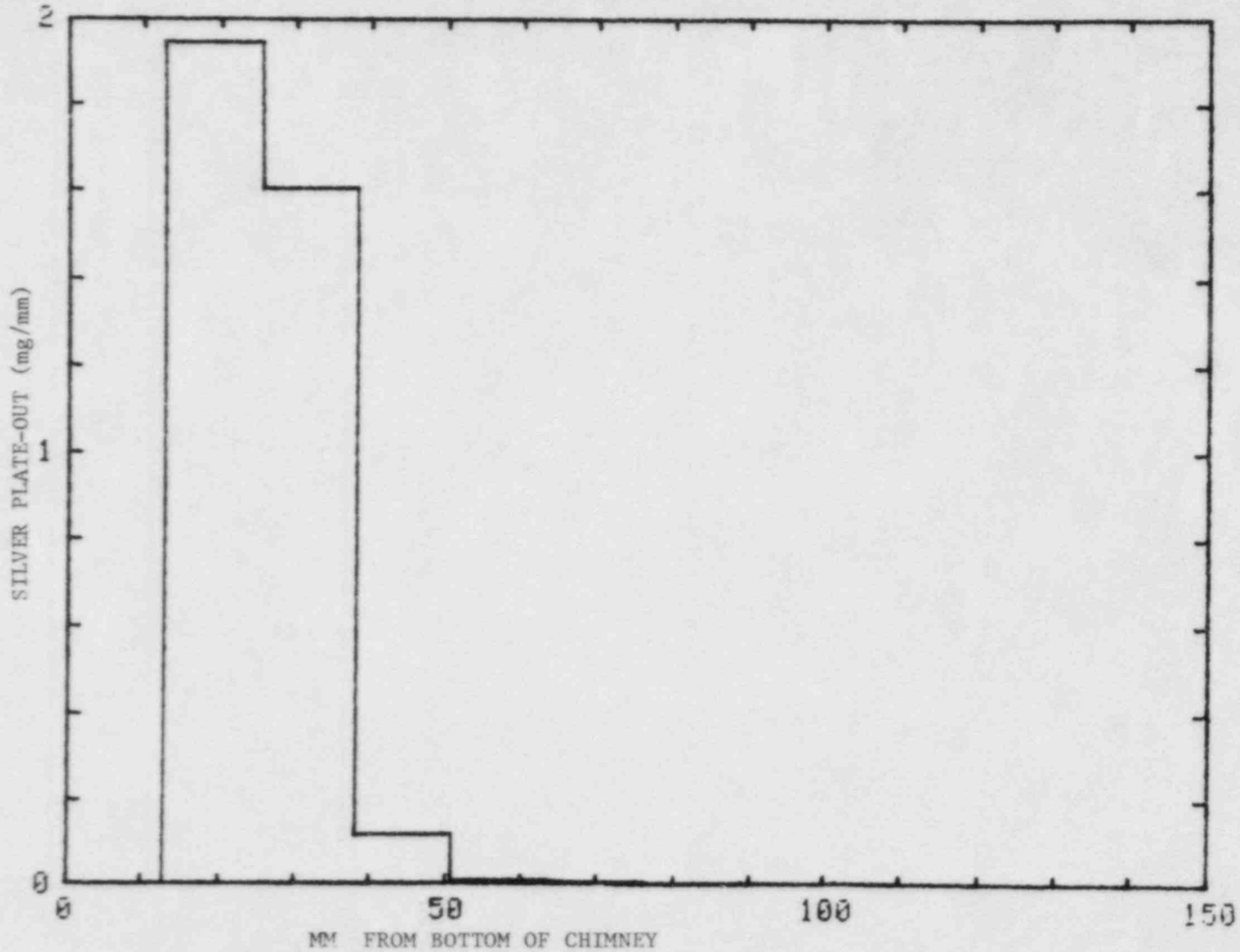

Figure 1.1.3 Silver Plate-Out as a Function of Distance From the Susceptor for Run #70884.

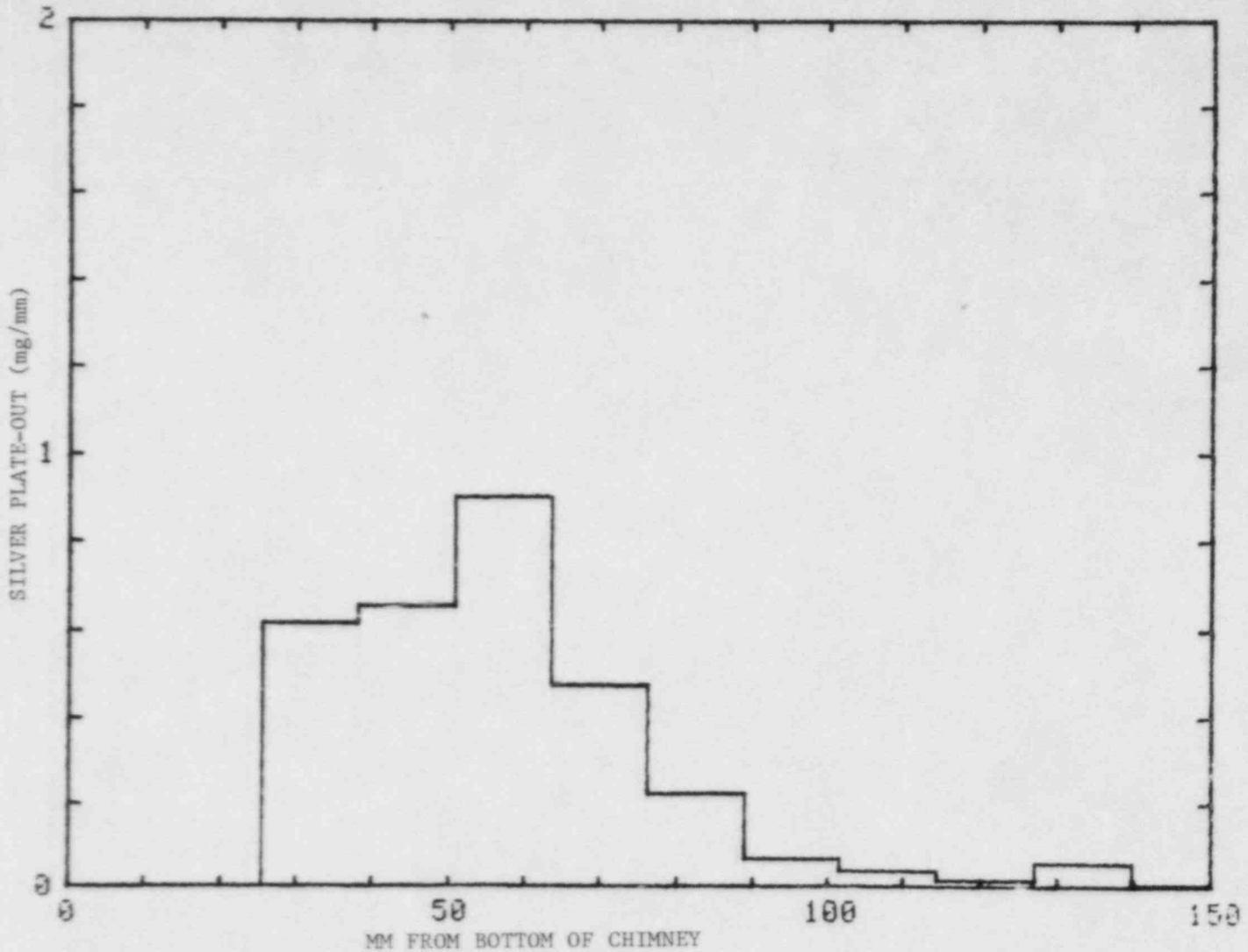

Figure 1.1.4 Silver Plate-Out as a Function of Distance From the Susceptor for Run #81484.

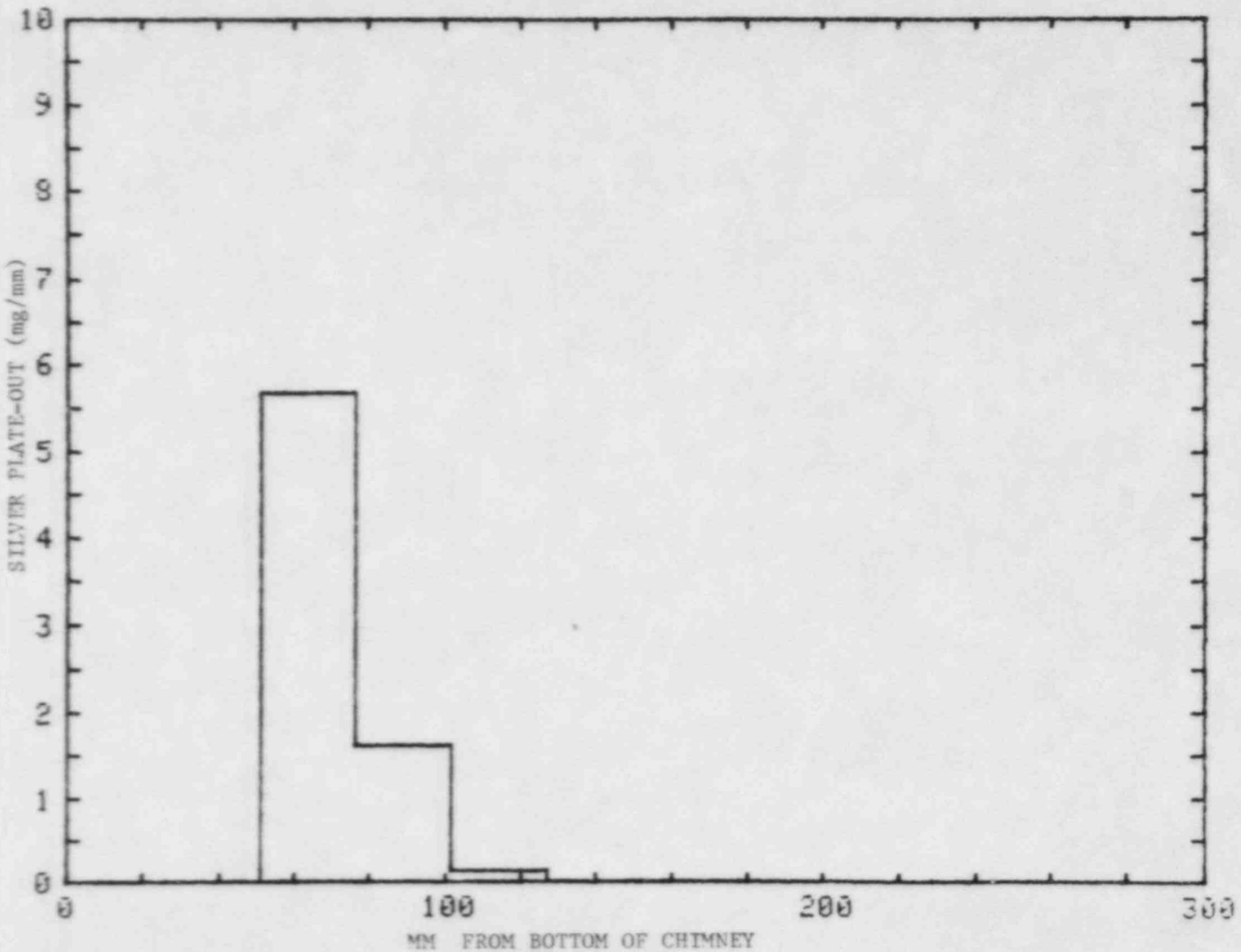

Figure 1.1.5 Silver Plate-Out as a Function of Distance From the Susceptor for Run #51884.

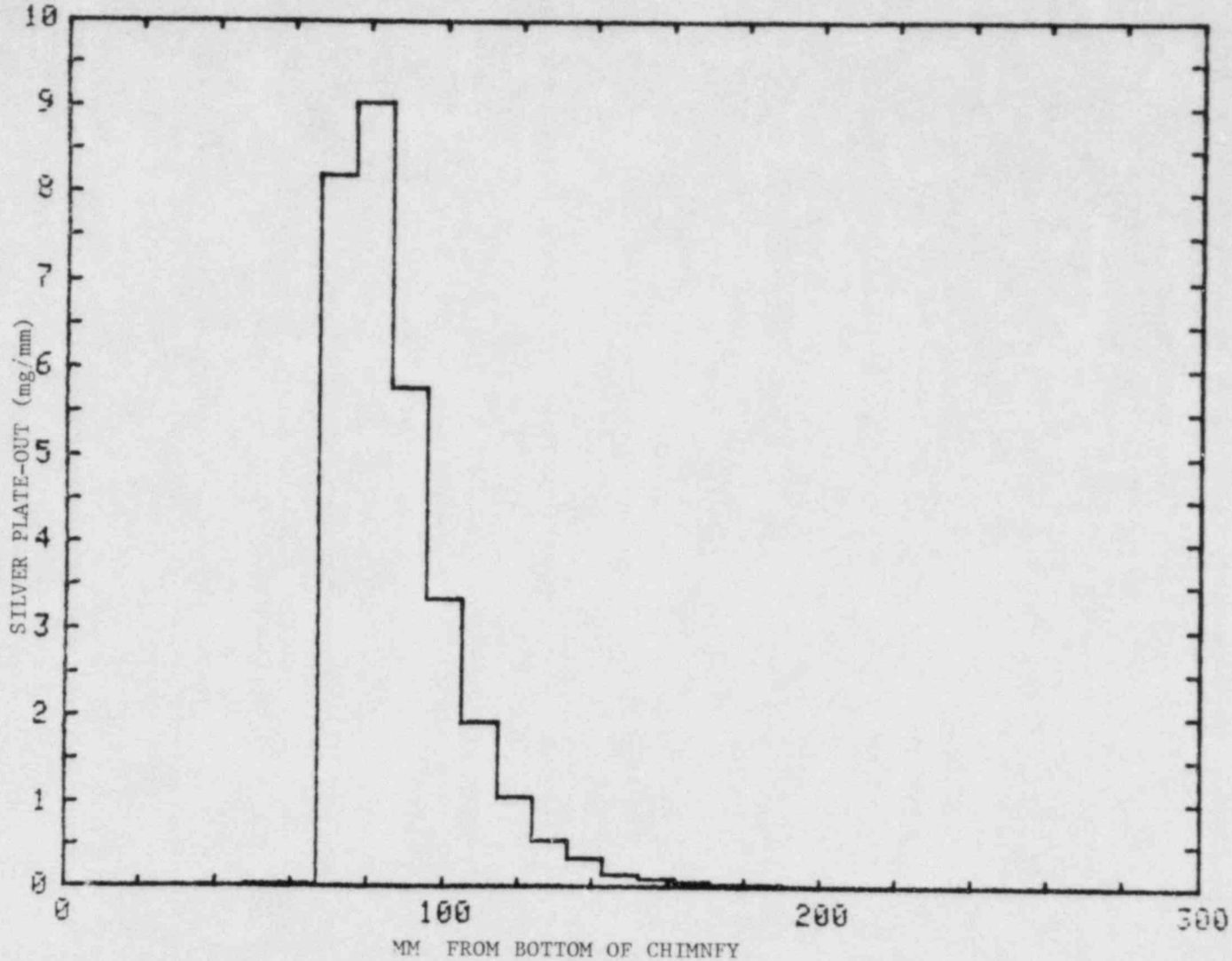

Figure 1.1.6 Silver Plate-Out as a Function of Distance From the Susceptor for Run #92884.

1.3 Analytical

1.3.1 Vapor Migration in Concrete (P. G. Kroeger)

Our previous work (Kroeger & Shiina, 1984; and Kroeger, April - June 1984) was extended to include the effects of chemically bound water in concrete, which is generally released in the temperature range of 200 to 600°C. In the selected sample application 140 kg/m^3 of physically bound water and 40 kg/m^3 of chemically bound water were used as initial water content of the concrete structure. The pressures behind the liner remained about equal to the previous results with only 140 kg/m^3 of physically bound water, and the water ingress into the core cavity increased about proportional to the increase in total water available i.e., by about 28%. Our previous conclusions that the water ingress remains at least an order below earlier estimates remains therefore unaffected.

1.3.2 Containment Building Atmosphere (P. G. Kroeger)

Based on our previous assessment of containment building (CB) atmosphere heat transfer conditions during UCHA scenarios without functioning LCS (Kroeger and Chan, Jan. - March 1984). a solution of the energy equation for the CB atmosphere and a model for transient conduction into the solid structures of the CB were added to our ATMOS code.

With this addition we can now evaluate CB temperatures during such transients, and some typical results are shown in Figures 1.3.1 and 1.3.2. Figure 1.3.2 (a) includes the gas temperature and the average wall surface temperature. These temperatures actually confirm the rough estimates that had to be used with the source term study (H. Reilly, et al, 1984). Liner failure and beginning water ingress occurred at 60 hrs, and CO_2 ingress began at 90 hrs. The resulting CB atmosphere pressure is shown in Figure 1.3.1 (b) as "Base Case", indicating that the assumed building failure pressure of 7 bar or 100 psi is reached after about 10 days.

A very essential but uncertain parameter is the effective surface area of the CB structure, including the PCRV outside surface. While the upper dome structures will certainly absorb heat, only part of the surface in the annular space between PCRV and CB walls will participate. The base case of Figure 1.3.1 used an effective surface of 11,900 m^2 which includes about one half of the annular region surfaces. Included in Figure 1.3.1 (b) is the pressure response for a limiting case which excluded all of the annular space, and used an active surface of only 6,400 m^2. The resulting pressure is clearly an upper limit, since part of the side structure will always participate in the heat exchange between gas and wall. For this limiting case the used failure pressure of 100 psi was reached at 190 hrs rather than at 240 hrs. Thus, even if our base case assumption of 11,900 m^2 effective surface area were high, CB failure times would lie between 190 and 240 hrs.

All the above runs were made with the water ingress rates of the source term study (136,000 kg between 60 and 240 hrs). From further work (see Section 1.3.1 of this report) we now know that those ingress rates were at least one order too high. An additional case is, therefore, shown here, with reduced water ingress of 20,000 kg between 60 and 240 hrs. This ingress rate

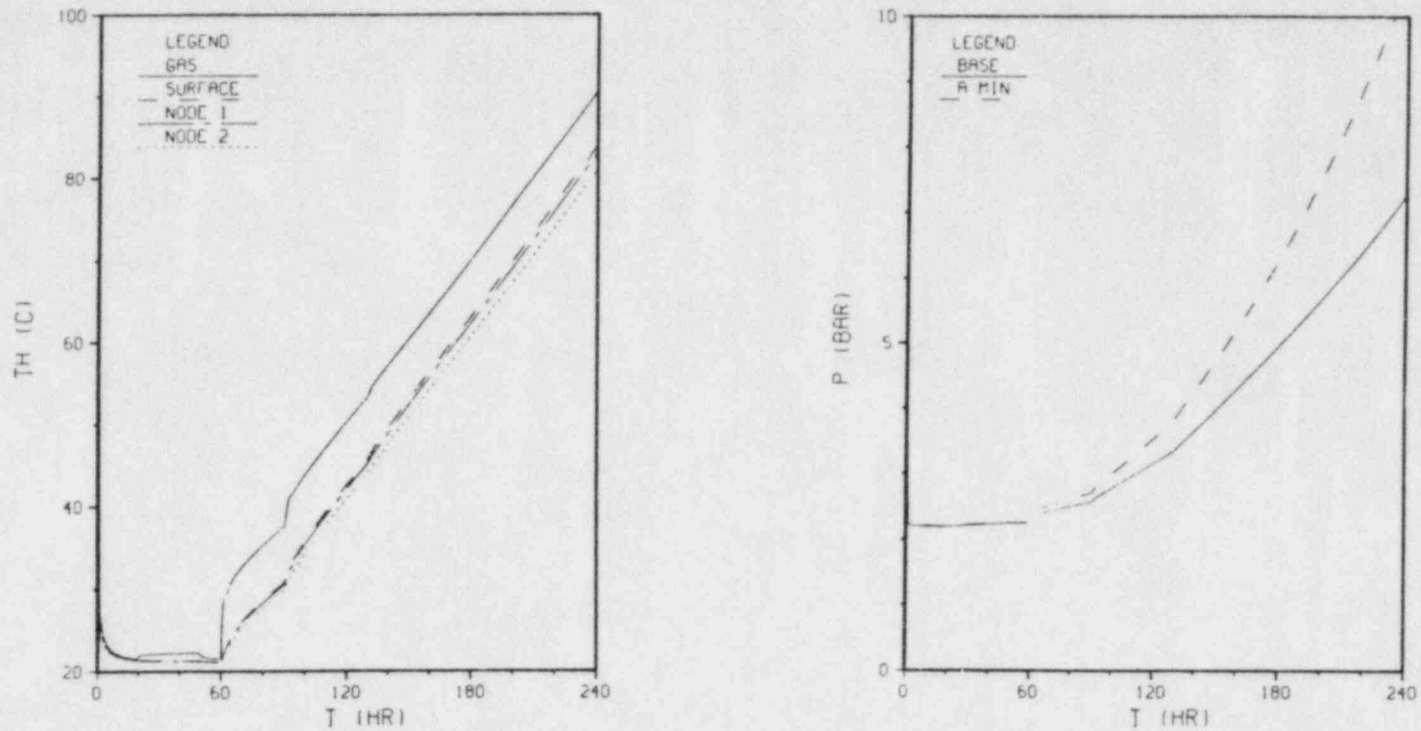

(a) (b)

Figure 1.3.1 Containment Building Temperatures and Pressures During Unrestricted Core Heatup Accidents (Frame a: Gas and Structure Temperatures, Frame b: CB Atmosphere Pressures For Base Case and Limiting Case of Reduced Wall Surface).

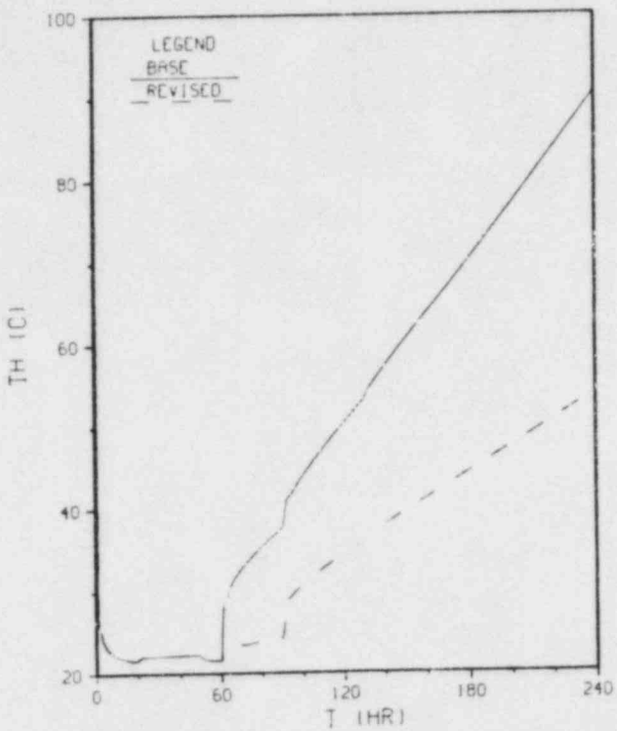

(a)

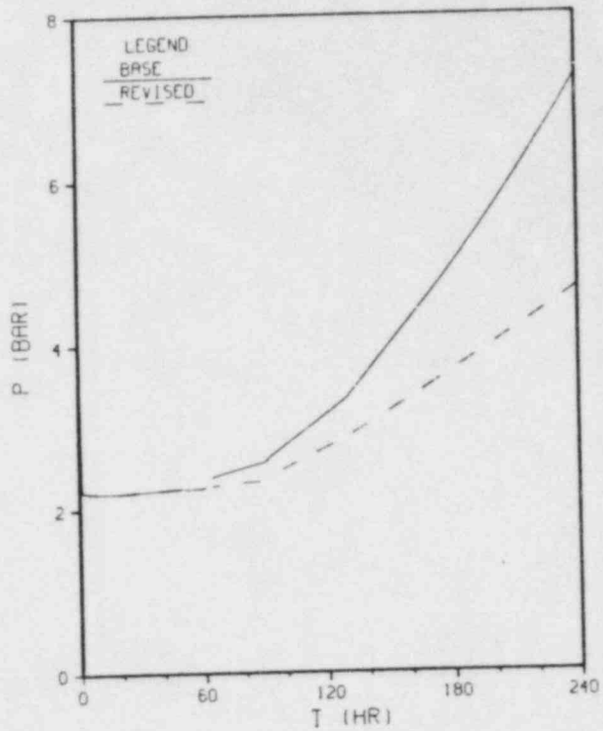

(b)

Figure 1.3.2 Containment Building Temperatures and Pressures During Unrestricted Core Heatup Accidents, Comparing Base Case of 130,000 kg Water Ingress Vs. Revised Water Ingress of 20,000 kg.

is still too high based on our current knowledge, but was used to qualitatively assess the effect of reduced water ingress. Figure 1.3.2 clearly show the reduced temperatures and pressures, and even for this conservative case failure pressures would now be expected only after more than 350 hrs.

1.3.3 Severe Accident Transient for Modular Pebble Bed Reactor

With the current emphasis on modular HTGR's and the recent interest in pebble bed core designs, the severe accident of loss of forced circulation with depressurization was analyzed using our THATCH code. A 250 MW pebble bed core reactor was modeled with a nominal power density of about 4.2 W/cc (Bechtel Group, 1984). As many of the material and design data are not finalized at this time, assumptions had to be made in particular with respect some of the support structure materials. Some of these data are based on information reported for the DOE program (Lutz et al, 1982) or from KFA Germany (Jahn et al, 1983).

These results represent the first application of the general THATCH code to a modular pebble bed reactor. Aside from very few debug problems which typically occur with new codes, the application was straightforward. The model includes a pebble bed core, side reflectors, top and bottom reflectors, support structure, reactor vessel, cavity, and cavity cooling systems. The initial results shown here used 400 nodes, which was ample, and assumed a cavity cooling system operating in the passive emergency mode. Computer running costs for 100 hrs transients were negligible.

Typical core, side reflector and reactor vessel temperatures are shown in Figure 1.3.3 (a). Heat flows out of the core, and out of the reactor vessel are compared against the decay heat in Figure 1.3.3 (b). The core peaks at about 1820°C at about 50 hrs and at about 60 hrs the heat transfer out of the core exceeds the decay heat production. Similarly the heat transfer out of the reactor vessel peaks at about 95 hrs from which time on all reactor component begins to cool down. The initial drop in heat flow out of the rector vessel is due to the change to the emergency cooling mode.

The current set up of the THATCH code, applying it to such modular reactor accident scenarios, can be readily modified to accommodate changes in geometry, power level, or different material properties. While the quantitative values will be revised as better material descriptions and dimensions become available, this work establishes a base for understanding the accident behavior of modular pebble bed or prismatic fuel reactors.

One of the objectives of this work was to establish the capability to compute expected gas flows from the core to the cavity for various severe accident scenarios which will provide inputs for the assessment of confinement/containment building transients during such accidents. At the prevailing cavity temperature levels it was found that radiation will be the dominant mode of heat transfer across the cavity, from reactor vessel to the

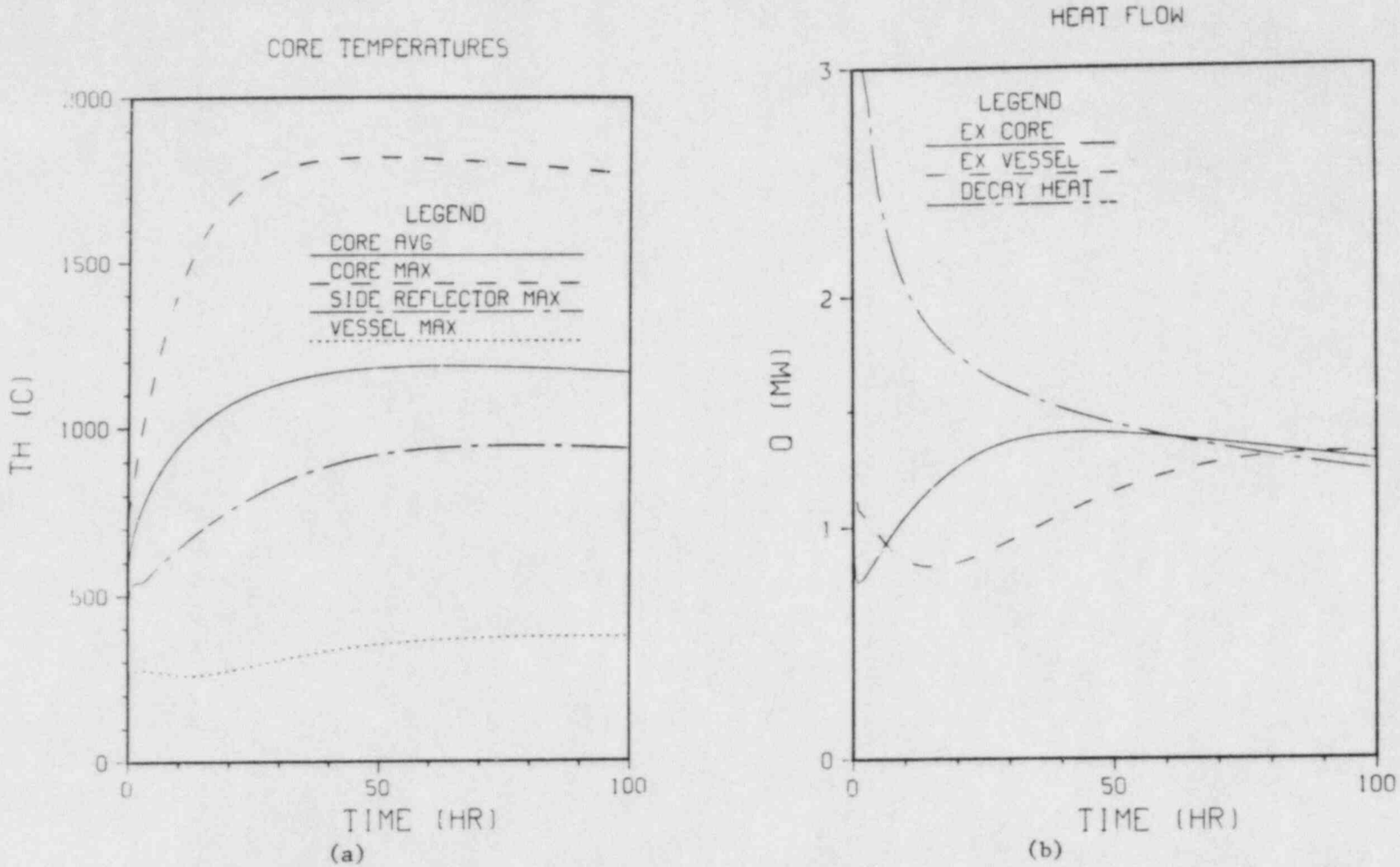

Figure 1.3.3 Transient Response for Typical Modular Pebble Bed Reactor to Loss of Forced Circulation With Depressurization Accident. (Frame a: Reactor Temperatures; Frame b; Decay Heat and Heat Flows).

cavity cooling system. For typical 2 to 3 ft. wide cavities, significant natural circulation currents will exist in the cavity, but their net effect on total heat transfer appears to remain small. The code currently applies a correlation for two-dimensional cavity convection and uses one-dimensional radiation. Two-dimensional radiation would be more correct. It can be readily included as the code is set up for it. However, its effect would be to predict only slightly lower vessel temperatures and its inclusion is premature at this time.

References

BECHTEL GROUP, INC., "Evaluation of Small Modular High Temperature Gas-Cooled Reactors Applied to Electricity Generation," GCRA 84-002, May 1984.

JAHN, W., et al, Spezielle Analysen zum Temperatur-und Spaltproduktverhalten von HTR-MODUL-Anlagen, KFA, JUEL-SPEZ-235, Germany, 1983.

KROEGER, P. G. and SHIINA, Y., "Transient Moisture Migration in Concretes During Severe Reactor Accidents," TS 13.7, Proceeding of the Fifth Meeting on-Thermal Nuclear Reactor Safety, Karlsruhe, W. Germany, September 1984.

KROEGER, P. G., Sect. 1.3.2, Quarterly Progress Report, Brookhaven National Laboratory, April - June, 1984.

KROEGER, P. G. and CHAN, B. C., Sect. 1.3.2, Quarterly Progress Report, Brookhaven National Laboratory, January - March, 1984.

LEE, B. S. et al, Quarterly Progress Report, Brookhaven National Laboratory, April - June 1983, BNL-NUREG-51454, Vol. 3 No. 2.

LEE, B. S., HEISER, J. H, III, and WALES, D. R., Quarterly Progress Report, Brookhaven National Laboratory, April - June 1984.

LUTZ, D. E., et al, "Modular Pebble-Bed Reactor Reforming Plant Design for Process Heat, General Electric Co., Calif., GEFR-00630, 1982.

REILLY, H. et al, "Preliminary Evaluation of HTGR Severe Accident Source Terms, EG&G Idaho National Engineering Laboratory, EGG-REP-6565, April 1984.

2. SSC Development, Validation and Application (J. G. Guppy)

The Super System Code (SSC) Development, Validation and Application Program deals with advanced thermohydraulic codes to simulate transients in liquid metal-cooled reactors (LMRs). During this reporting period, work continued on three codes in the SSC series. These codes are: (1) SSC-L for simulating short-term transients in loop-type LMRs; (2) SSC-P which is analogous to SSC-L except that it is applicable to pool-type designs and (3) SSC-S for long-term (shutdown) transients occurring in either loop- or pool-type LMRs. In addition to these code development and application efforts, validation of these codes is an ongoing task. Reference is made to the previous quarterly progress report (Guppy, 1984) for a summary of accomplishments prior to the start of the current period.

2.1 SSC-L Code (W. C. Horak)

2.1.1 Pipe Insulation Test (W. C. Horak, R. J. Kennett)

To determine the effect of rock wool insulation on a complete loss-of-heat sink accident, a transient was simulated using SSC for a reactor similar to FFTF, i.e., a 400 MWth loop type reactor with three parallel heat transport trains. In this hypothetical plant, the primary piping in all three loops was assumed to have a 0.152m (6") layer of rock wool insulation. At time t = 0, all heat transfer across the IHXs was stopped, followed by a reactor scram with pump trip at 0.6(s). The reactor vessel is considered to be adiabatic. The only heat loss is through the piping to the reactor containment, which is assumed to be at a constant temperature of 295.6°K (72°F). It was intended that the transient be simulated until the temperatures were on an established downward trend or until the coolant boiled.

The piping thermal model currently in SSC is a one-dimensional, discrete parameter representation, with two radial nodes (coolant, pipe wall) and a user specified number of axial nodes. The coolant flow is single phase and incompressible. Axial conduction in the walls and frictional heating are neglected.

In addition to the above assumptions, the pipe walls were assumed to be perfectly insulated on the outside. For plants of the CRBR type with standard insulation, this assumption was adequate especially at full power operation or during relatively short term transients (less than 1 hour). The adequacy of this assumption for extremely long time transients was not addressed in an earlier report, (Madni, 1980).

These assumptions lead to energy balance equations for a single axial node of the form:

Coolant:

$$\rho_i V_i \frac{d}{dt} h_{i+1} = W(h_i - h_{i+1}) - (UA)_{CW} (T_i - T_i^p) \qquad (2.1)$$

Pipe Wall:

$$M_i^p \, C_i^p \, \frac{d}{dt} \, T_i^p = (UA)_{CW} \, [T_i - T_i^p] \qquad (2.2)$$

where,

ρ_i = density of coolant in the i-th pipe node

V_i = volume of coolant in the i-th node

h_{i+1} = exit coolant enthalpy

W = coolant mass flow rate

h_i = inlet coolant enthalpy

$(UA)_{CW}$ = overall heat transfer coefficient between the coolant and pipe wall

$\overline{T}_i$ = average coolant temperature in the i-th wall

M_i^p = mass of the pipe wall in the i-th node

C_i^p = heat capacity of the pipe wall in the i-th node

T_i^p = pipe wall temperature in the i-th node

A "donor cell" approach was used in the development of these equations.

To model the effect of piping insulation, Eq. 2.2 was modified as:

$$M_i^p \, C_i^p \, \frac{d}{dt} \, T_i^p = (UA)_{CW} \, [\overline{T}_i - T_i^p] - (UA)_{WA} \, [T_i^p - T_A] \qquad (2.3)$$

where,

$(UA)_{WA}$ = overall heat transfer coefficient (including the thermal resistance of the insulation) between the pipe wall

T_A = ambient (atmospheric) temperature

In this model, the heat capacity of the insulation was neglected since this contribution was a fraction of the thermal mass of the node. This assumption increased the computational efficiency and was clearly conservative since any additional thermal mass would reduce the temperature increase during a loss of heat sink accident.

The expressions for the overall heat transfer coefficients are:

$$1/(UA)_{CW} = \frac{1}{2\pi L}\left\{\frac{1}{r_i h} + \frac{1}{k_p}\ln\left(\frac{r_o + r_i}{2r_i}\right)\right\} \qquad (2.4)$$

$$1/(UA)_{WA} = \frac{1}{2\pi L}\left\{\frac{1}{k_p}\ln\left(\frac{2r_o}{r_o + r_i}\right) + \frac{1}{k_I}\ln\left(\frac{r_s}{r_o}\right) + \frac{1}{r_s h_a}\right\} \qquad (2.5)$$

where,

L = length of axial node

r_i = pipe wall inner radius

h = convective heat transfer coefficient between the coolant and pipe wall

k_p = thermal conductivity of the pipe wall

r_o = pipe wall outer radius

k_I = thermal conductivity of the insulation

r_s = radius of the outer surface

h_a = the combined convective and radiative surface heat transfer coefficient

The convective heat transfer coefficient, h, and the pipe wall thermal conductivity, k_p, were determined using functions already present in SSC. The piping insulation thermal conductivity was obtained using the relation (Vossebrecker and Kellner, 1979):

$$k_I\ [W/m\ ^\circ K] = 0.003 + 10^{-4}\ T + 2.10 \times 10^{-10}\ T^3 \qquad (2.6)$$

The combined surface heat transfer coefficient was taken to be (Van Tuyle, et al., 1984):

$$h_a = 0.8512\ (T_S - T_A)^{0.25} + 2.3035 \times 10^{-9}\ (T_S^4 - T_A^4)/(T_S - T_A)\ , \qquad (2.7)$$

where T_S is the surface temperature of the insulation.

Figure 2.1 shows the core average coolant temperature and reactor vessel outlet temperature. During the first day of the transient, both the core average and reactor outlet temperatures show a cyclic pattern which is typical of transients with natural circulation. The reactor outlet temperature oscillations are damped and delayed in time with respect to the core average temperature because of the volume of coolant in the reactor upper plenum. After 24 hours, the coolant enters a stage of adiabatic heat-up. Without an additional heat sink, the coolant temperatures would continue to rise until the coolant reached saturation (~1200°K). In this case, the pipe radiative losses slow the rise until approximately 5 days into the transient, when the temperatures essentially remain constant at approximately 920°K. The temperature reaches a peak slightly below 923°K at 6.5 days. The temperatures then begin a slow, but established decline to 915°K at 8 days, when the calculation was terminated.

The IHX inlet and outlet temperatures are shown in Figure 2.2. They show the same behavior as the core temperatures, although somewhat delayed in time. The peak temperature reached in the IHX is lower than the core peak temperature due to the radiative pipe loss.

The primary loop flow rate is shown in Figure 2.3. It shows a cyclic pattern during the first day of the transient, then rises slightly between days 2 and 6. The noticeable increase in the flow rate, which occurs at around 6.5 days, is due to the re-establishment of positive flow in the cold channel of the reactor core. Due to buoyancy-driven flow redistribution, this channel had experienced reverse flow since the very early stages of this LOHS event. At this particular time in the transient, conditions in the core are such that a positive flow rate can once again be established in this channel. Once re-established, the frictional forces (which increase sharply at very low flow rates, Spencer and Markley, 1981) are reduced, thus permitting the overall loop flow rate to increase as well. Even though, as seen in the figure, the flow rate has remained relatively constant at slightly greater than 4 kg/s. This behavior is consistent with the behavior of the coolant temperatures.

2.1.2 Inter-Assembly Heat Transfer (W. C. Horak, R. J. Kennett)

The development and coding of the inter-assembly heat transfer model was completed during this quarter.

The model developed for SSC utilized certain assumptions and features so that an adequate portrayal of the important processes involved was accomplished while minimizing computation. The model also was designed to easily interface with the previously developed low heat flux boiling model (Khatib-Rahbar and Cazzoli, 1982) and the intra-assembly heat transfer model (Khatib-Rahbar and Cazzoli, 1983).

The model was written for a cluster of assemblies composed of a central assembly which transfers heat with one ring of adjacent neighbors (see Fig. 2.4). The model can be applied to more than one cluster during a simulation. The outer surfaces of the adjacent assemblies are considered to be adiabatic. Each assembly duct wall is divided into two constant temperature regions.

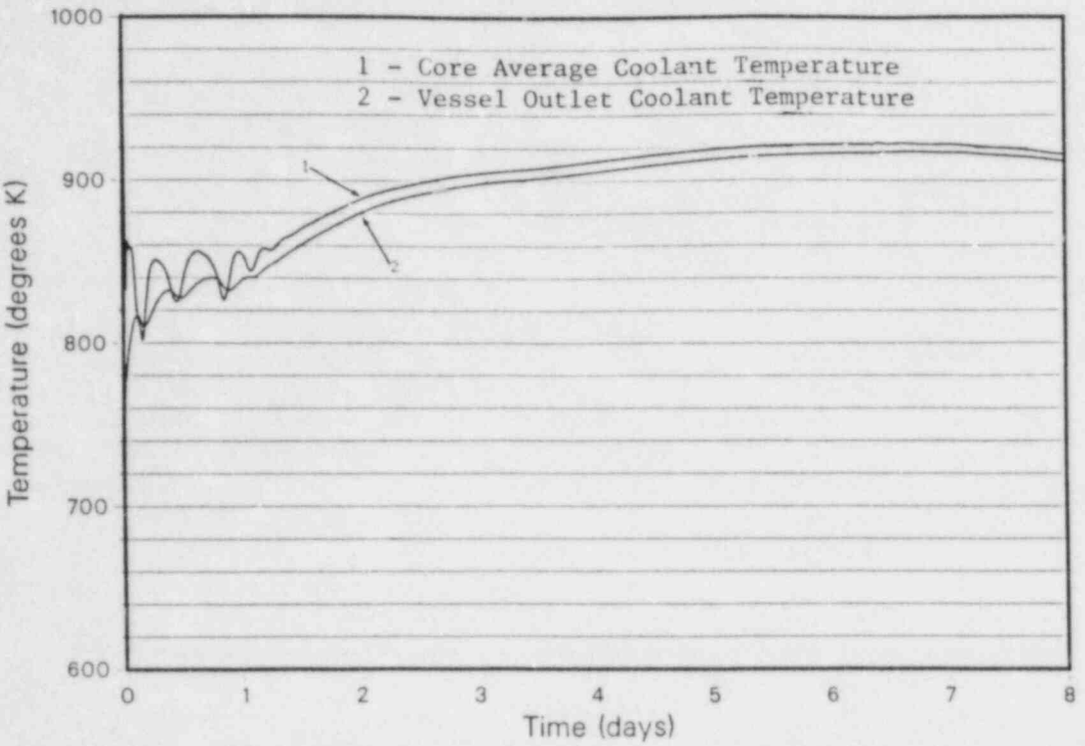

Figure 2.1 Core Average and Vessel Outlet Coolant Temperature for LOHS Event

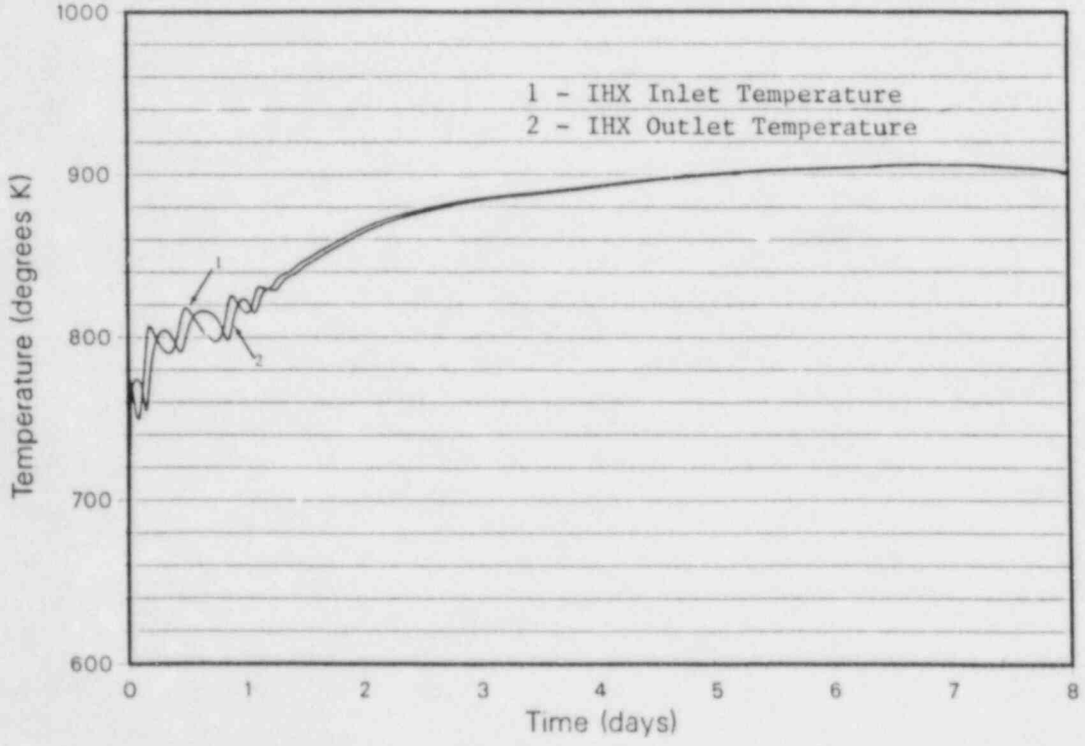

Figure 2.2 IHX Inlet and Outlet Coolant Temperatures for LOHS Event

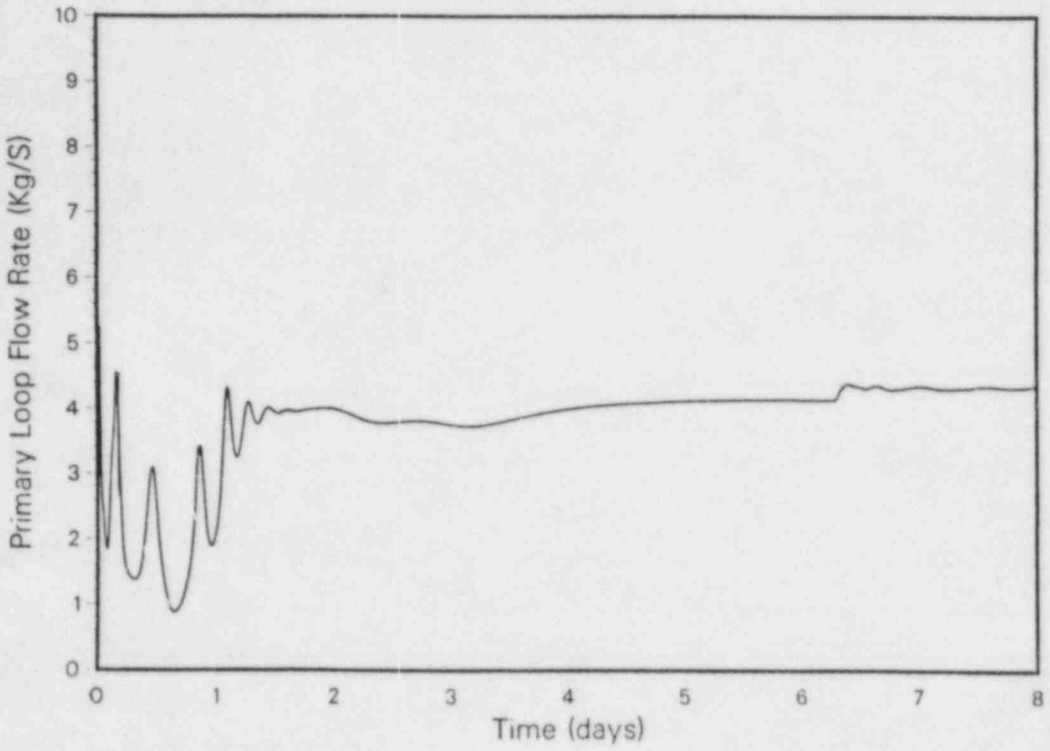

Figure 2.3 Primary Loop Flow Rate for LOHS Event

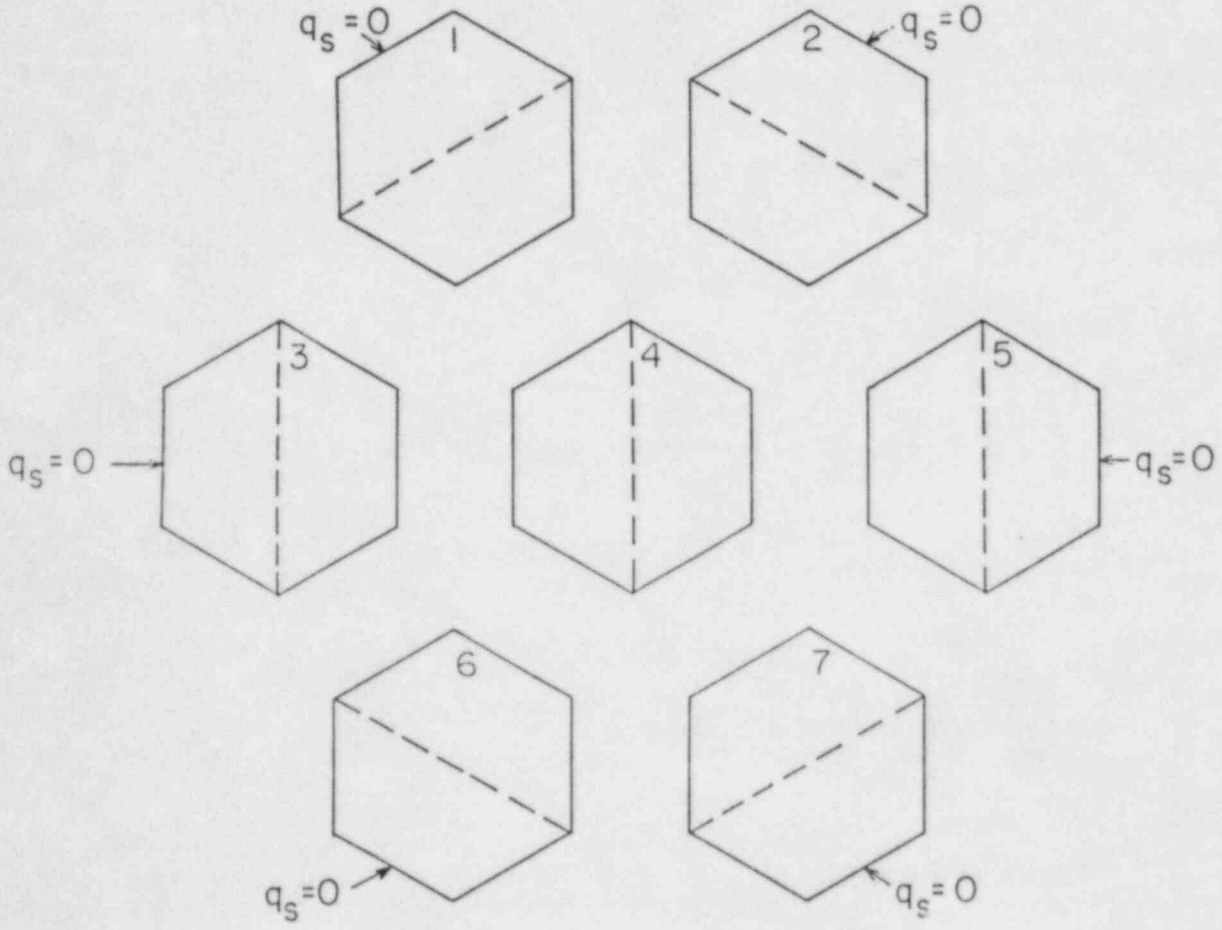

Fig. 2.4 Seven-Assembly Cluster Model for Inter-Assembly Heat Transfer

The sodium in the interstices between the assemblies is assumed to be stagnant. Future models will allow for natural convection of the interstitial sodium. The heat capacity of the interstitial sodium is also neglected permitting the interstices to be represented as thermal resistances between the duct walls.

In the steady-state, all the duct wall temperatures and assembly coolant properties at a particular axial level are solved for simultaneously using matrix methods. Since the heat transfer coefficients and material properties are temperature dependent, an iterative procedure is employed. Once the temperatures are converged, the procedure is then repeated for the next axial level, marching in the direction of flow.

For the six outer (adiabatic) surfaces, the temperatures are given by:

$$UC\ [TD - TC] = QD \tag{2.8}$$

where,
- TD = duct wall temperature
- TC = assembly coolant temperature
- QD = power deposited directly into the duct, and
- UC = overall heat transfer coef icient between the duct and coolant

The duct wall temperatures for the eight inner surfaces are given by

$$UC\ [TD - TC] + \sum_{j=1}^{3} UI_j\ (TD - TD_j) = QD \tag{2.9}$$

where the summation is over the three adjacent duct walls and UI is the overall heat transfer coefficient from duct wall to duct wall across the interface.

These 14 equations, along with the appropriate equations for the assembly coolant temperature, form a banded matrix which is solved using standard techniques. Since the overall heat transfer coefficients are temperature dependent, an iterative procedure is employed at each axial level until the temperatures are converged.

In the transient, the heat flux from the duct wall to the coolant is handled explicitly. This enables the module to interface with the previously developed low heat flux boiling model. The transient equation (in implicit finite difference form) for the six outer surfaces is:

$$(mc_p)\ (TD - TD^{-})/\Delta t = QD - QC^{-} \tag{2.10}$$

where m is the mass of the duct wall, c_p, the heat capacity of the duct wall, and QC, the heat flux from the duct wall to the assembly coolant. The superscripted values are evaluated at the previous timestep. The timestep size is Δt.

The eight inner duct wall temperatures are given by a similar expression:

$$(mc_p)\ (TD - TD^-)/\Delta t + \sum_{j=1}^{3} UI_j\ (TD - TD_j) = QD - QC^- \qquad (2.11)$$

where the summation is over the three adjacent duct wall surfaces. This heat flux among the duct walls is evaluated implicitly.

The 14 transient equations also form a banded matrix, which is inverted using standard techniques. The heat transfer coefficients and material properties are evaluated from the temperatures calculated at the previous timestep. The maximum change in the duct wall temperatures is calculated for use in the automatic timestep control.

The model has been interfaced into SSC where it is currently being debugged and validated against FFTF natural circulation tests. Validation will be completed in the next quarter, with release of the completed documentation and revised SSC library expected by the end of the calendar year.

2.1.3 Interactive Computer Graphics (J. Brown, R. J. Kennett)

An enhanced computer graphics output has now been developed. This extended capability is intended for use in an interactive version of SSC, but will initially be used to provide "snapshots" of the plant condition during various times of the transient. The FFTF plant was the first design analyzed, with data provided from the long term simulations done earlier.

Before the graphics begin, the user is presented with a menu. This allows him to choose two of seven variables to be shown on the graphs. These variables are:

1) primary loop flow rate, W1ONE (1)
2) primary hot leg temperature, T1NA (13)
3) primary cold leg temperature, T1NA (77)
4) secondary loop flow rate, W2ONE (1)
5) secondary hot leg temperature, T2NA (81)
6) secondary cold leg temperature, T2NA (140)
7) normalized fission power, F5PRMT

The expected input is two integers separated by a comma.

Next, the user chooses what time, t, he wishes to see during the transient. The choice is 0.0 to 3600.0 seconds in four second intervals. The input should be a real number. The schematic will be labeled with the variables at the time, t, and the graphs will show a two hundred second interval prior to that time for $t \geq 200.$ secs. For $t < 200.$ secs., the interval will be t secs. The program checks to be sure that the input is evenly divisible by four and that it is in the specified range and requires another input if either of these criteria is not met.

The user now chooses whether to use automatic or user specified scaling. The automatic scaling may give odd looking curves because the y-axis scale is often quite small. There are recommended scales for all of the variables which should encompass all of the data points, but the user may choose any scale he wishes. The input should be two real numbers, separated by a comma, for each variable.

Figure 2.5 shows a typical graphic generated using this program.

2.2 SSC-S Code

2.2.1 Large Timesteps for Long Term Simulations (J. G. Guppy)

Testing has shown that very long timesteps (30 seconds or longer) can be taken by SSC during a slowly changing transient, as long as certain explicit calculations in the IHX representation are suppressed. In order to allow such long timesteps on a routine basis, two potential problems have to be worked out. First, some type of implicit formulation and/or re-nodalization will be needed for the IHX calculations. Second, abrupt changes, resulting from controller actions, must be anticipated when the timestep size is determined.

Previous testing has indicated that the explicit numerical treatment for the time integration in the IHX is the key reason why timesteps must be kept on the order of 1.0 to 2.0 seconds for long term, slowly varying transients. The lagging of the heat flux term across the tube wall causes numerical instabilities when the timesteps become too large. To circumvent this situation for long term transients, a new option is being developed which will allow the user to switch to a fully implicit integration technique for the IHX energy calculations when desired. The first model being created uses full Gaussian elimination for the matrix inversion. This will be replaced later with a more efficient solver which will take advantage of the fact that the resulting matrix is fairly well banded.

Work on implementing this new option for handling the numerical time integration for the IHX is progressing. This implicit scheme, which presently utilizes a full Gaussian elimination method for the matrix inversion, has been coded and debugged. Initial testing is being conducted using the FFTF long term simulation deck.

REFERENCES

GUPPY, J. G., et al., (1984), "SSC Development, Validation and Application," Safety Research Programs Sponsored by Office of Nuclear Regulatory Research Quarterly Progress Report, April 1 - June 30, 1984, Brookhaven National Laboratory Report to be published.

KHATIB-RAHBAR, M. and CAZZOLI, E. G., (1982), "Modeling and Analysis of Low Heat Flux Natural Convection Boiling in LMFBRs," Brookhaven National Laboratory, NUREG/CR-2006, BNL-NUREG-51541.

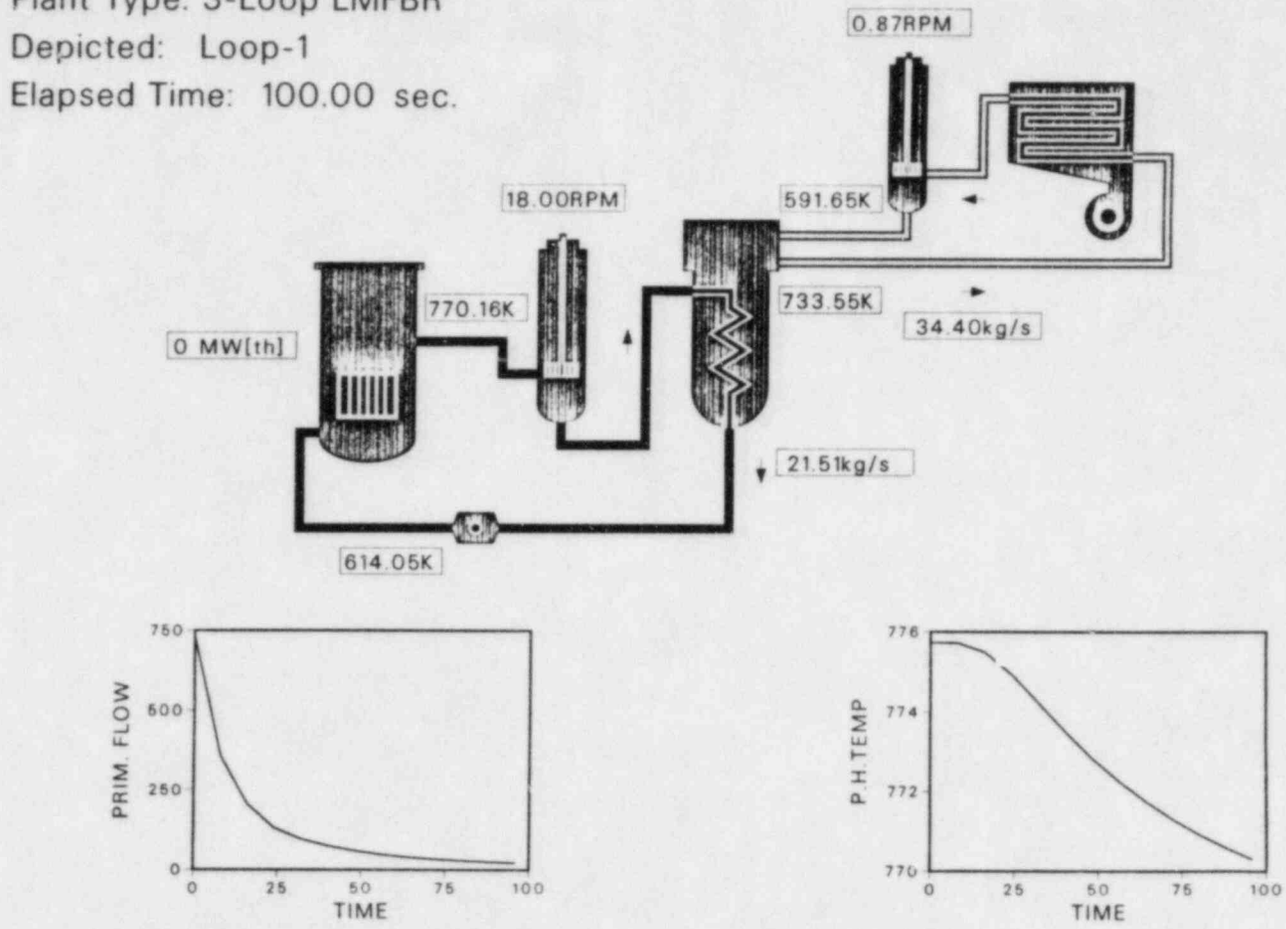

Fig. 2.5 Sample Output for Extended SSC Graphics Capability

KHATIB-RAHBAR, M. and CAZZOLI, E. G., (1983), "Two-Dimensional Modeling of Intra-Assembly Heat Transfer and Buoyancy-Induced Flow Redistribution in LMFBRs", Brookhaven National Laboratory, NUREG/CR-3498, BNL-NUREG-51713).

MADNI, I. K., (1980), "Transient Analysis of Coolant Flow and Heat Transfer in LMFBR Piping Systems," Brookhaven National Laboratory, NUREG/CR-1404, BNL-NUREG-51179, April 1980.

SPENCER, D. R. and MARKLEY, R. A., (1981), "Friction Factor Correlation for 217-Pin Wire-Wrap-Spaced LMFBR Fuel Assemblies," Trans. Am. Nucl. Soc., V. 39, 1014.

VAN TUYLE, G. J., NEPSEE, T. C., and GUPPY, J. G., (1984), "MINET Code Documentation," Brookhaven National Laboratory, NUREG/CR-3668, BNL-NUREG-51742, February 1984.

VOSSEBRECKER, H. and KELLNER, A., (1979), "Inherent Safety Characteristics of Loop-Type LMFBRs," Proc. Int. Mtg. Fast Reactor Safety Technology, Vol. II, p. 554, American Nuclear Society.

PUBLICATIONS

CHAN, B. C., "A Buoyancy-Dominated Model for LMFBR Upper Plenum Flows," Brookhaven National Laboratory Report to be published, 1985.

CHAN, B. C., KENNETT, R. J., GUPPY, J. G., "A Numerical Investigation of Buoyancy-Induced Flow Stratification in the LMFBR Upper Plenum," Brookhaven National Laboratory Report to be published, 1985.

HORAK, W. C., GUPPY, J. G. and WOOD, P. M., "The Effect of Pipe Insulation Losses on a Loss-of-Heat Sink Accident for an LMR," Proceedings of the 2nd Specialists' Meeting on Decay Heat Removal and Natural Convection in LMFBRs, to be published, 1985.

3. Generic Balance of Plant Modeling (J. G. Guppy)

The Generic Balance of Plant (BOP) Modeling Program deals with the development of safety analysis tools for system simulation of nuclear power plants. It provides for the development and validation of models to represent and link together BOP components (e.g., steam generator components, feedwater heaters, turbine/generator, condensers) that are generic to all types of nuclear power plants. This system transient analysis package is designated MINET to reflect the generality of the models and methods, which are based on a momentum integral network method. The code is to be fast-running and capable of operating as a self-standing code or to be easily interfaced to other system codes. Reference is made to the previous quarterly progress report (Guppy, 1984) for a summary of accomplishments prior to the start of the current period.

3.1 Balance of Plant Models (G. J. Van Tuyle)

Models for the soon to be exported Version 1 of MINET have been completed. Major new models for the plant control system and the rotor module are planned for incorporation into Version 2 of MINET. In the meantime, various enhancements to Version 1 are to be made, so as to improve on the system modeling capabilities. This intermediate version of MINET will be designated Version 1A, as the name "Version 2" is to be reserved for the version that includes the control system models.

The model enhancement currently in process is a trapped cover gas option for the MINET volume module. This model will be useful for 1) BOP tanks where air is normally trapped above a region of subcooled water and 2) sodium loops where gas (e.g., argon) is trapped above sodium. A major objective of this effort is to incorporate the appropriate models without significantly perturbing Version 1 of MINET. A formulation has been worked out that looks a great deal like the volume formulation already in MINET, and incorporation of the trapped cover gas option into the code will begin shortly.

Designs for two major extensions for Version 2 of MINET, i.e., the control system model and the rotor module have been completed and await implementation in the code. Several improvements to the current modules, such as height dependent area and port orientation (i.e., angle from vertical) for the volumes, are also currently envisioned.

3.2 MINET Code Improvements (G. J. Van Tuyle, T. C. Nepsee)

Several relatively minor adjustments and improvements are being made in preparation for exporting Version 1 of MINET. A plotfile option has been incorporated in order to output values for plotting. As plot-support computer software tends to vary between systems, the program that reads data from the planned MINET plotfile and generates the time (t) vs. f(t) plots may not be exportable, in general. An effort is also underway to purge the MINET program library of other system dependent routines, which were used in the testing process.

The MINET input processor error testing has been upgraded to include bounds test for both REAL and INTEGER input data types. Tests are performed for each field value as it is read, allowing error messages to be printed as part of the input data listing. This places the messages close to the source of the errors, making it easier for the user to debug the input. As a further enhancement, the allowable data range will be explicitly printed for each field in error.

A set of comprehensive data option tests is now in the coding phase. Their purpose is to define optional and default data values in addition to detecting missing data.

Several other areas of input data error testing and verification are also now being upgraded. These include

- Network connectivity tests to identify unconnected module ports
- Missing data tests
- Consistency tests for optional data

These upgrades will be included in the first MINET export version.

We are in the process of incorporating a set of fluid properties for helium, so helium would become the fifth fluid type available in MINET simulations (H_2O, Na, NaK, Air). Helium is one coolant type being discussed for advanced reactor designs under consideration, and incorporation of helium properties into MINET will thus increase the flexibility of SSC/MINET in simulating advanced reactor systems.

3.3 MINET Standard Input Decks (G. J. Van Tuyle, J. Guillen)

For Version 0 of MINET, executing with SSC Cycle 41, two standardized input decks are being maintained. MINET Deck E1, already tested against plant transient data, is being used to further test the combined SSC/MINET representation of the EBR-II facility. Deck S3, used in development and testing of the SNR-300 control system representation, is kept available for further analysis pending feedback from German engineers.

MINET Decks X1, X2, E1, and BF1 were used to test recently created Version 1.8 of MINET. All decks for stand-alone MINET have been updated to run with Version 1.8.

In order to provide attendees of the MINET code workshop (8/23 and 8/24) with hands-on experience using the code, we developed a sample problem which exercised several of the code capabilities and options. This deck is to be standardized as MINET deck SP1, and will be maintained for further use as a teaching tool.

Our recent efforts have been focused on simulating the Browns Ferry feedwater, High Pressure Coolant Injection (HPCI), and Reactor Core Isolation Cooling (RCIC) systems. The initial deck, BF1, was designed to simulate the latter portion of the feedwater train, but contained many estimates regarding the system design and behavior. A second deck, recently documented as MINET Standard Deck BF2, was created by adding representations for the HPCI and RCIC systems to the BF1 deck. A third deck, recently documented as Deck BF3 (see Figure 3.1), includes only the line from the junction where the HPCI and RCIC lines join the feedwater line. This BF3 deck contains almost no guesswork and is to be used in the combined RAMONA/MINET representation until more detailed decks can be improved and checked out. A fourth deck, to be designated BF4, was created from deck BF2 by eliminating the feedwater train representation, leaving the HPCI and RCIC representation. Because much more information is available on the HPCI and RCIC systems than the feedwater train, deck BF4 is currently more usable than BF1 or BF2.

In developing our Browns Ferry decks we are confronted with a shortage of information about the plant design, a problem that is likely to recur with other plants. This is occurring because much of the BOP was not included in prior plant safety analysis, and important design data have not been placed into Safety Analysis Reports or other open literature sources. We are currently compiling a list of information needed for Browns Ferry, and will need to seek help from TVA.

3.4 MINET Validations and Applications (G. J. Van Tuyle, E. G. Cazzoli, J. Guillen)

The initial RAMONA/MINET interface, through the feedwater line, has been completed and we are beginning to look at differences in the results between RAMONA/MINET and those generated by RAMONA alone. In applying RAMONA standalone, the user either specifies the feedwater flow and temperature vs. time or requests a control system representation. When the RAMONA control system option is invoked, the feedwater temperature (into the vessel) is switched (to room temperature) as soon as HPCI and RCIC come on line. Essentially, this instantly converts all the water in the feedwater line from 464 K to 293 K. In Browns Ferry this piping run is 70 meters long, and it causes a transport delay of nearly 1 1/2 minutes at combined HPCI and RCIC flow rates. When using the RAMONA/MINET combined representation, we have developed MINET Deck BF3 to account for this delay (see Figure 3.1). We are still working to quantify the results of this change in the representation. It should be noted that much of the important SASA analysis performed using RAMONA was done with table-driven feedwater flows and temperatures obtained from more detailed thermal hydraulic analysis. Thus, these runs were not affected by the missing transport delay.

When advancing in time, RAMONA-3B; 1) uses a predictor approach in computing neutronics transient steps, 2) waits for thermohydraulics to reach the same point in time, and then 3) corrects the neutronics results. A back step is taken if predicted - corrected values do not agree within an acceptance criterion. Provisions were made for MINET to be able to step back at the same time and "restart" from known values.

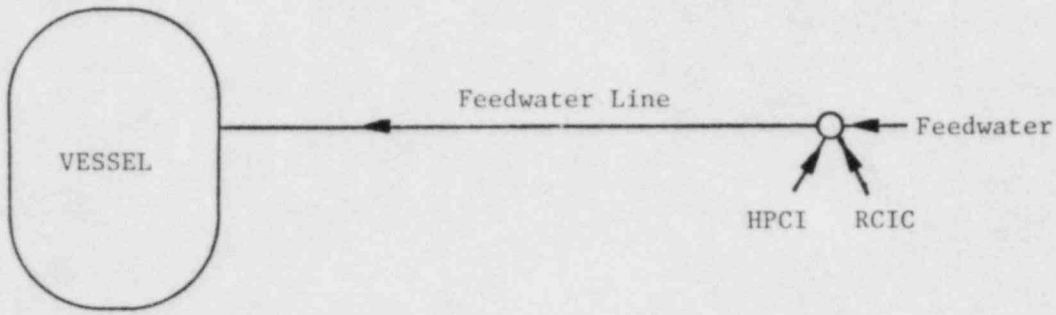

Figure 3.1 MINET Deck BF3 Modules

An improved restart capability was also added to RAMONA, making it possible to save data at a user-specified frequency; the same capability has been extended to the interface with MINET.

We have completed a preliminary design for the second RAMONA/MINET interface through the safety/relief valve line. Once this interface is completed, representation of the pressure suppression pool will be possible.

3.5 User Support (G. J. Van Tuyle, T. C. Nepsee, J. G. Guppy, W. C. Horak, J. Guillen, E. G. Cazzoli)

We hosted our first MINET code workshop on August 23 and 24, during which the MINET models and coding were discussed at length. A sample problem was utilized to better familiarize attendees with the code. The response of the attendees was quite positive with respect to both the MINET code and the workshop, and we expect to be exporting the code in the coming weeks.

One immediate benefit on the workshop is that we received a considerable amount of useful feedback from the attendees. Among the various items of interest were:

1) They considered the MINET code to be very user-friendly, and suggested ways to make it even more so. Those from industry suggested an option whereby input and output could be in British Units, as SI units are relatively unfamiliar to them. We feel that many of the suggested changes can be implemented as time permits.

2) Our plans to develop a module that will read the MINET input deck and draw a schematic diagram of the system (as specified) received very strong interest. While this option will take some time to implement, it may well be worth the effort.

3) There was wide-spread agreement that a simulator assessment effort is overdue, as there is considerable doubt about the accuracy of these machines when conditions are off-normal. Use of MINET for such assessment was considered to be a logical application.

4) The interface between RAMONA and MINET and other potential interfaces proved to be very interesting to the attendees. One feature of great interest is that the host code is virtually unaffected by the interface, and a code's capabilities can be extended without the arduous process of re-establishing the accuracy of the code with the NRC. This is very important with the licensing codes, which are currently almost untouchable.

We expect to be sending out two copies of MINET, Version 1 in the near future, one to a utility and one to a nuclear steam supply system vendor. The utility is already using the RAMONA code, and has expressed interest in executing the composite RAMONA/MINET as well as the stand-alone MINET code.

REFERENCES

GUPPY, J. G., et al., (1984), "Generic Balance of Plant Modeling," Safety Research Programs Sponsored by Office of Nuclear Regulatory Research Quarterly Progress Report, April 1 - June 30, 1984, Brookhaven National Laboratory Report to be published.

PUBLICATIONS

VAN TUYLE, G. J., NEPSEE, T. C., GUPPY, J. G., "MINET Code Documentation, "Brookhaven National Laboratory, NUREG/CR-3668, BNL-NUREG-51742, February 1984.

VAN TUYLE, G. J., "Simulation of a Helical Coil Sodium/Water Steam Generator, Including Structural Effects," Brookhaven National Laboratory, NUREG/CR-3765, BNL-NUREG-51766, April 1984.

VAN TUYLE, G. J., "MINET Validation Study Using EBR-II Transient Data," Second Proceedings of Nuclear Thermal Hydraulics, 1984 ANS Annual Meeting, New Orleans, June 1984.

VAN TUYLE, G. J., et al., "Analysis of Postulated BWR ATWS for the Brown's Ferry Plant Using RAMONA/MINET," Brookhaven National Laboratory Report to be published.

VAN TUYLE, G. J., "MINET Validation Study Using Steam Generator Transient Data," Brookhaven National Laboratory , NUREG/CR-3813, BNL-NUREG-51775, May 1984.

VAN TUYLE, G. J., "MINET Validation Study Using Steam Generator Test Data," Proceedings of the International Conference on Power Plant Simulation, Cuernavaca, Mexico, November 19-21, 1984. To be published.

4. Thermal-Hydraulic Reactor Safety Experiments

4.1 Core Debris Thermal-Hydraulic Phenomenology: Ex-Vessel Debris Quenching

(T. Ginsberg, N. K. Tutu, J. Klein, J. Klages, C. E. Schwarz and Lianhei Wei)

During this quarter final reduction of the superheated debris bed quench data was performed. This included calculation of quench-front propagation speeds and average bed heat flux. A final report is in preparation.

In addition, the quench experiments were redone with beds of 1-mm steel particles. Analysis of prior 1-mm bed data had shown the heat balances (comparison of initial stored energy with integral of steam generation rate) to be inaccurate (2 by 30-40%). These experiments were reperformed. The results yielded heat balances which were accurate to within 5-10%. Calibration difficulties with the turbine flowmeter used in these experiments was the most likely cause of the early discrepancies.

4.2 Core Debris Thermal-Hydraulic Phenomenology: In-Vessel Debris Quenching

(N.K. Tutu, T. Ginsberg, J. Klein, J. Klages and C.E. Schwarz)

The purpose of this task is to develop an understanding of the transient quenching of in-vessel debris beds (formed in the reactor core region) when the coolant is injected from below. The experimental results would, in addition, generate a data base for verifying the transient thermal-hydraulic models for the quenching process. The present experimental and model development effort is directed towards the case where the coolant is being injected at a constant rate.

4.2.1 Modifications in Experimental Facility and Instrumentation

The first series of debris bed quench experiments with bottom-flood were performed with a debris bed height of 0.42 meters. In order to verify the change in quench behavior due to the variation in bed height as predicted by the transient model, the debris bed height for the next series of experiments will be doubled. This required several modifications in the test apparatus, and these have been accomplished.

To find out the actual instantaneous rate of heat loss experienced by the solid particles (3.18-mm stainless steel spheres) during the quenching process, special thermocouple probes, with the thermocouple junction inside the particle, were fabricated as follows. First, a 0.8-mm-diameter and 1.59-mm-deep hole was drilled into the spherical particle. Next, a grounded junction Chromel-Alumel thermocouple with a 0.79-mm-diameter stainless steel sheath was inserted into the hole. This assembly was held in a copper jig which exposed only the top portion of the stainless steel sphere. By using the helium-arc welding process the sphere was then heated to its melting point in order to get a good thermal bond between the thermocouple and the sphere interior. The "particle" thermocouples formed in this manner were tested by the following procedure. The thermocouples were superheated to an initial temperature in excess of 650 K, and were then quenched in a saturated pool of water. Figure 4.1 shows the temperature transient for one of the thermocouples. Assuming

the particle temperature to be uniform, the temperature transient can be used to construct the "transient boiling curve." This is shown in Figure 4.2. We see that the film boiling regime and the transition boiling regime are clearly delineated. This indicates that the thermocouple junction is indeed within the particle interior. Four of these thermocouples will be used in the next series of debris bed quench experiments. The temperature history from these thermocouples should help us in the modeling of local solid-fluid heat transfer coefficients.

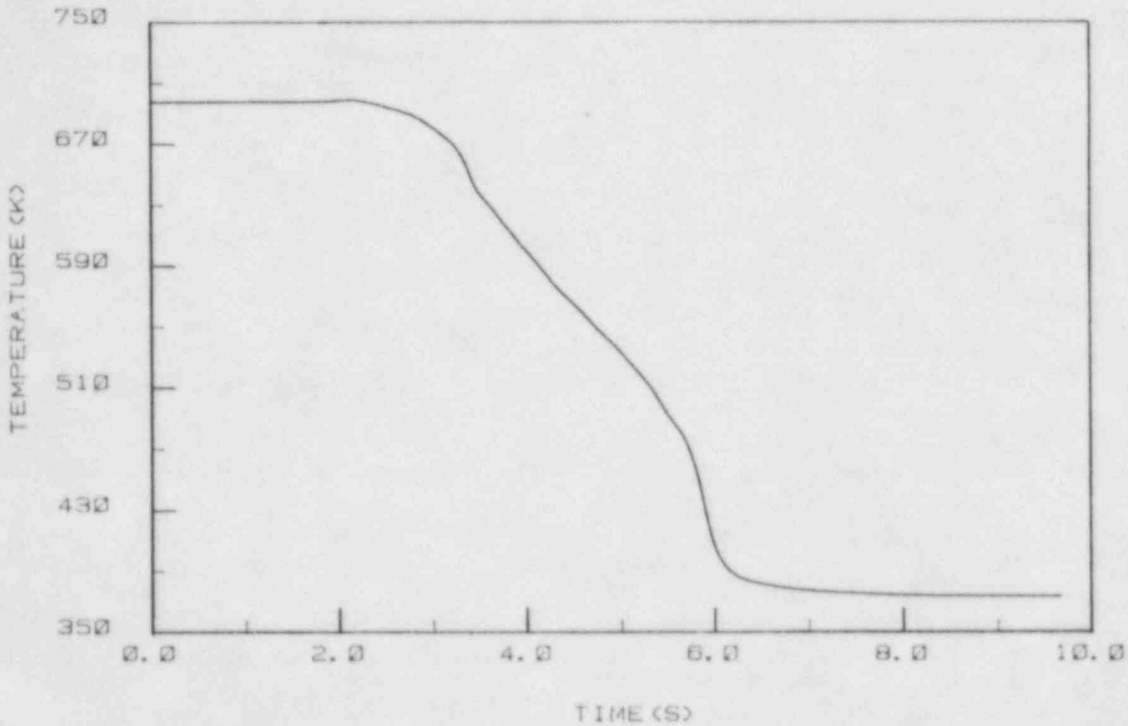

Figure 4.1 Transient Temperature History of a Particle Thermocouple Being Quenched in a Saturated Pool of Water

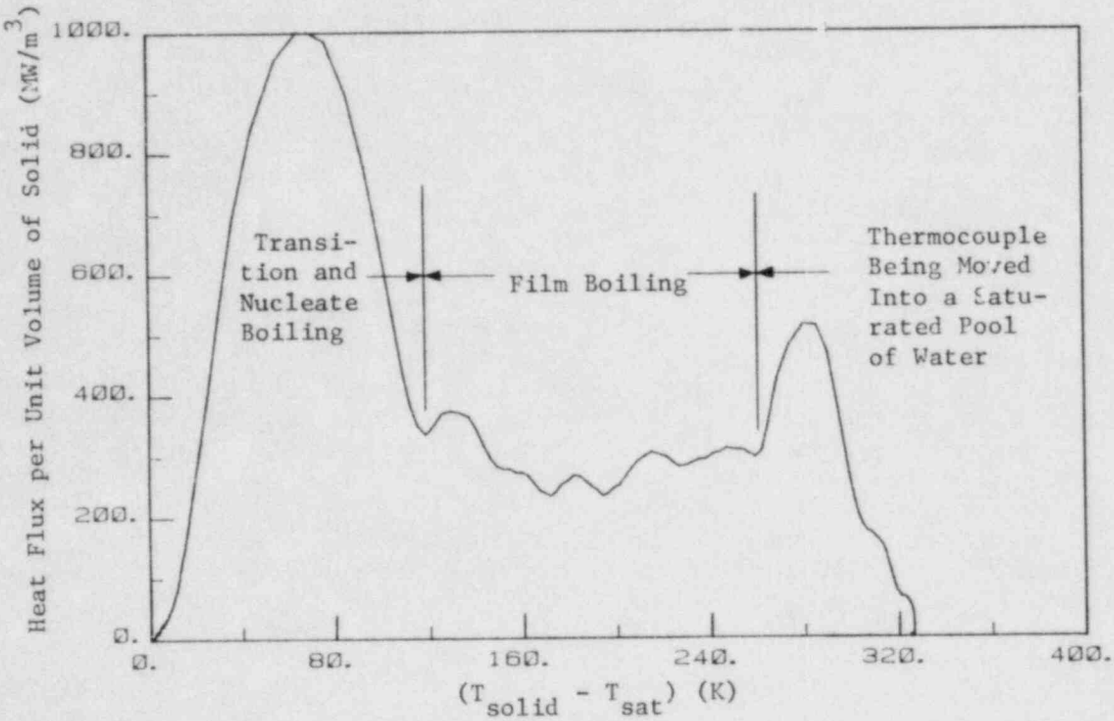

Figure 4.2 Instantaneous Volumetric Heat Flux as a Function of Particle Superheat. Particle Being Quenched in a Saturated Pool of Water.

4.3 Core-Concrete Heat Transfer Studies: Coolant Layer Heat Transfer (G.A. Greene and T.F. Irvine, Jr. (SUSB))

The purpose of this task is to study the mechanisms of liquid-liquid boiling heat transfer and its effect on the ex-vessel attack of molten core debris on concrete. This effort is in support of the CORCON development program at Sandia National Laboratories.

4.3.1 Analysis of Experimental Data

Analysis of the compiled R11/liquid metal and H_2O/liquid metal liquid-liquid film boiling data continued. The tests with R11 as the boiling fluid include a large number of two-phase boiling experiments with noncondensable gas blowing from below to simulate the effect of concrete decomposition gases bubbling through the melt-coolant interface.

So far the boiling heat flux data with R11 and without gas bubbling lie, on the average, approximately twenty percent higher than the Berenson

model predictions of the data. The boiling heat flux appears to increase linearly with the gas superficial velocity over the range of the experiments performed. However, the experiments always remained in the stable boiling regime and no vapor explosions occurred with R11. With the liquid metal pools used, the melts were observed to cool isothermally throughout and freeze suddenly, suggesting that formation of a slurry may be the dominant mode of solidification of a metal melt.

4.3.2 Experimental Development

A series of liquid-liquid film boiling experiments with water as the boiling fluid were begun (Series 300). These experiments do not yet include the effect of gas bubbling. In the first two tests, Runs 301 and 302 with Wood's metal, minor steam explosions occurred early in the tests, terminating the data acquisition. The visual observations of violent boiling and splashing substantiate early observations of intense liquid-liquid contact and unstable film boilng. It has been suggested that some form of nucleate boiling is being induced in these tests in spite of the high initial melt temperature, possibly due to surface oxidation. Although considered unlikely, this explanation is being pursued. However, it is clear that the data exceed the Berenson model by a significant margin, as much as a factor of five or more, for water boiling on liquid metal melts, and that Berenson is not applicable under such conditions. Also, under such conditions, steam explosions must be considered when analyzing such occurrences as containment pressurization, direct heating of the containment, and release of fission products from the melt.

5. Development of Plant Analyzer
(W. Wulff)

5.1 Introduction

This program is being conducted to develop an engineering plant analyzer, capable of performing accurate, real-time and faster than real-time simulations of plant transients and Small-Break Loss of Coolant Accidents (SBLOCAs) in LWR power plants. The engineering plant analyzer is being developed by utilizing a modern, interactive, high-speed, special-purpose peripheral processor, which is designed for time-critical systems simulations. The engineering plant analyzer primarily supports safety analyses, but it also serves as the basis of technology development for nuclear power plant monitoring, for on-line accident diagnosis and mitigation, and for upgrading operator training programs and existing training simulators.

Originally, there were three activities related to the LWR Plant Analyzer Development Program; namely, (1) the assessment of the capabilities and limitations of existing simulators for nuclear power plants, (2) the selection and acquisition of a special-purpose, high-speed peripheral processor suitable for real-time and faster than real-time simulation of power plant transients, and (3) the development of mathematical models and the software for this peripheral processor.

Below is a brief summary of previous results and a detailed summary of achievements during the current reporting period.

5.2 Assessment of Existing Training Simulators (W. Wulff and H. S. Cheng)

The assessment of then current simulator capabilities consisted of evaluating qualitatively the thermohydraulic modeling assumptions in the training simulator and comparing quantitatively the predictions from the simulator with results from the detailed systems code RETRAN.

The results of the assessment have been published earlier in three reports (Wulff, 1980; Wulff, 1981a; Cheng and Wulff, 1981). It had been found that the reviewed training simulators were limited to the simulation of steady-state conditions and quasi-steady transients within the parameter range of normal operations. Most PWR simulators delivered before 1980 cannot simulate two-phase flow conditions in the primary reactor coolant loops, nor the motion of the two-phase mixture level beyond the narrow controls range in the steam generator secondary side. Most BWR simulators delivered before 1980 cannot simulate two-phase flow conditions in the recirculation loops or in the downcomer and lower plenum, nor can they simulate coolant level motions in the steam dome, the lower regions of the downcomer (below the separators), or in the riser and core regions. These limitations arise from the lack of thermohydraulic models for phase separation and mixture level tracking (Wulff, 1980; 1981a).

The comparison between PWR simulator and corresponding RETRAN results, carried out for a reactor scram from full power, showed significant discrepancies for primary and secondary system pressures and for mean coolant temperatures of the primary side. The discrepancies were found even after the

elimination of differences in fission power, feedwater flow and rate of vapor discharge from the steam dome. Good agreement was obtained between simulator and RETRAN calculations for only the early part (narrow control range) of the water level motion in the steam generator. The differences between simulator and RETRAN calculations have been explained in terms of modeling differences (Cheng and Wulff, 1981).

5.3 Acquisition of Special-Purpose Peripheral Processor and Ancillary Equipment (A.N. Mallen, R.J. Cerbone and S.V. Lekach)

The AD10 had been selected earlier as the special-purpose peripheral processor for high-speed, interactive systems simulation through integrating large systems of nonlinear ordinary differential equations. A brief description of the processor has been published in a previous Quarterly Progress Report (Wulff, 1981b). A PDP-11/34 DEC computer serves as the host computer.

Two AD10 units, coupled directly to each other by a bus-to-bus interface and equipped with a total of one megaword of memory, have been installed with the PDP-11/34 host computer, two 67 megabyte disc drives, a tape drive and a line printer. On-line access is facilitated by a model 4012 Tektronix oscilloscope terminal and a 28-channel signal generator. The system is accessed remotely via four ADDS CRT terminals and two DEC Writer terminals, one also equipped with a line printer. An IBM Personal Computer will also be used to access the PDP-11/34 host computer, but is now used primarily to generate labelled, multicolored graphs from AD10 results. An advanced multicolor graphics terminal is needed, however, for extensive on-line display of simulated parameters generated by the AD10 at real-time for faster computing speeds.

5.4 Model Implementation on AD10 Processor and Developmental Assessment

A four-equation model for nonhomogeneous, nonequilibrium two-phase flow had been formulated and supplemented by constitutive relations from an existing BWR reference code, then scaled and adapted to the AD10 processor to simulate the Peach Bottom-2 BWR power plant (Wulff, 1982a). The resulting High-Speed Interactive Plant Analyzer code (HIPA-PB2) has been programmed in the high-level language MPS10 (Modular Programming System) of the AD10. After implementing the thermohydraulics of HIPA-PB2 on the AD10, we compared the computed results and the computing speed of the AD10 with those of the CDC-7600 mainframe computer, to demonstrate the feasibility of achieving engineering accuracy at high simulation speeds with the low-cost AD10 minicomputer (Wulff, 1982b).

It has been demonstrated (Wulff, 1982b) that (i) the high-level, state equation-oriented systems simulation language MPS10 compressed 9,950 active FORTRAN statements into 1,555 calling statements to MPS10 modules, (ii) the hydraulics simulation occupies one-fourth of available program memory, (iii) the difference between AD10 and CDC-7600 results is only approximately $\pm 5\%$ of total parameter variations during the simulation of a severe licensing base transient, (iv) the AD10 is 110 times faster than the CDC-7600 for the same transient, and (v) the AD10 simulates the BWR hydraulics transients up to 10 times faster than real-time process speed. It has been demonstrated now that even after the inclusion of models for neutron kinetics, conduction, balance

of plant dynamics and controls, the AD10 still achieves 10 times real-time simulation speed for all transients reported earlier (Wulff, 1983c).

The HIPA-PB2 hydraulics program used earlier for the feasibility demonstration has been expanded to simulate neutron kinetics (point kinetics), thermal conduction in fuel elements and the thermohydraulics of the components of the balance of plant shown in Figure 5.1. The expanded version is called HIPA-BWR/4 and is capable of simulating all BWR/4 reactor plants.

The stand-alone program modules for neutron kinetics with reactivity feedback and automatic reactor trips, for thermal conducton in fuel elements, for compressible flows in the steam line and for the control logic for operating the safety and relief valves tested earlier (Wulff, 1982c; 1983a) have been implemented in HIPA-BWR/4. Models had been formulated and tested separately for the control and plant protection systems and the plant components forming a closed loop through turbines, condensers and the feedwater trains.

During the previous reporting period, the boron tracking model (Wulff, 1983d) had been implemented first as a stand-alone module (Wulff, 1984a). This module is now part of HIPA-BWR/4.

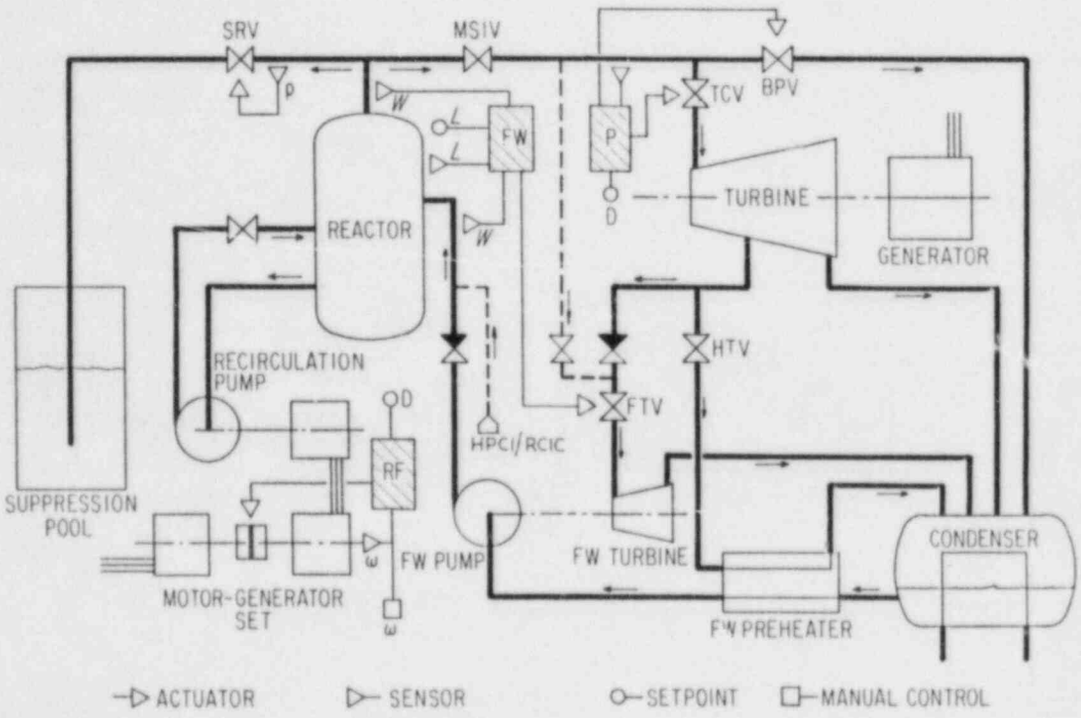

Figure 5.1 Flow Schematic and Control Blocks for BWR Simulation; FW - Feedwater Controller, P - Pressure Controller, RF - Recirculation Flow Controller

The graphics capabilities had been significantly enhanced during the previous reporting period to allow now the on-line display of two parameter variations versus time on the four-color monitor of the IBM PC. The parameters are displayed in separate colors on labelled diagrams. Also, a Local Area Network has been assembled to display on-line simulation results from the plant analyzer in a remote conference room (Wulff, 1984a).

Earlier, we presented results from the developmental assessment of the plant analyzer. We compared plant analyzer results with GE calculations (Wulff, 1984) and with calculations from the systems codes TRAC-BD1, RELAP5 and RAMONA-3B (Wulff, 1984a). We also established proper plant analyzer performance, where no best-estimate simulations were available, by comparison with FSAR results (Wulff, 1984a). The comparisons show that the plant analyzer simulates, reliably and accurately, a large number of severe abnormal transients in a BWR power plant, and that it produces the same results as TRAC-BD1, RELAP5 and RAMONA-3B but at a considerably lower cost and in much shorter time. We have demonstrated that the BNL Plant Analyzer can simulate 37 different transients in less than four days.

Specific accomplishments of the current reporting period are described below in Sections 5.5 and 5.6.

5.5 Further Model Improvements

5.5.1 Reactor Shutdown by Boron Injection (H.S. Cheng)

The previously tested boron transport model (Wulff, 1983d and 1984b) has been incorporated into the HIPA-BWR/4 code and successfully executed. Figure 5.2 shows for an Anticipated Transient without Scram (ATWS) after Main Steam Isolation Valve (MSIV) Closure, the boron concentration and the boron reactivity. Notice that the boron concentration in the core increases every time when the boron front reenters the core after circulating through the vessel. Figure 5.3 shows in the lower curve the transient fission power, peaking first at 210% of full power then oscillating under the influence of pressure-induced flashing and condensing in the core and, finally after approximately 1,330 seconds (22 minutes), dropping off to zero when the boron concentration becomes high enough. The system pressure is shown as the upper curve. As expected, the pressurization rate decreases as the heating power reduces from fission to decay heating and, consequently, the period of valve cycling increases.

Notice that the boron transport model in the plant analyzer does not involve any numerical integration. Instead, the plant analyzer evaluates dynamically the results from analytical integrations, using the liquid phase velocity as computed from the hydraulics simulation.

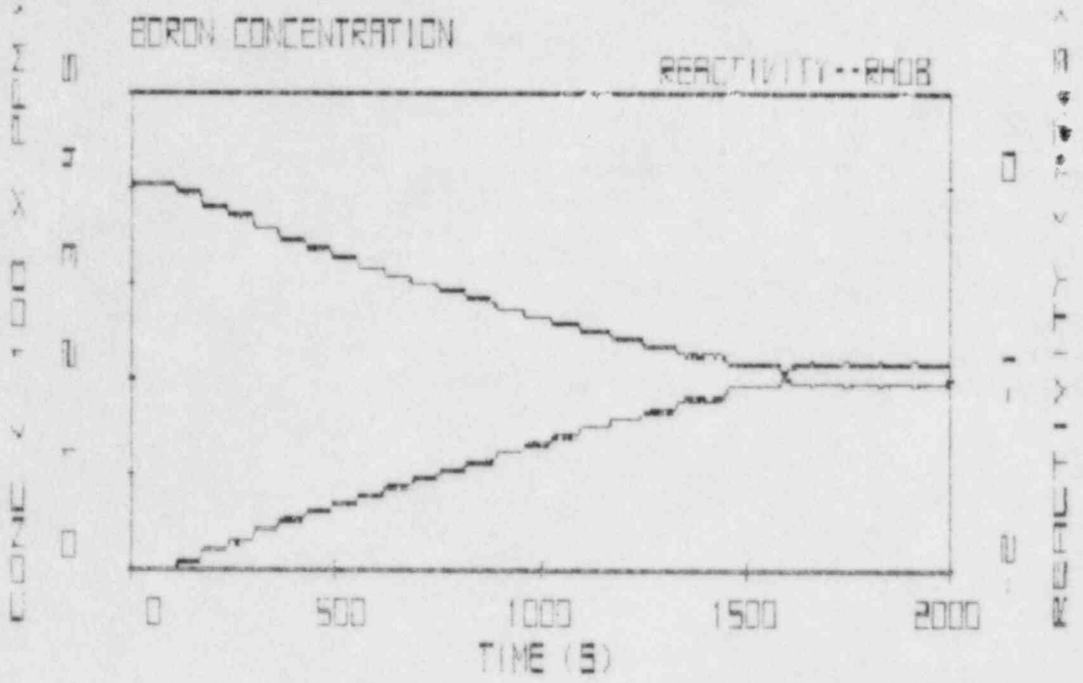

Figure 5.2 Boron Reactivity and Boron Concentration for MSIV-Induced ATWS

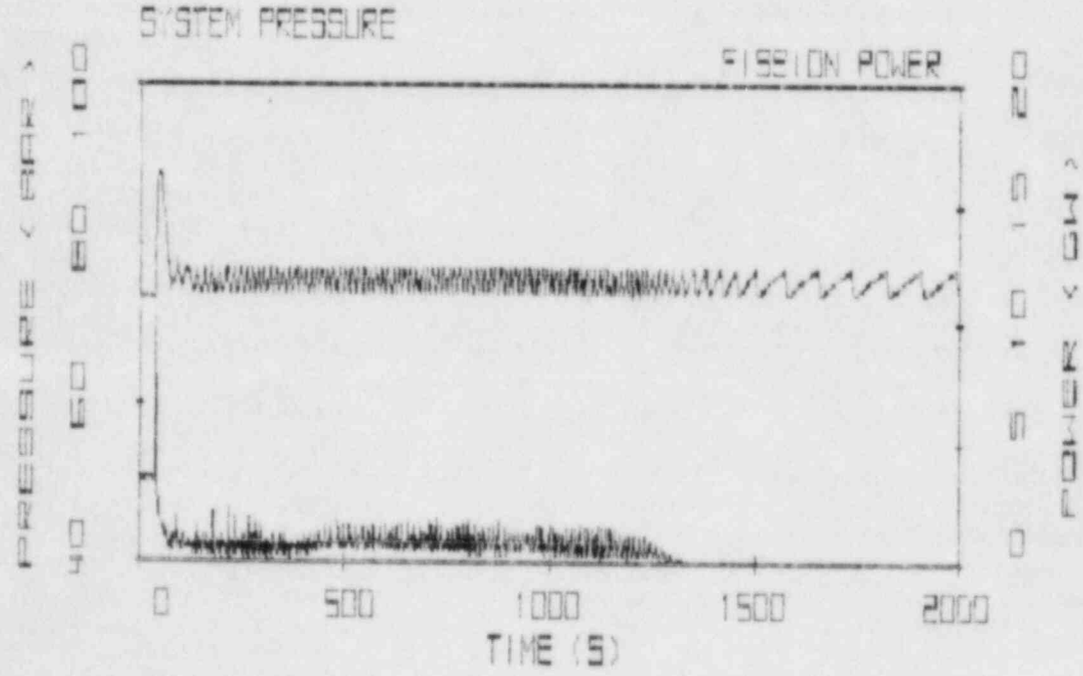

Figure 5.3 Fission Power and System Pressure for MSIV-Induced ATWS with Boron Injection

5.5.2 Modeling of Flow Reversal (H.S. Cheng and W. Wulff)

Vapor mass and phasic energy fluxes have been related to cell-averaged properties via donor-cell type relationships for both forward and backward flow conditions. This has been carried out to account properly for the transport of vapor mass and phasic energies and to maintain numerical stability for normal and reverse flows. Notice that the mixture mass and momentum balances have been integrated analytically and are therefore valid for both flow directions without special attention.

The phasic mass flux W_k, k=g (for vapor) and k=ℓ (for liquid) is computed for the cell boundary with index i from

$$(W_k)_i = \frac{1}{2}\left[(W_k)_{i(i)} + \left|(W_k)_{i(i)}\right| + (W_k)_{i(i+1)} - \left|(W_k)_{i(i+1)}\right|\right], \tag{5.1}$$

where

$$(W_k)_{i(i)} = W_k(\langle j_m\rangle_i , \bar{\alpha}_i)$$
$$(W_k)_{i(i+1)} = W_k(\langle j_m\rangle_i , \bar{\alpha}_{i+1}) \tag{5.2}$$

are the mass flow rates computed according to the drift flux model, with the area-averaged volumetric flux $\langle j_m\rangle_i$ at the i-th cell boundary and with the upstream (i) and downstream (i+1) cell-averaged void fractions $\bar{\alpha}$. Equation 5.1 guarantees continuity of $(W_k)_i$ while it changes sign. Notice that during a sign change of $(W_k)_i$, i.e., during flow reversal at a cell boundary, $(W_k)_i$ assumes temporarily the mean value between $(W_k)_{i(i+1)}$ and $(W_k)_{i(i)}$ if $(W_k)_{i(i)} > (W_k)_{i(i+1)}$, or it is temporarily zero if $(W_k)_{i(i)} < (W_k)_{i(i+1)}$. The transition period begins always when the first sign change occurs on either $(W_k)_{i(i)}$ or $(W_k)_{i(i+1)}$. The transition terminates when both mass flow rates have undergone a sign change.

This method has been successfully implemented in HIPA-BWR/4.

5.5.3 Level Tracking in Downcomer (A. Stritar and W. Wulff)

As the mixture level falls from the steam dome into the downcomer, a new flow pattern appears in the downcomer. The return flow from the separators discharges no longer into the two-phase mixture below the level, but instead, it falls as a liquid film along the stand pipes and the core shroud and then across the mixture level. A new model is being implemented to track the mixture level on the basis of the drift flux model and the mass jump conditions.

With the positive z-axis pointing upward, the liquid volumetric flux entering the downcomer is

$$(j_\ell)_{DCI} = (j_\ell)_{RSE} - V_{DOM}\langle\Gamma_V\rangle_{DOM} , \tag{5.3}$$

where $(j_\ell)_{RSE}$, V_{DOM} and $\langle\Gamma_V\rangle_{DOM}$ are, respectively, the volumetric flux of liquid discharged from the separators, the vapor volume in the dome and the mass transfer rate (positive for evaporation) for the dome.

The volumetric flux of the mixture at the downcomer entrance, $(j_m)_{DCI}$ is computed, as before, from the three loop momentum and the flux divergence equation. The void fraction above the level, $\langle\alpha\rangle_{up}$, is computed from Ishii's drift velocity correlation for annular flow (Ishii, 1977) (derived from the two-fluid momentum balances) by solving this implicit equation

$$[1+75(1-\langle\alpha\rangle_{up})][(1-\langle\alpha\rangle_{up})(j_m)_{DCI} - (j_\ell)_{DCI}] =$$

$$\langle\alpha\rangle_{up}^3 \frac{\rho_f}{\rho_g} \frac{(j_\ell)_{DCI}\left|(j_\ell)_{DCI}\right|}{\sqrt{\langle\alpha\rangle_{up}}} + 66.7(1-\langle\alpha\rangle_{up})^3 \frac{\rho_f-\rho_g}{\rho_g \sqrt{\langle\alpha\rangle_{up}}} gd_h \qquad (5.4)$$

iteratively for $\langle\alpha\rangle_{up}$. Here, the symbols ρ_f, ρ_g, g and d_h designate, respectively, liquid and vapor densities, gravitational constant and hydraulic diameter.

The result of Eq. 5.4 and the cell volume-averaged vapor void fraction $\bar{\alpha}$, known from the vapor mass balance, are used, along with the level position Z, to compute the void fraction below the level, $\langle\alpha\rangle_{\ell o}$. The level position Z is defined by the integral of the vapor mass jump condition

$$\frac{dZ}{d\tau} = \frac{(j_g)_{up} - (j_g)_{\ell o}}{\langle\alpha\rangle_{up} - \langle\alpha\rangle_{\ell o}} , \qquad (5.5)$$

where the vapor volumetric fluxes, $(j_g)_{up}$ and $(j_g)_{\ell o}$, above and below the level, respectively, are computed, via drift flux relations from the known void fractions $\langle\alpha\rangle_{up}$ and $\langle\alpha\rangle_{\ell o}$, and from the mixture mass jump condition

$$(j_m)_{up} = (j_m)_{\ell o} . \qquad (5.6)$$

This model has been implemented and is being checked out at this time.

5.6 Simulation for Emergency Procedure Guidelines (H.S. Cheng and S.V. Lekach)

5.6.1 Purpose

An anticipated transient without scram (ATWS) has been of concern because of its potentially severe consequences, even though it is an extremely unlikely event. In this transient, the only mechanism for removing energy from the reactor pressure vessel (RPV) is the steam discharge through safety and relief valves, which results in a heating up of the suppression pool water. In a boiling water reactor (BWR), if the suppression pool temperature exceeds the heat capacity limit, it could induce a severe vibration which might threaten the integrity of the reactor containment. Thus, the reactor power must be reduced during an ATWS in order to preserve the containment integrity.

Under the proposed Emergency Procedure Guidelines (EPG) for the ATWS event by the BWR owner's group, the RPV water level and pressure would be lowered to reduce the reactor power, thereby minimizing the heat dumped into the suppression pool. Steady-state analyses have been made to evaluate the degree of power reduction that can be achieved by reducing the RPV water level and system pressure (Chexal, 1984). The purpose of the present work is to provide a dynamic analysis of the EPG, using the complete system simulation code HIPA-BWR/4 in the plant analyzer.

5.6.2 Scope of Simulations

The scope of the present study covered the subject of interest to the EPG; namely, the effect of proposed operator actions regarding the level and pressure control on core power and flow.

The BWR analyzed in this study is a 251/764 BWR/4 (251-in. inside diameter pressure vessel with 764 fuel bundles) with a rated core thermal power of 3293 MW. The balance of plant including the control and protection systems is typical of a BWR/4 such as Browns Ferry 1.

The ATWS analyzed was assumed to be initiated by an inadvertent closure of all Main Steam Isolation Valves (MSIV) from full power operating conditions. Since the long-term behavior of the transient is of primary interest, the transient was run for 2000 seconds. Four cases were run:

Case 1 - This was the base case where the High Pressure Coolant Injection (HPCI) system, in conjunction with the Reactor Core Isolation Cooling (RCIC) system, automatically controlled the RPV level and the Safety/Relief Valves (SRV) controlled the pressure. No boron was injected into the RPV for reactor shutdown.

Case 2 - This was similar to the base case except that the RPV water level was lowered to just above the top of active fuel (TAF) by reducing the the HPCI flow rate from the control panel and the RPV pressure was controlled automatically by SRVs.

Case 3 - This was similar to the base case except that the RPV pressure was lowered manually to 4.8 MPa via the first bank of SRVs and the RPV water level was controlled automatically by the HPCI and RCIC systems with 100% flow capacity.

Case 4 - This was similar to the base case except that both RPV water level and pressure were lowered so that the level was just above the TAF and the pressure at 4 MPa.

5.6.3 Results of Simulations

The results for the base case (Case 1) are presented in Figures 5.4 and 5.5. It is clear that, without any mitigative actions, the system pressure and reactor power would experience a sustained oscillation for an extended period of time due to the continued valve cycling of the first bank of SRVs. Thus, the extended discharge of steam into the suppression pool would heat up the pool water temperature beyond the safe limit, and would, hence, threaten the integrity of the containment.

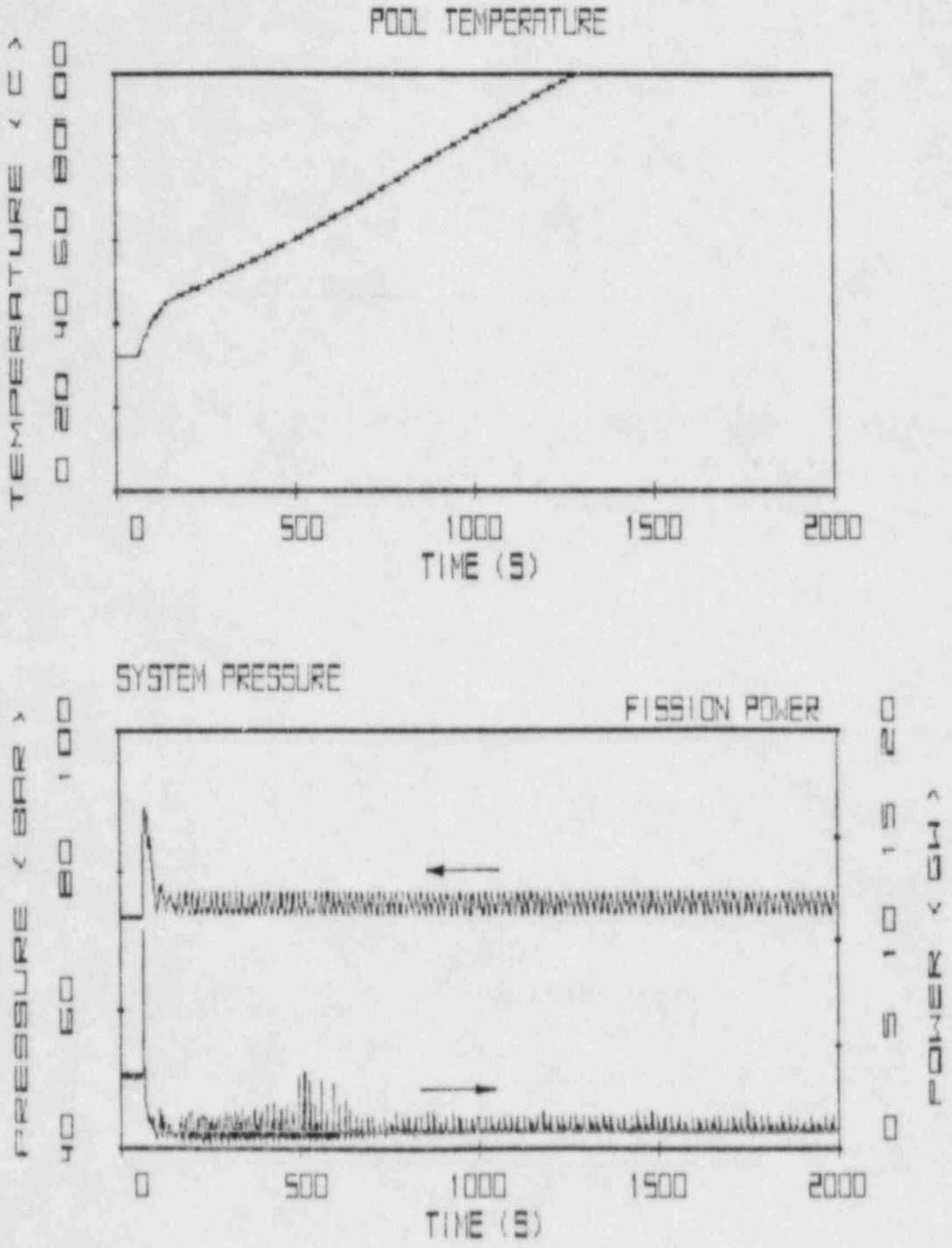

Figure 5.4 Results for Case 1: Top Graph is for Suppression Pool Temperature, Bottom Graph for System Pressure and Reactor Power

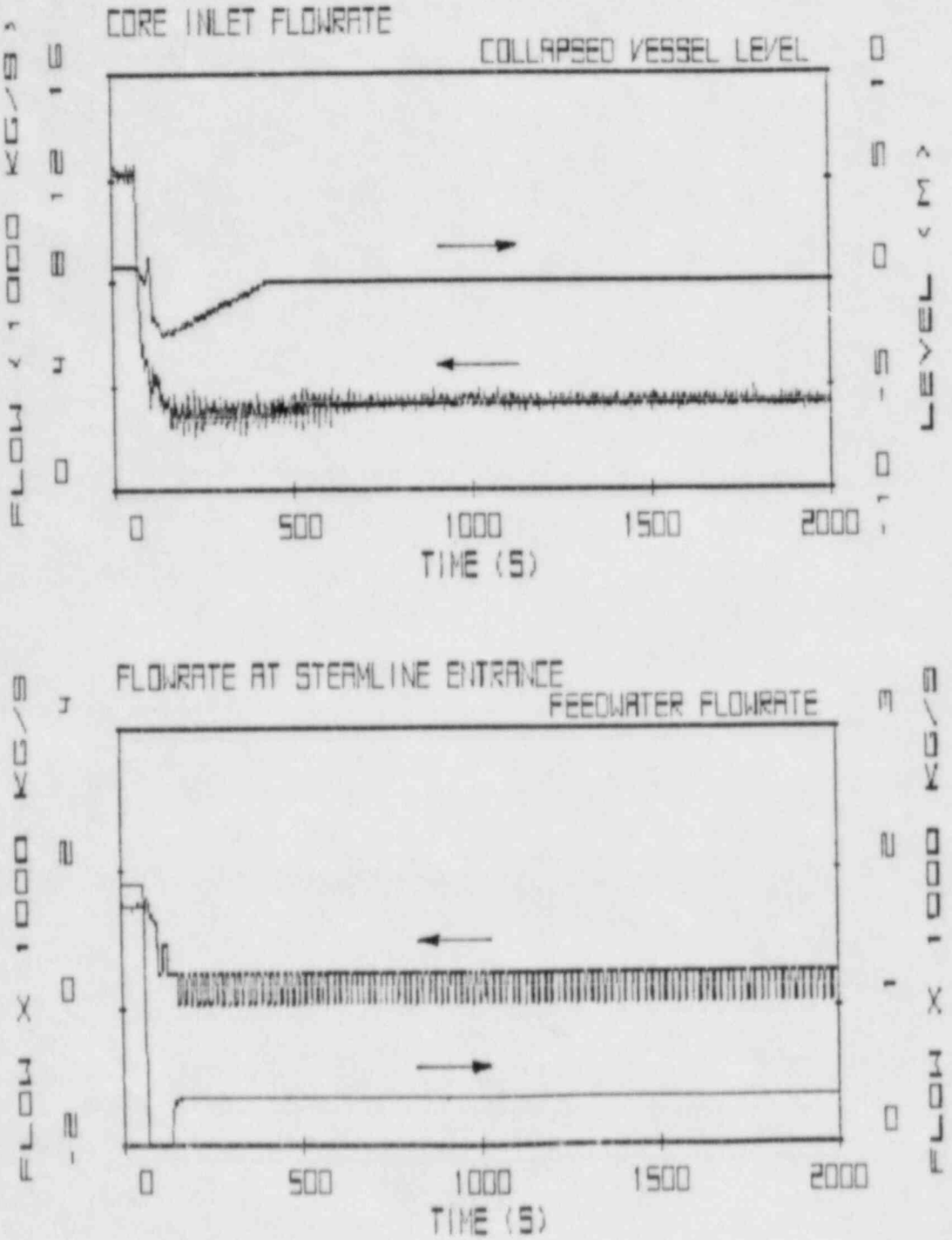

Figure 5.5 Results for Case 1: Top Graph is for Core Inlet Flow Rate and Collapsed Liquid Level, Bottom Graph for Steam Line Flow Rate and Feedwater Flow Rate

The results for Case 2 are shown in Figures 5.6 and 5.7. In this case, the RPV water level was kept just above the TAF by controlling the HPCI flow rate, while the system pressure was controlled automatically by the first bank of SRVs in accordance with its setpoints. This is the case of level control on core power and flow as proposed in the EPGs. We see a significant reduction in the fission power* and core inlet flow rate, which reduced the amount of steam discharged into the suppression pool and, thus, helped reduce the suppression pool water temperature.

The results for Case 3 are shown in Figures 5.8 and 5.9. In this case, the RPV pressure was lowered to about 4.8 MPa via partial opening of the first bank of SRVs, while the water level was controlled automatically by the HPCI and RCIC systems with full capacity. This is the case of pressure control on the core power and flow as proposed in the EPG. The results indicate that decreasing system pressure has a complex effect on core power and flow. At low flow conditions, the total core pressure drop is dominated by the elevation pressure drop in the core, which is proportional to the core liquid fraction or one minus void fraction. Therefore, the void fraction has a strong influence not only on core reactivity, but also on core pressure drop. Thus,

(a) As pressure is reduced, some liquid in the core flashes to vapor and the void fraction in the core increases. This introduces a negative void reactivity into the core to help reduce core power.

(b) On the other hand, the increase in core void fraction causes a decrease in total core gravity head. Thus, for a given water level in the downcomer, the driving head in the flow loop increases and flow through the core also increases which reduces the core void fraction. This introduces a positive void reactivity into the core, which tends to increase core power.

The net result of these two competing effects is apparently to increase slightly the core flow and to reduce very slightly the reactor power (compare Figures 5.8 vs. 5.4). Thus, the reduction in core power by reducing system pressure is insignificant without also lowering the water level at the same time. It should be noted that reducing system pressure by forcing partial opening of SRVs in this case has actually aggravated the suppression pool temperature (compare Figures 5.9 with 5.4). It seems unwise to reduce system pressure during an ATWS without also controlling the water level just above TAF.

The results for Case 4 are shown in Figures 5.10 and 5.11. In this case, both the system pressure and water level were lowered to control core power and flow. Again, the effect of reducing system pressure is complex. However, the combination of level and pressure controls did help reduce the core power significantly and the core flow slightly. Most of the power reduction apparently comes from the level control rather than the pressure control.

*Notice that Figures 5.6, 8 and 10 show fission power, without decay heat.

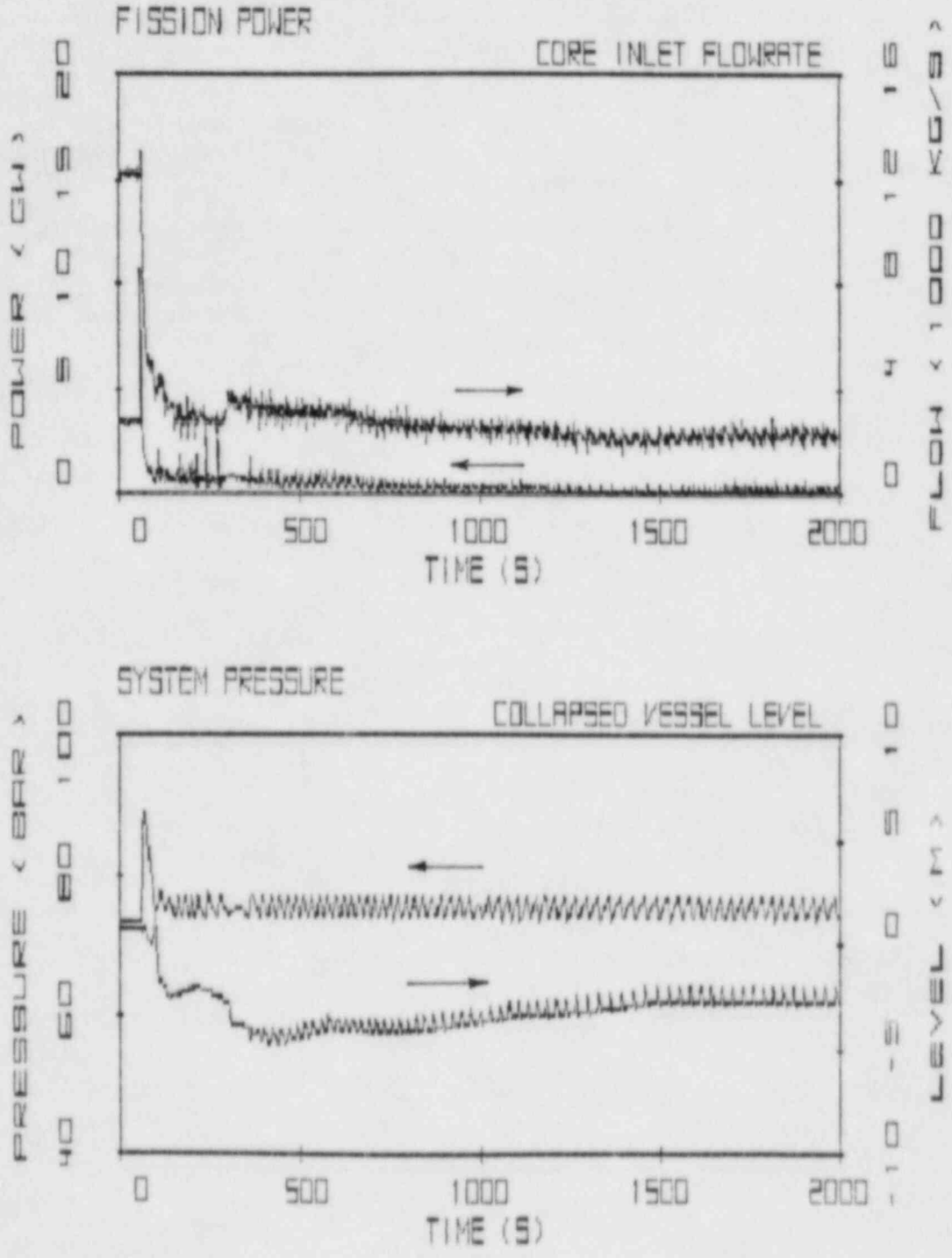

Figure 5.6 Results for Case 2: Top Graph is for Reactor Power and Core Inlet Flow Rate, Bottom Graph for System Pressure and Collapsed Liquid Level

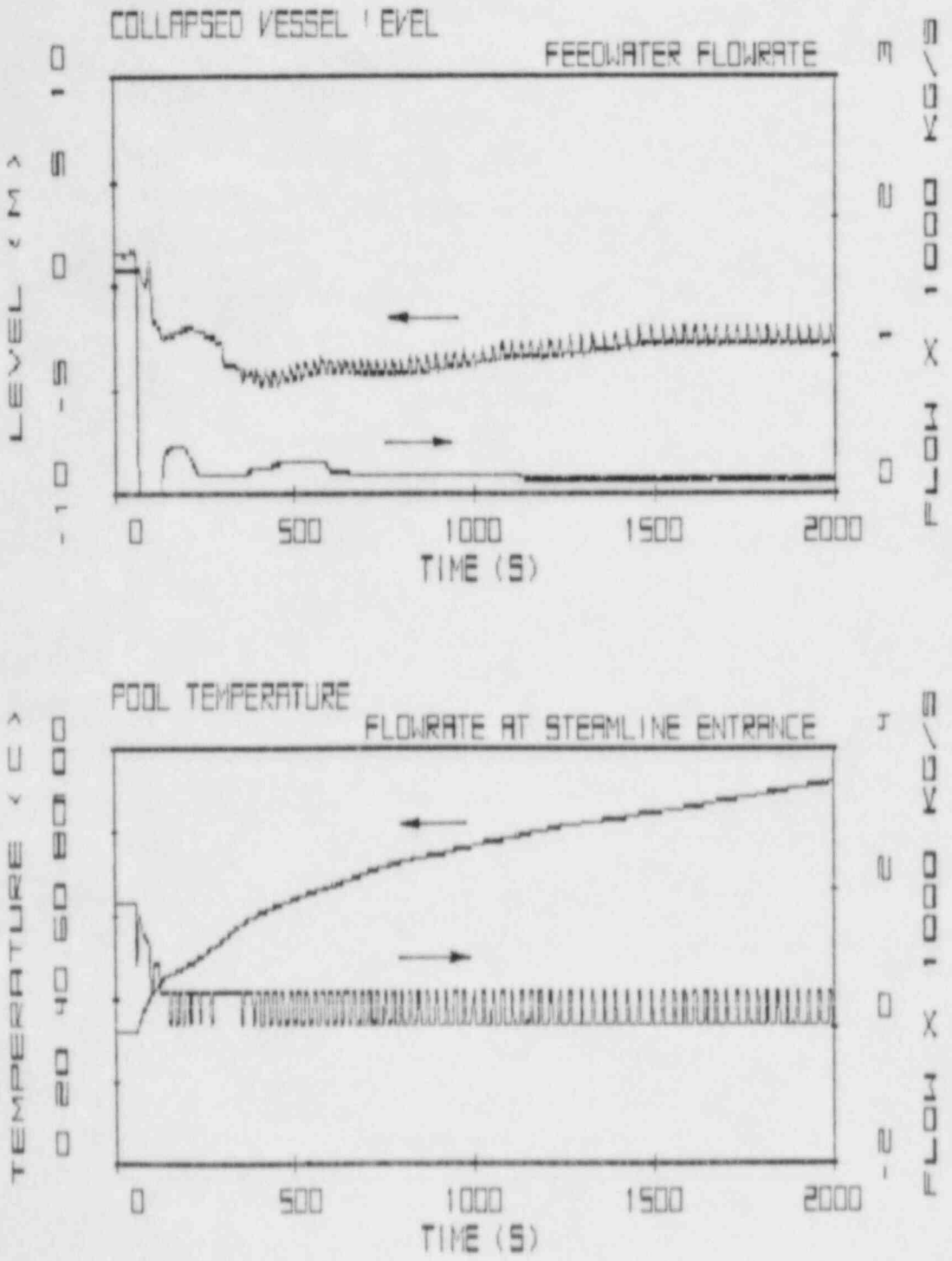

Figure 5.7 Results for Case 2: Top Graph is for Collapsed Liquid Level and Feedwater Flow Rate, Bottom Graph is for Pool Temperature and Flow Rate at Steam Line Entrance

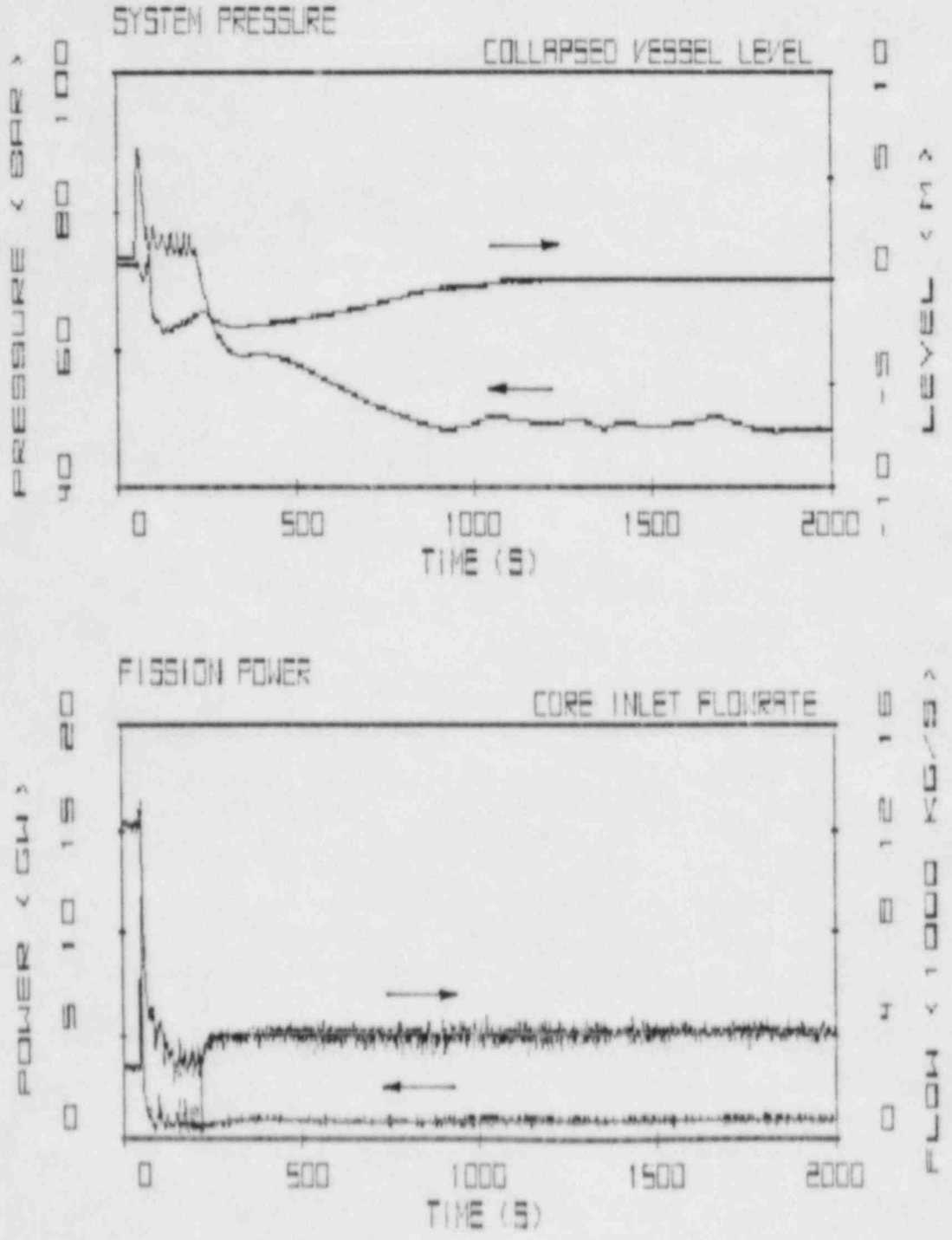

Figure 5.8 Results for Case 3: Top Graph is for System Pressure and Collapsed Liquid Level, Bottom Graph for Fission Power and Core Inlet Flow Rate

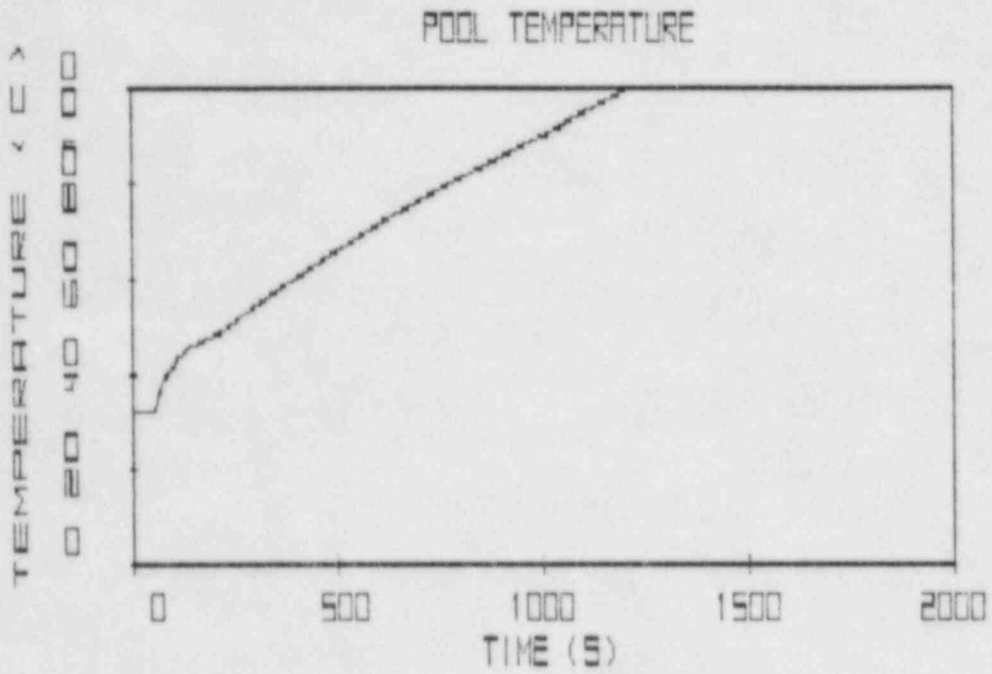

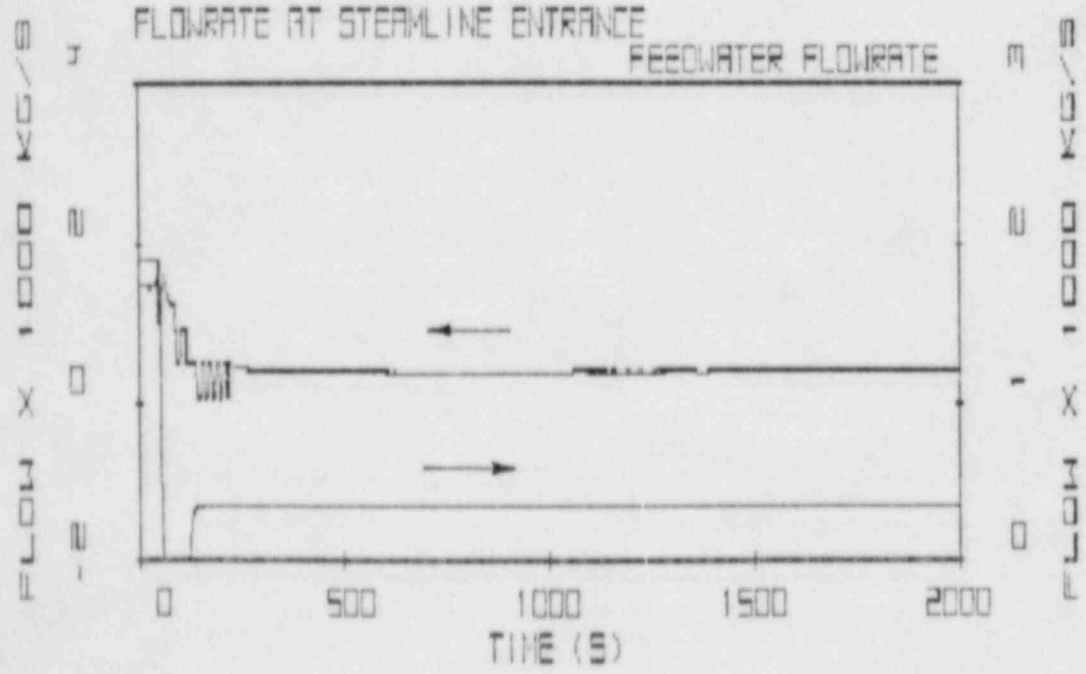

Figure 5.9 Results for Case 3: Top Graph is for the Suppression Pool Temperature, Bottom Graph for Steam Line Flow Rate and Feedwater Flow Rate

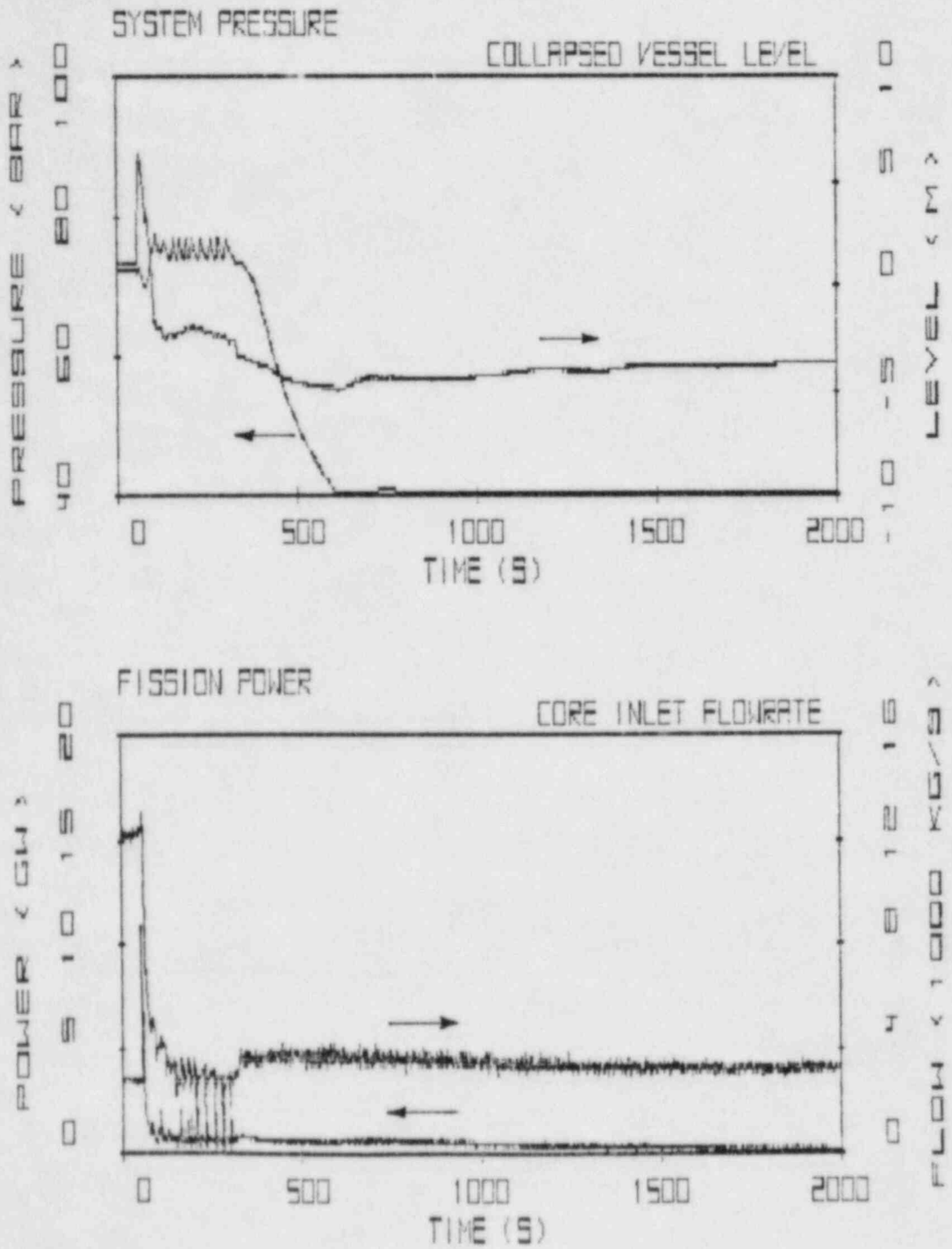

Figure 5.10 Results for Case 4: Top Graph is for System Pressure and Collapsed Liquid Level, Bottom Graph for Fission Power and Core Inlet Flow Rate

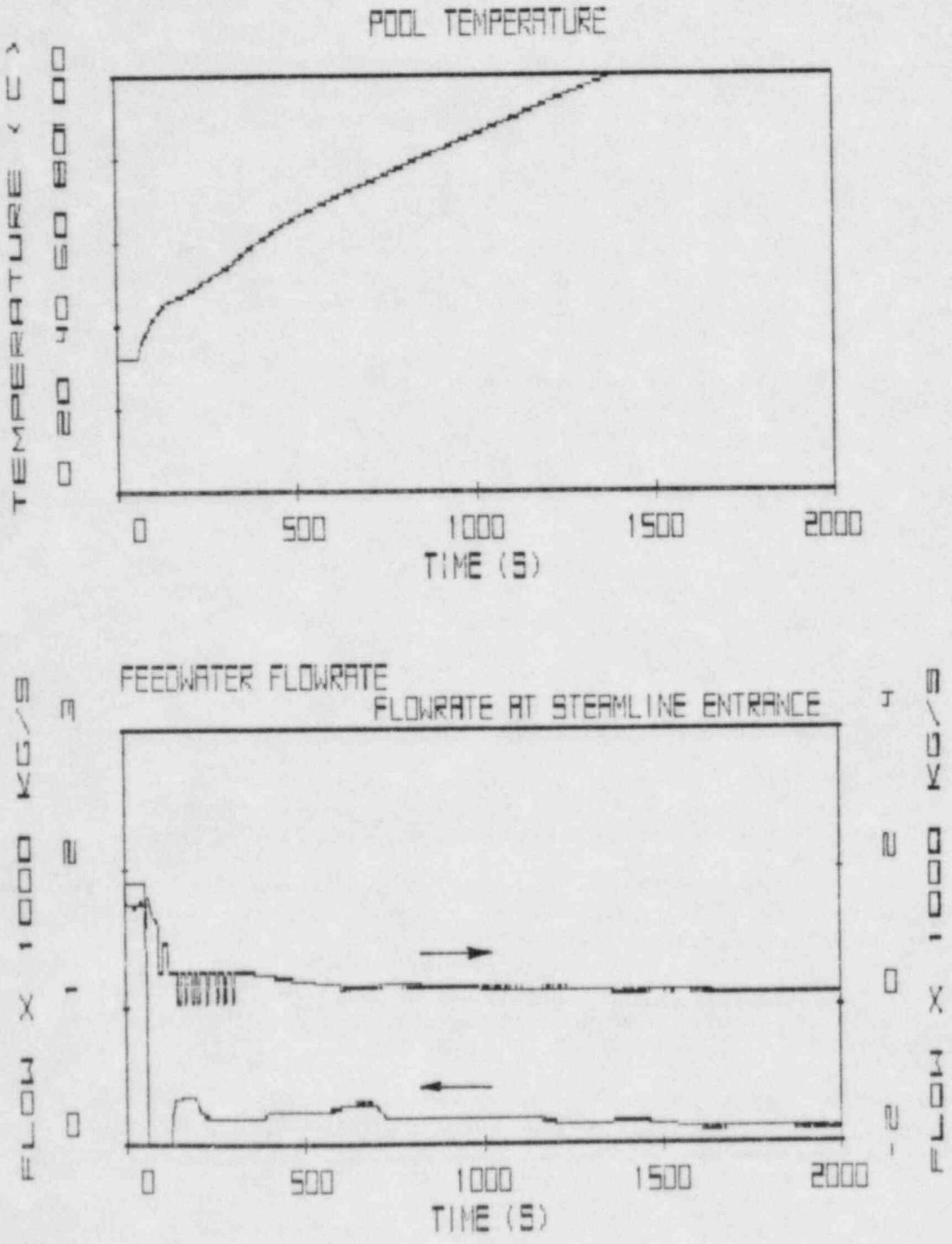

Figure 5.11 Results for Case 4: Top Graph is for Suppression Pool Temperature, Bottom Graph for Feedwater Flow Rate and Steam Line Flow Rate

In conclusion, significant power reduction during an ATWS can be achieved by means of either the level control through HPCI or the combination of the level and pressure controls. The level control is preferable from the standpoint of suppression pool temperature to preserve the containment integrity. However, in either case, the final suppression pool temperature appears to be too high so that additional mitigative measures such as boron injection via SLCS may be necessary.

5.7 Future Plans

Assessment work will continue. A module will be implemented to compute the critical power ratio. A scheme will be developed for remote access of the plant analyzer. Work will continue on the development of the preprocessor for input data.

The plant analyzer will be presented and demonstrated to domestic industries and foreign institutions interested in nuclear power plant simulation for the purpose of developing cooperative programs directed toward PWR simulations.

REFERENCES

CHENG, H. S. and WULFF, W., (1981), "A PWR Training Simulator Comparison with RETRAN for a Reactor Trip from Full Power," Informal Report, BNL-NUREG-30602, Brookhaven National Laboratory, September 1981.

CHEXAL, B., et al., (1984), "Reducing BWR Power by Water Level Control During an ATWS - A Quasi-Static Analysis," Nuclear Safety Analysis Center, Electric Power Research Institute , NSAC-69, May 1984.

ISHII, M. (1977), "One-Dimensional Drift-Flux Model and Constitutive Equations for Relative Motion Between Phases in Various Two-Phase Flow Regimes," Argonne National Laboratory, Argonne, IL., ANL-77-47.

WULFF, W., (1980), "PWR Training Simulator, An Evaluation of the Thermohydraulic Models for its Main Steam Supply System," Informal Report, BNL-NUREG-28955, September 1980.

WULFF, W., (1981a), "BWR Training Simulator, An Evaluation of the Thermohydraulic Models for its Main Steam Supply System," Informal Report, BNL-NUREG-29815, Brookhaven National Laboratory, July 1981.

WULFF, W., (1981b), "LWR Plant Analyzer Development Program," Ch. 6 in Safety Research Programs Sponsored by the Office of Nuclear Regulatory Research, Quarterly Progress Report, April 1-June 30, 1981; A. J. Romano, Editor, NUREG/CR-2231, BNL-NUREG-51454, Vol. 1, No. 1-2, 1980.

WULFF, W., CHENG, H. S., DIAMOND, D. J. and KHATIB-RAHBAR, M., (1981c), "A Description and Assessment of RAMONA-3B MOD.0 CYCLE4: A Computer Code with Three-Dimensional Neutron Kinetics for BWR Systems Transients," NUREG/CR-3664, BNL-NUREG-51746, Manuscript completed 1981, published 1984.

WULFF, W., CHENG, H. S., LEKACH, S. V. and MALLEN, A. N., (1984), "The BWR Plant Analyzer," Final Report, BNL-NUREG-51812, NUREG/CR-3943.

WULFF, W., (1982a), "LWR Plant Analyzer Development Program," Ch. 5 in Safety Research Programs Sponsored by the Office of Nuclear Regulatory Research, Quarterly Progress Report, January 1-March 31, 1982; A. J. Romano, Editor, NUREG/CR-2331, BNL-NUREG-51454, Vol. 2, No. 1, 1982.

WULFF, W., (1982b), "LWR Plant Analyzer Development Program," Ch. 5 in Safety Research Programs Sponsored by the Office of Nuclear Regulatory Research, Quarterly Progress Report, July 1-September 30, 1982; compiled by Allen J. Weiss, NUREG/CR-2331, BNL-NUREG-51454, Vol. 2, No. 3, 1982.

WULFF, W., (1982c), "LWR Plant Analyzer Development Program," Ch. 5 in Safety Research Programs Sponsored by the Office of Nuclear Regulatory Research, Quarterly Progress Report, October 1-December 31, 1982; compiled by Allen J. Weiss, NUREG/CR-2331, BNL-NUREG-51454, Vol. 2, No. 4, 1982.

WULFF, W., (1983a), "LWR Plant Analyzer Development Program," Ch. 5 in Safety Research Programs Sponsored by the Office of Nuclear Regulatory Research, Quarterly Progress Report, January 1-March 31, 1983; compiled by Allen J. Weiss, NUREG/CR-2331, BNL-NUREG-51454, Vol. 3, No. 1, 1983.

WULFF, W., (1983b), "LWR Plant Analyzer Development Program," Ch. 5 in Safety Research Programs Sponsored by the Office of Nuclear Regulatory Research, Quarterly Progress Report, July 1-September 30, 1983; compiled by Allen J. Weiss, NUREG/CR-2331, BNL-NUREG-51454, Vol. 3, No. 3, 1983.

WULFF, W., (1983c), "NRC Plant Analyzer Development," Proc. Eleventh Water Reactor Safety Research Information Meeting, held at National Bureau of Standards, Gaithersburg, MD, Oct. 24-28, 1983, U.S. Nuclear Regulatory Commission. To be published.

WULFF, W., (1983d), "LWR Plant Analyzer Development Program," Ch. 5 in Safety Research Programs Sponsored by the Office of Nuclear Regulatory Research, Quarterly Progress Report, October 1-December 31, 1983; compiled by Allen J. Weiss, NUREG/CR-2331, BNL-NUREG-51454, Vol. 3, No. 4, 1983.

WULFF, W., (1984a), "LWR Plant Analyzer Development Program," Ch. 5 in Safety Research Programs Sponsored by the Office of Nuclear Regulatory Research, Quarterly Progress Report, January 1-March 31, 1984; compiled by Allen J. Weiss, NUREG/CR-2331, BNL-NUREG-51454, Vol. 4, No. 1, 1984.

WULFF, W., (1984b), "LWR Plant Analyzer Development Program," Ch. 5 in Safety Research Programs Sponsored by the Office of Nuclear Regulatory Research, Quarterly Progress Report, April 1-June 30, 1984; compiled by Allen J. Weiss, NUREG/CR-2331, BNL-NUREG-51454, Vol. 4, No. 2, 1984.

6. Code Assessment and Application (Transient and LOCA Analyses)

(P. Saha, J. H. Jo, H. R. Connell, U. S. Rohatgi and C. Yuelys-Miksis)

This project includes the independent assessment of the latest released versions of LWR safety codes such as TRAC, RELAP5, and RAMONA-3B, and the application of these codes to the simulation of plant accidents and/or transients. Two major code application tasks namely, the RESAR-3S large break LOCA study and the BWR/4 MSIV closure ATWS analysis, have been completed, and are being documented in two separate topical reports.

The TRAC-BD1/MOD1 (Version 22) code has been implemented on the BNL computer and significant progress has been made in developing a TRAC-BD1/MOD1 input deck for simulating the FIST facility. A part of the NUFREQ-NP code has also been implemented at BNL.

The major activities performed during the reporting period of July to September 1984 are described below.

6.1 Code Implementation and Assessment

6.1.1 Simulation of FIST Experiments with TRAC-BD1/MOD1
(J. H. Jo and H. R. Connell)

The TRAC-BD1/MOD1 code (Version A22 plus the correction set E1Z1) has been implemented and tested with the sample problem. The data for FIST tests were accessed from the Reactor Safety Research Data Bank in the INEL computer and selected plots for the 4PMC1 FIST test were obtained. These data are needed to set up the input deck for the FIST test.

The efforts are continuing to obtain the steady-state for Test 4PMC1 of the Phase 1 FIST test. There were many difficulties in achieving the steady state. The first problem experienced was with the use of the water packing option (IPAK=1) of the TRAC-BD1/MOD1 code. This option was recommended in the draft version of the manual; however, it was found that this option was neither exercised in any of the sample problems which were received with the code nor used in the INEL FIST input deck. This option has been turned off in the BNL input deck for the FIST test.

There were other difficulties in obtaining the steady-state, such as recirculation flow, core inlet flow, steam downflow or carry-under in the downcomer, etc. These difficulties have been resolved and the input deck is being tested for the final steady-state. A deck for the transient calculation has also been prepared which will be run after the final steady-state is obtained.

6.1.2 Transmittal of BNL TRAC-BD1/MOD1 to General Electric
(H. R. Connell)

At the request of NRC, the BNL implementation of the TRAC-BD1/MOD1 code on the CDC-7600 computer was transferred to General Electric Company at San Jose, California. All the files necessary to implement the BNL version of the code on the GE CDC-7600 computer were written onto a magnetic tape and transmitted to GE.

6.1.3 NUFREQ-NP Implementation (H. R. Connell)

The BWR stability analysis code, NUFREQ-NP, acquired from Rensselaer Polytechnic Institute was implemented in part on the BNL CDC 7600 computer. NURFRQ-NP is a dual program system code consisting of a thermal hydraulic program system and a nuclear (NU) program system. The thermal hydraulic (TH) program system was made operational at BNL and the sample problem distributed with the code was successfully run.

Both program systems were written for an IBM 370 computer. The adaptation of the TH-system to the CDC 7600 computer at BNL was possible by means of code revisions, but the memory requirements of the NU-system are so great as to make implementation possible only by means of extensive code changes. However, this code could be implemented in the VAX system but would run exceedingly slow.

6.2 Code Application

6.2.1 Analysis of Westinghouse RESAR-3S Plants (U. S. Rohatgi and C. Yuelys-Miksis)

The BNL best-estimate and evaluation type calculations for the 200% cold leg break in a Westinghouse 4-loop RESAR-3S plant using TRAC-PD2/MOD1 code have been completed. The EM-type calculation followed the Appendix-K guideline regarding the transient scenario. However, there were two possible situations for the reactor coolant pumps (RCP) in the reflood phase, i.e., pump coasting down or pumps with locked rotor. The first BNL EM-type calculation followed the pumps coastdown option with locked rotor to occur only when the rotor had stopped. Another EM-type calculation was initiated to follow the second option on the RCP status in order to study the effect of the locked rotor resistance in the reflood phase. This calculation was started from the plant conditions at the end of the refill stage (48.5 seconds) in the previous EM-type calculation. The calculation will be continued until 300 seconds, at which time the hot rods are expected to cooldown. Furthermore, the peak clad temperature is also expected to be higher and to occur later than in the previous EM-type calculation.

7. Thermal Reactor Code Development (RAMONA-3B)

(P. Saha, L. Neymotin, G. C. Slovik, H. R. Connell, and E. Cazzoli)

This project includes the modifications, improvements and preliminary (or developmental) assessment of the BWR transient analysis code called RAMONA-3B. This is the only BWR systems transient code with three-dimensional neutron kinetics, and it is now available, at no cost, to U. S. organizations for the analysis of U. S. reactors.

During this reporting period of July to September 1984, several improvements and corrections have been made to the RAMONA-3B code. The details of the progress achieved during the reporting quarter are described below.

7.1 RAMONA-3B Improvement

7.1.1 Feedwater Control System Implementation
(L. Neymotin and H. R. Connell)

The objective of the BWR feedwater control (FWC) system is to maintain the reactor vessel water level at a prescribed optimum elevation during the plant nominal operation as well as at operational transient situations. The control scheme adopted for implementation in the RAMONA-3B code is based mainly on information obtained from FSARs of various BWR plants including Quad Cities (BWR/3), Browns Ferry (BWR/4) and Grand Gulf (BWR/6). Several other documents were also consulted (Forkner, 1978 and Linford 1973). The major features of the FWC system are briefly described below.

Two "error" signals are used in the system to generate the appropriate value of the feedwater flow rate ("error" signal is a difference between the current value of a variable and its requested or steady state value). Those are the water level error signal

$$E_L = L_R - L_m \,, \tag{1}$$

where L_m is the measured water level and L_R is the requested (optimal) water level, and the "inventory" error signal

$$E_W = W_{stm,m} - W_{fw,m} \,, \tag{2}$$

where $W_{stm,m}$ and $W_{fw,m}$ are the measured steam line and feedwater flow rates, respectively. The feedwater and steam flow rate measurements can be described by the following differential equations

$$\tau_{fw} \frac{dW_{fw,m}}{dt} = W_{fw} - W_{fw,m} \tag{3}$$

$$\tau_{stm} \frac{dW_{stm,m}}{dt} = W_{stm} - W_{stm,m} \tag{4}$$

where τ_{fw} and τ_{stm} are corresponding time constants of the measuring systems and W_{fw} and W_{stm} are real values of the system variables. Equations (3) and (4) are solved by the explicit Euler method in Subroutine FWCTRL which also contains most of the FORTRAN coding relevant to the control system.

The requested water level L_R can be a function of the reactor operating conditions (the present model assumes that the requested water level is the water level at the steady-state reactor condition).

The level error signal, E_L is supplied to a Proportional-Integral-Derivative (PID) controller which generates an intermediate signal, S_L:

$$S_L = K_S\left(E_L + \frac{1}{\tau_{I,S}} \int_0^t E_L dt + \tau_{D,S} \frac{dE_L}{dt}\right) . \qquad (5)$$

This intermediate signal from Equation (5) is put through a "limiter" to prevent an excessively strong response of the control system on variations of the water level:

$$S_L = \begin{cases} S_{L,max} & \text{if } S_L > S_{L,max} \\ S_{L,min} & \text{if } S_L < S_{L,min} \end{cases} \qquad (6)$$

The trimmed signal, S_L is then combined with the inventory error signal, Equation (2) thus producing the final error signal, E_T (note, that some BWR control systems use only the water level error signal, S_L):

$$E_T = S_L + K_W E_W \qquad (7)$$

Finally, the combined error signal, E_T is supplied to another PID controller

$$T_r = K_T\left(E_T + \frac{1}{\tau_{I,T}} \int_0^t E_T dt + \tau_{D,T} \frac{dE_T}{dt}\right) \qquad (8)$$

$$T_r = \begin{cases} T_{r,max} & \text{if } T_r > T_{r,max} \\ T_{r,min} & \text{if } T_r < T_{r,min} \end{cases}$$

in order to generate the input signal T_r to a feedwater system regulator (it can be either a pump or a valve) and calculate the sought feedwater flow rate according to the following correlation

$$W_{fw} = K_p T_r + W_{fw,o} \quad (9)$$

where $W_{fw,o}$ is the feedwater flow rate at the steady-state condition at the beginning of a transient.

In order to test the FORTRAN implementation and model performance, a sample calculation is being run for a prototype case when the steam line flow rate and downcomer water level may vary considerably. The results of this calculation will be discussed in the next quarterly report.

7.1.2 Improvements for Reverse Flow (L. Neymotin)

As a first step in the work on improvements in calculating the reverse flow situation, the boundary conditions for the mixture energy equation at the riser entrance junction have been corrected to account for possible flow reversal at the exit of the core channels. The liquid enthalpy at the riser entrance is calculated assuming perfect mixing of the liquid exiting from the core channels, thus excluding from consideration the liquid flowing downwards at the channel exits.

7.1.3 Modification to Restart Capability (H. R. Connell)

The current RAMONA-3B option for restart has been extended so that more frequent restart dumps can be generated at user specified time intervals. Previously, the restart dump was created only upon normal termination of the code execution (i.e., on user specified time). The new capability will allow a more efficient code operation in the event of an unexpected job termination and/or code modification during a calculation.

7.1.4 Time Step Corrections (H. R. Connell and L. Neymotin)

It has been discovered that the time step evaluations for the thermal-hydraulics part in RAMONA-3B were done incorrectly when the maximum number of hydraulic channels permitted by the code was used for the reactor core representation. The errors have been corrected and a test case was successfully run.

7.2 RAMONA-3B User Support
(L. Neymotin, G. C. Slovik, H. R. Connell and P. Saha)

Continuous support has been provided for a Control Rod Drop Accident (CRDA) calculation being performed at BNL under the NRC/NRR sponsorship. The rod drop velocity (15 ft/second) in this calculation is three times higher than that used in the previous CRDA calculations performed at BNL.

A BNL/INEL/NRC meeting was held at BNL on July 25, 1984 and subsequent RAMONA-3B calculations were performed to resolve the discrepancies between the TRAC-BD1/MOD1 and RAMONA-3B results using 1-D neutronics for the Peach Bottom Turbine Trip Test 3 (PBTT3). The major problem which developed was the fact that the steady state corresponding to the PBTT3 could not be calculated by TRAC-BD1/MOD1 while the RAMONA-3B code not only calculated the

steady state but also the transient with reasonable success. It was found that the problem was in the 1-D fitting coefficients which were sent to INEL from the RAMONA-3B 3-D to 1-D collapser without accounting for the different hydraulic models of TRAC-BD1/MOD1. This was verified when TRAC-BD1/MOD1 and RAMONA-3B printed out their steady state converged cross sections (i.e., D_1, D_2, Σ_{r1}, Σ_{a1}, $\nu\Sigma_{f1}$, Σ_{a2}, and $\nu\Sigma_{f2}$). These were used in subsequent calculations at BNL with RAMONA-3B and INEL with TRAC-BD1/MOD1. The results demonstrated that both codes predict similar trends when the same 1-D cross section are used instead of the same fitting coefficients. Therefore, the 3-D to 1-D collapser must make allowances for the different hydraulics when generating the 1-D fitting coefficients for cross section calculations.

A number of telephone consultations were given to the GPU Nuclear Company staff who have recently has implemented the RAMONA-3B code on an IBM computer and are now performing plant transient calculations.

7.3 Nuclear Cross Sections for Browns Ferry Cycle 5
(G. Slovik and E. Cazzoli)

During this quarter, two different cross section sets have been calculated for RAMONA-3B using the CASMO cross sections reported earlier (Slovik, 1984) and the BLEND2 code developed at BNL. To accomplish this task, the TVA-supplied description of the core, along with the exposure and void histories of the reactor at several times during Cycle 5 of Unit 3, was also used.

The two cross section sets were calculated at a state point of 8876 MWD/MT which is the end of Cycle 5. The first set has 13 cross section sets to represent the core which lumped nodes together using an acceptance criterion of 5291 MWD/MT and 0.39 on the void history. The second set used an acceptance criterion of 4233 MWD/MT and 0.3 on the void history which resulted in a set of 20 cross sections to represent the core. Both of these cross section sets have been used in the RAMONA-3B steady state calculation and the results agree well with the TVA-supplied core power distribution.

REFERENCES

FORKNER, S. L., (1978) , "Calculation of Generator Load Rejection Transient for 3293 MW BWR with RETRAN-01-RET128," TVA Report, July 1, 1978.

LINFORD, R. B., (1973), "Analytical Methods of Plant Transient Evaluation for the General Electric Boiling Water Reactor," NEDO-10802, February 1973.

SLOVIK, G. C., and KOHUT, P., (1984), "Generation of Browns Ferry Cycle 5 Nuclear Cross Sections," in Safety Research Program Sponsored by the Office of Nuclear Regulatory Research, Quarterly Progress Report, April 1 - June 30, 1984, NUREG/CR-2331, BNL-NUREG-51454, Vol. 4, No. 2, Section 7.3.

8. Calculational Quality Assurance in Support of PTS

(P. Saha, J. H. Jo, U. S. Rohatgi and C. Yuelys-Miksis)

The objective of this project is to provide a peer review of the thermal-hydraulic calculations that have been performed at LANL (using the TRAC-PWR code) and INEL (using the RELAP5 code) for the NRC Pressurized Thermal Shock (PTS) study. Specifically, this includes a review of the plant decks and the calculations, and an assessment of the reasonableness of the results. The major activities performed during July to September 1984 are described below.

8.1 Assessment of RELAP5 Thermal-Hydraulic Analysis of PTS Transients of H. B. Robinson Unit 2

(C. Yuelys-Miksis, J. H. Jo and U. S. Rohatgi)

Eleven transient scenarios, specified by Oak Ridge National Laboratory, were simulated by INEL (Fletcher, 1983) for the H. B. Robinson-2 PWR plant. These were qualitatively reviewed and reported in the previous quarterly. Six of these transients were selected for quantitative in-depth review using the simple method developed at BNL. Four of these transients were reviewed based on the information available at BNL by the end of September 1984 and are summarized in the remaining section. (It is our understanding that some of these transients, i.e., Transients 1 through 4 have been recomputed at INEL. However, no information on these recalculations were available at BNL by the end of September 1984.)

Transient 1: Main Steam Line Break from Hot Standby Conditions

This transient was initiated by a 1 ft^2 break in the steam line at hot standby operation. The break is upstream of the main steam isolation valve and there is no failure of any automatic equipment. The operator is assumed to stop the auxiliary feedwater flow 600 seconds after the initiation of the transient and to trip the reactor coolant pumps when the safety injection actuation signal is generated and the primary system pressure falls to 1300 psig.

The RELAP5/MOD1.6 code was used to calculate the transient to 1800 seconds and the key parameters were extrapolated to 7200 seconds. Figure 8.1 shows the downcomer temperatures calculated by RELAP5 with the system average temperature obtained by the BNL hand calculation. In addition, the figure shows the INEL extrapolation of the downcomer temperature. The BNL temperature shown is that calculated without accounting for the heat stored in the metal structure. This assumes that the relatively slow wall heat transfer between the liquid and the metal structures of the reactor and other components will not affect the temperature of the liquid in the early stages of the transient. Calculations were also performed with the assumption that the wall heat transfer is instantaneous, so that the metal and the liquid

temperatures change simultaneously. The actual temperature would initially be close to that calculated without the metal structure and eventually approach that calculated with the metal stored heat accounted for since the metal cooling is considerably slower than that for the liquid.

In the code calculations, there was stagnation in Loops B and C which prevented the injected cooling water from circulating, hence, keeping the cold leg temperatures very low. This lack of natural circulation forced the Loop B and C hot leg temperatures to remain very high. In the affected Loop A there is greater natural circulation and therefore its hot leg temperature is lower than the other loops and its cold leg temperature is closer to the downcomer temperature.

Figures 8.2 to 8.4 show the hot and cold leg temperatures of each loop and the BNL calculated temperatures with and without the metal stored heat. Due to stagnation in the loops, there are large temperature spreads between the hot and cold legs in Loops B and C and the BNL calculated temperatures fall between the two extremes. In Loop A the BNL predicted system average temperature without the metal heat accounted for is very close to the hot leg temperature. Since the BNL values are system average temperatures, these results are to be expected. Figure 8.2 also shows the temperature spread between the hot leg and the cold leg as calculated by BNL, based on the flow rates calculated by RELAP5. This temperature spread is compared to the RELAP5 temperature difference between the hot leg and the cold leg, and it can be seen that the RELAP5 calculated temperature spread is realistic and to be expected.

Figure 8.5 shows the cold leg temperatures as extrapolated by INEL and the BNL temperatures with and without the heat stored in the metal structures. The INEL extrapolations approach the system average temperature with the metal, as would be expected, in Loops A and C but not in Loop B. These extrapolations assume a constant rate of temperature increase or decrease based upon the temperatures calculated at 1800 seconds. However, these calculations appear to have been prematurely terminated since the key parameters still have not stabilized and there is insufficient information to accurately extrapolate the results. As was found in the Calvert Cliffs calculation (Jo, 1984) the effect of the metal stored heat is significant up to 4000 seconds after which the heat transfer rate may decrease.

Figure 8.6 shows the system pressures as calculated by RELAP5 and BNL. The BNL pressures are calculated with the assumption of adiabatic compression during the filling stage which is expected to provide the upper bound of the actual pressure. Also shown is the saturation pressure corresponding to the BNL calculated system average temperature. As expected, the RELAP5 pressure remained below the BNL pressure. Similar results were observed in the Calvert Cliff case (Jo, 1984). However, RELAP5 exhibited less non-equilibrium effect than did TRAC. As expected, the secondary pressure of the broken loop corresponds closely with the saturation pressure corresponding

to the BNL system average temperature. The pressure in the intact steam generators remains high and stable because the primary loops stagnate and there is no heat transfer in the two intact steam generators.

Transient 4: Three Steam Dump Valves Fail Open at Hot Full Power Condition

This transient is similar to Transient 1 except that it started during hot full power operation and three out of the five main steam line dump valves were stuck open. The reactor trips 41.1 seconds into the transient.

The RELAP5 code was used to calculate the scenario to 2500 seconds and key parameters were extrapolated to 7200 seconds. Figure 8.7 compares the INEL prediction of downcomer temperature and the BNL system average temperature with the metal structures accounted for. Both curves match very well, and converge to the saturation temperature at ambient conditions.

The pressurizer normalized levels are shown in Figure 8.8. Both the RELAP5 and BNL calculations show level maintenance later in the transient. The difference in the two levels is probably due either to the lack of shrinkage in the RELAP5 calculation as the cold inflow is injected into the primary system or to the voiding in the upper head. When a level is calculated by injecting all of the inflow directly into the pressurizer without accounting for any cooling or shrinkage effects, the results are nearly identical to the pressurizer levels calculated by RELAP5. It is therefore assumed that either shrinkage has not been accounted for or there is additional mass inflow into the pressurizer due to a mass shift from the upper head or additional mass flow into the primary system.

The downcomer pressure calculated by RELAP5 and extrapolated by INEL is shown in Figure 8.9. The INEL extrapolation assumes adiabatic pressurization after the first two cells of the pressurizer are full. The BNL pressure which was also based on the adiabatic assumption matches the INEL extrapolation up to approximately 1000 seconds. At this time, the INEL extrapolated pressure levels off at the RELAP5 calculated pressure. The reason for the pressure stabilization at this time is not clear since the INEL pressurizer level continues to increase up to 1250 seconds. The BNL pressure continues to rise until 1250 seconds. At this time, the BNL calculated pressurizer level also stabilizes and the pressure then levels off to approximately 1500 psia.

In summary, with the exception of the pressurizer level calculation, the RELAP5 code results appear reasonable.

Transient 6: Small Hot Leg Break LOCA at Hot Full Power Conditions

In this transient there is a 0.0635m (0.2 ft) diameter break in the pressurizer loop hot leg during hot full power operation. All systems operate automatically and there are no equipment failures.

The RELAP5 code was used to calculate the transient to 2800 seconds and key parameters were extrapolated to 7200 seconds. Figure 8.10 shows the downcomer and hot leg temperatures calculated by RELAP5 and the BNL system average temperature without metal structures. In this scenario multidimensional effects are seen when only two of the three loops experience stagnation. Since RELAP5 has a one-dimensional core model it may not permit adequate analysis of a transient with strong multidimensional effects. However, since this behavior is seen only in the early portion of the transient, the results should not be appreciably affected. The broken loop experienced natural circulation until about 1000 seconds. At this time the cold HPI and makeup inflow caused the large drop in the downcomer temperature as stagnation prevented this cold injection from reaching the hot legs. The BNL system average temperature agrees well with the RELAP5 calculation until stagnation occurs. After this point the BNL temperature is between the hot leg temperature and the downcomer temperature, as expected.

In the temperature extrapolation, shown in Figure 8.11, INEL has predicted a sharp drop of the downcomer temperature at around 2700 seconds. This drop levels off at the ECC fluid temperature. Yet, as the decay power input still exists and there are upper plenum to downcomer leakage flows, it is not likely that the downcomer temperature will experience such a sudden decrease in a relatively short time period. However, this assumption is conservative and it is likely that the actual temperature will fall between the INEL extrapolated values and the BNL system average values.

Figure 8.12 shows the pressurizer level. In both the RELAP5 and BNL calculations the pressurizer lost inventory rapidly. After this point it is expected that the downcomer pressure will be maintained at the saturation level associated with the hot leg temperature. This can be seen in Figure 8.13. Since the BNL system average temperature is lower than the RELAP5 hot leg temperature, it is expected that its saturation pressure will also be lower, but will eventually converge with the pressure predicted by INEL. However, since stagnation only affects the cold leg temperature, it is expected that the pressure will follow a gradual decrease as opposed to a rapid pressure drop, as predicted by INEL.

In summary, the RELAP5 calculated results appear reasonable. The INEL extrapolations are conservative and follow the expected trends.

Transient 8: Small Hot Leg Break LOCA at Hot Zero Power Conditions

This transient, like Transient 6 was initiated by a small break in the pressurizer hot leg. At the time of the break the reactor was at hot standby conditions, as opposed to Transient 6 where the reactor was at hot full power operation. The code calculation was terminated at 1740 seconds due to large oscillations and the remainder of the transient is extrapolated.

Figure 8.14 shows the RELAP5 downcomer and hot leg temperatures and the BNL system average temperature. This transient exhibits the same phenomena observed in Transient 6. There is considerable stagnation in the loops and therefore the cold injection has a significant effect on the downcomer temperature. However, the hot leg temperature, which represents the system average temperature, is very close to the BNL temperature.

The extrapolation of the downcomer temperature to 7200 seconds is shown in Figure 8.15. The INEL extrapolation shows a sudden downcomer temperature drop to the HPI/LPI temperature at about 3000 seconds. This temperature would only occur if there was complete stagnation in the system. Even in this case, the decrease should probably be more gradual and take longer than 7200 seconds because of warm leakage from the upper plenum, downcomer bypass regions and upper head mixing in the downcomer with the cold HPI. Moreover, it is not clear how it was determined that this leakage caused the 6°K (10°F) difference between the HPI/LPI temperature and the final downcomer temperature.

Also shown are the saturation temperature corresponding to the downcomer pressure calculated by INEL and the BNL system average temperature which decreases gradually. The saturation temperature is expected to be the highest system temperature. The BNL temperature is expected to fall between this saturation temperature and the downcomer temperature, as is the case except between 1200 and 4000 seconds. This is probably due to the metal stored heat that has not yet fully affected the liquid temperature calculated by RELAP5.

The saturation pressure corresponding to the BNL system average temperature is compared with the RELAP5 downcomer pressure in Figure 8.16. As expected for a LOCA these two pressures are very close.

In summary, it appears that the results calculated by RELAP5 are reasonable except for the extrapolation of the downcomer temperature which drops to a very low temperature very quickly.

REFERENCES

FLETCHER, C.D., et al, (1983), "RELAP5 Thermal-Hydraulic Analyses of Pressurized Thermal Shock Sequences for the H. B. Robinson Unit 2 Pressurized Water Reactor," EGG-SAAM-6476, December 1983.

JO, J.H., and ROHATGI, U.S., (1984), "Review of TRAC Calculations for Calvert Cliffs PTS Study," BNL-NUREG Report in publication.

CAUTION: The scenario simulated contains significant conservatisms in operator actions and equipment failures.

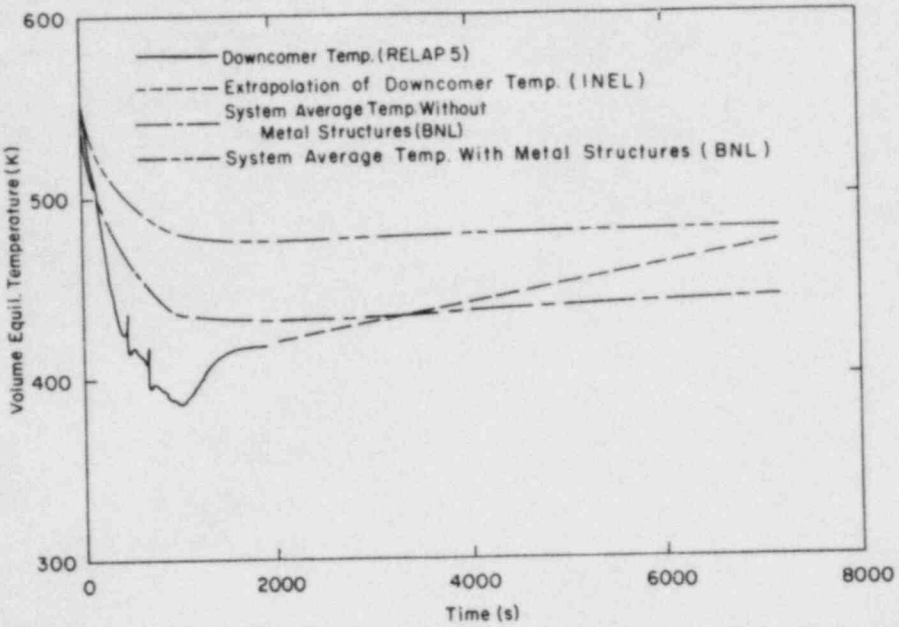

Figure 8.1 Transient 1: Liquid Temperature in the Downcomer

CAUTION: The scenario simulated contains significant conservatisms in operator actions and equipment failures.

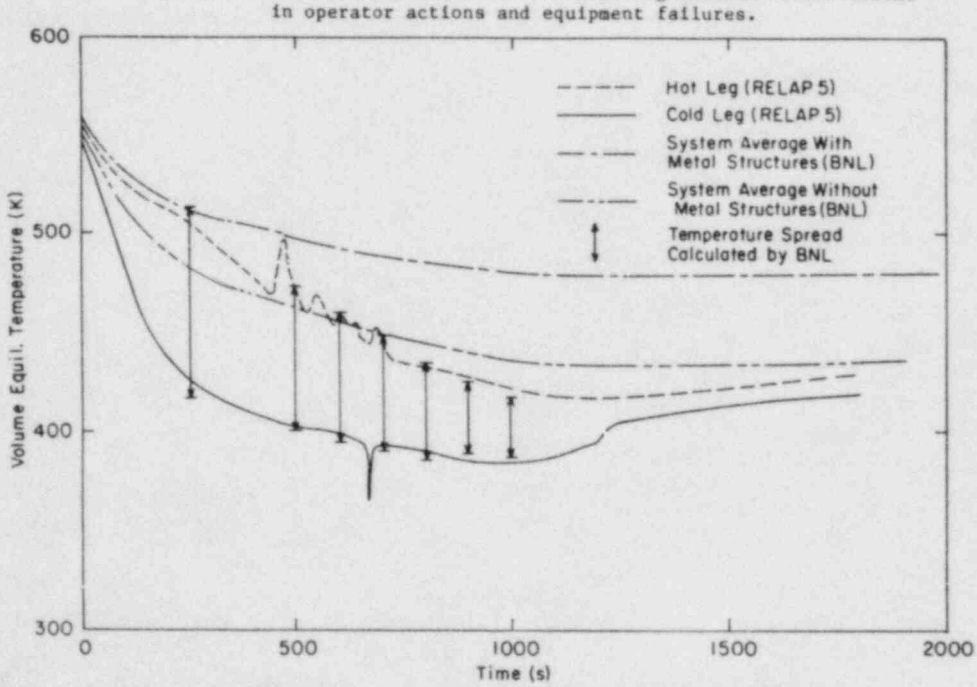

Figure 8.2 Transient 1: Loop A Liquid Temperature

CAUTION: The scenario simulated contains significant conservatisms in operator actions and equipment failures.

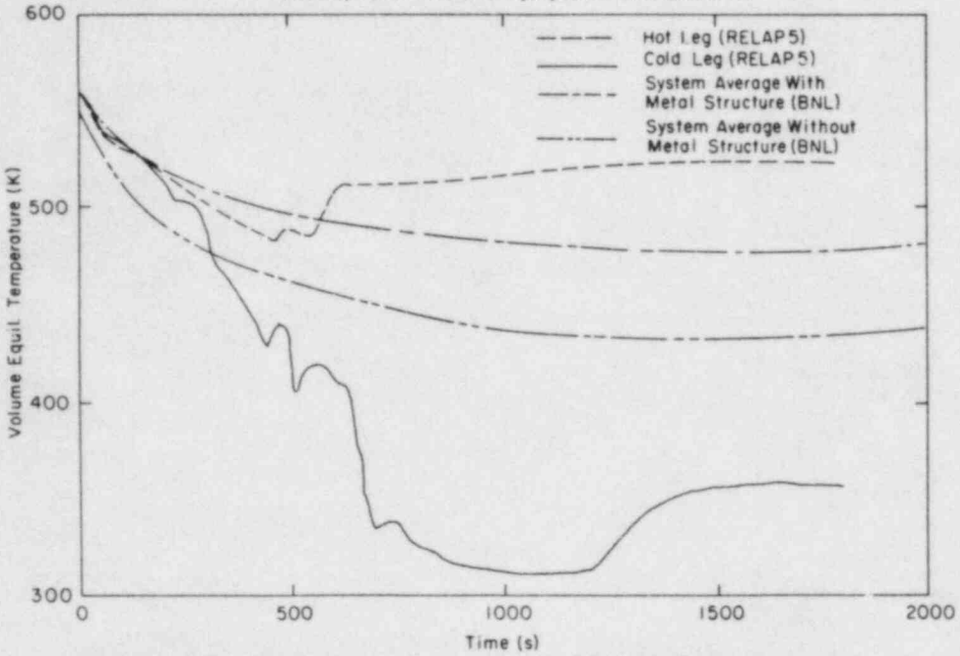

Figure 8.3 Transient 1: Loop B Liquid Temperature

CAUTION: The scenario simulated contains significant conservatisms in operator actions and equipment failures.

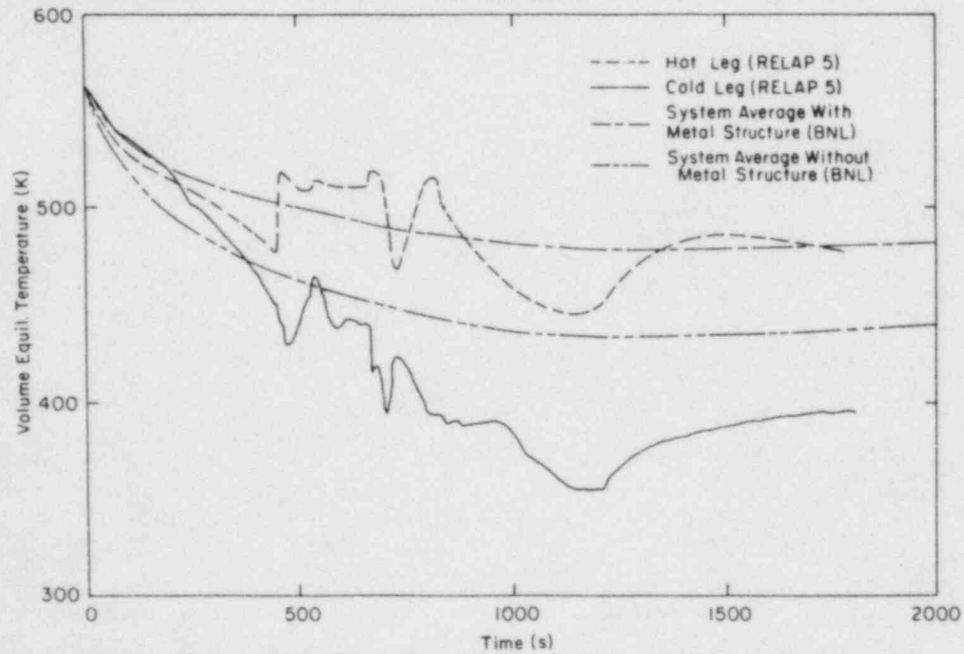

Figure 8.4 Transient 1: Loop C Liquid Temperature

CAUTION: The scenario simulated contains significant conservatisms in operator actions and equipment failures.

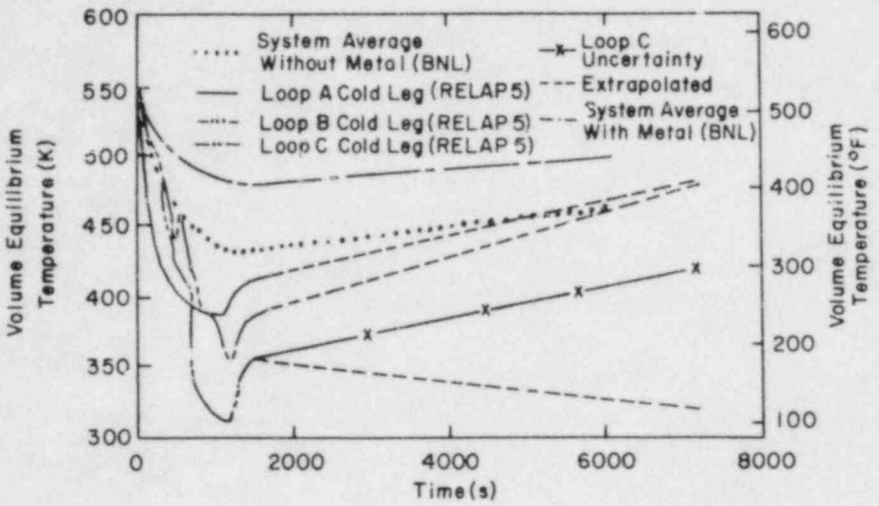

Figure 8.5 Transient 1: Cold Leg Liquid Temperatures

CAUTION: The scenario simulated contains significant conservatisms in operator actions and equipment failures.

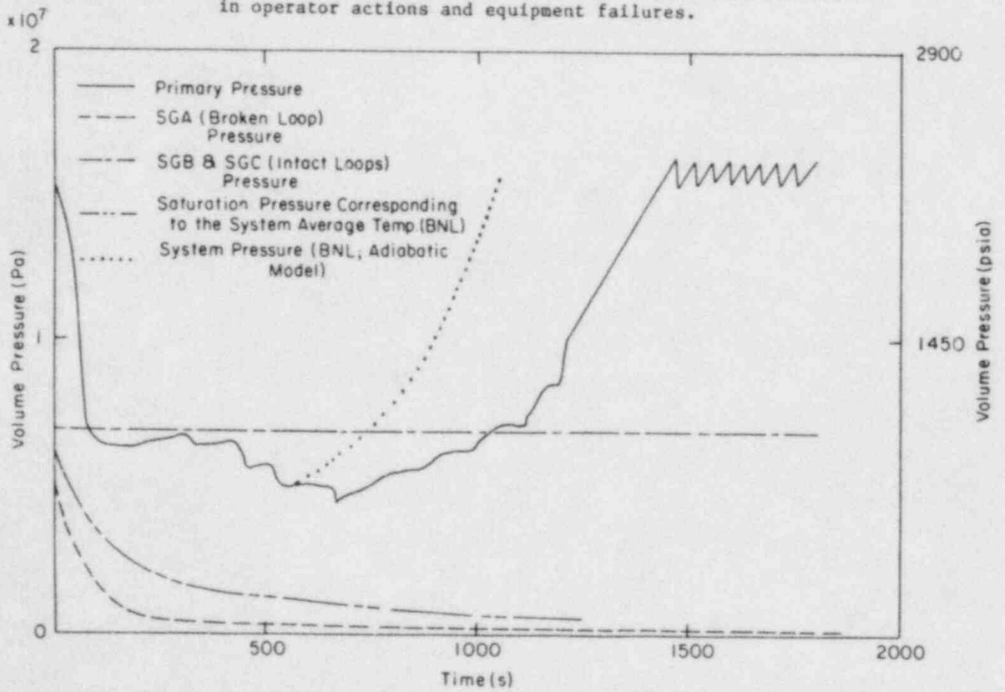

Figure 8.6 Transient 1: Primary and Secondary Pressure

CAUTION: The scenario simulated contains significant conservatisms in operator actions and equipment failures.

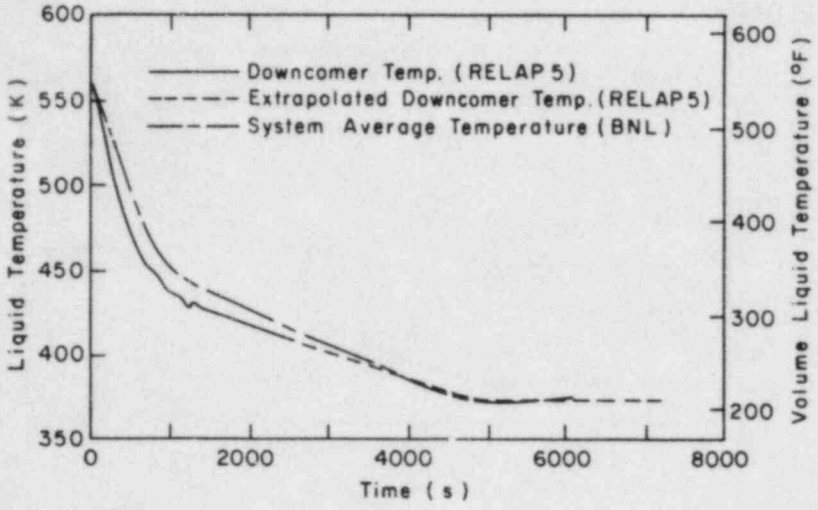

Figure 8.7 Transient 4: Liquid Temperature in the Downcomer

CAUTION: The scenario simulated contains significant conservatisms in operator actions and equipment failures.

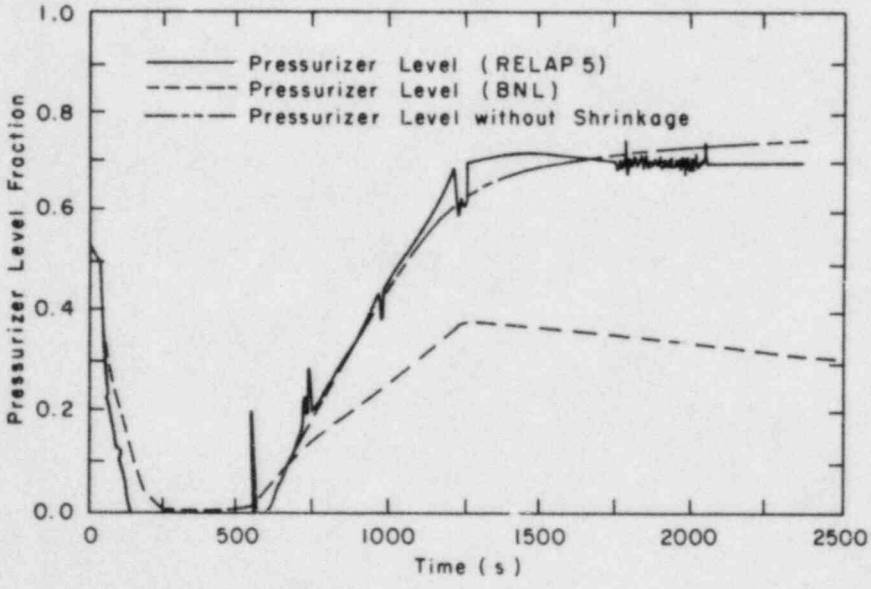

Figure 8.8 Transient 4: Normalized Pressurizer Level

CAUTION: The scenario simulated contains significant conservatisms in operator actions and equipment failures.

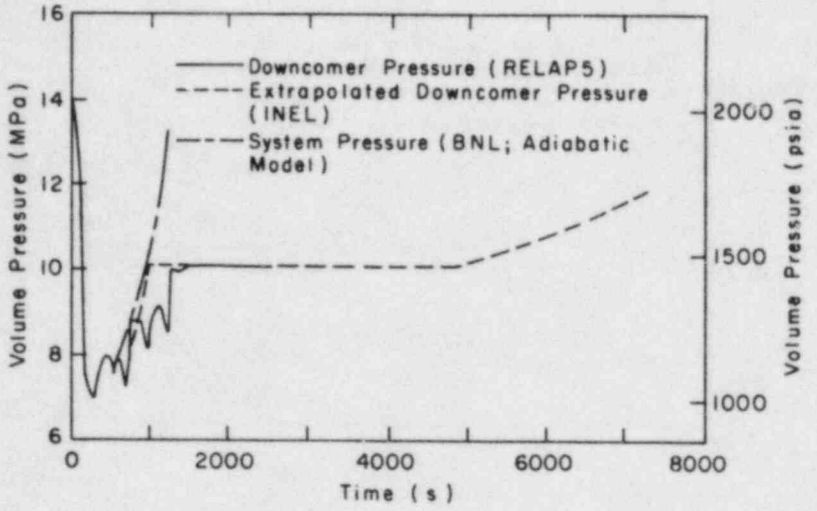

Figure 8.9 Transient 4: Downcomer Pressure

CAUTION: The scenario simulated contains significant conservatisms in operator actions and equipment failures.

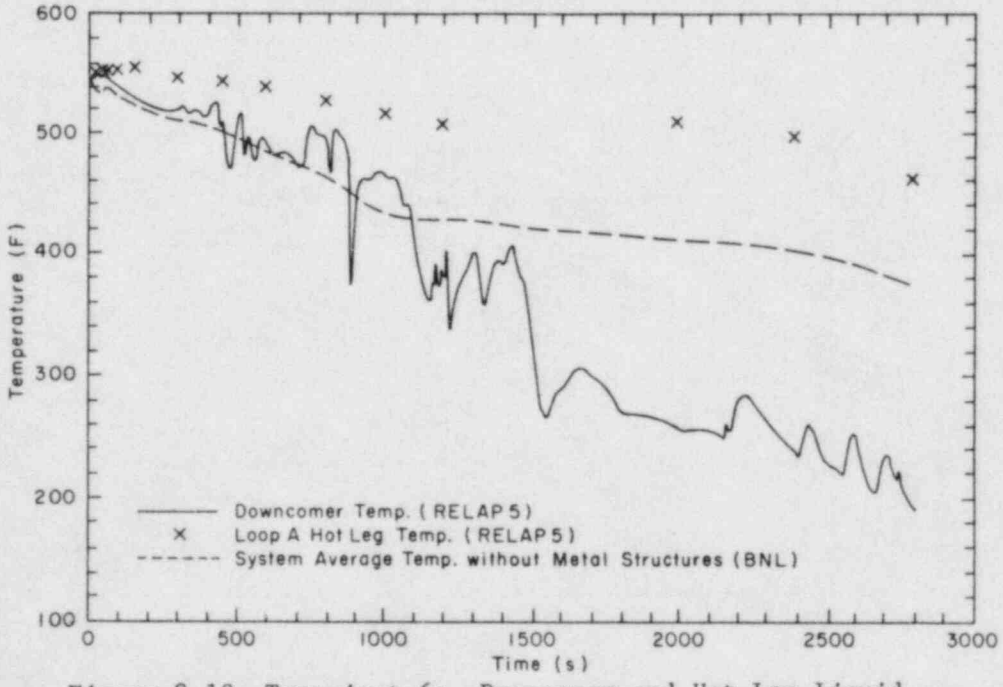

Figure 8.10 Transient 6: Downcomer and Hot Leg Liquid Temperature

CAUTION: The scenario simulated contains significant conservatisms in operator actions and equipment failures.

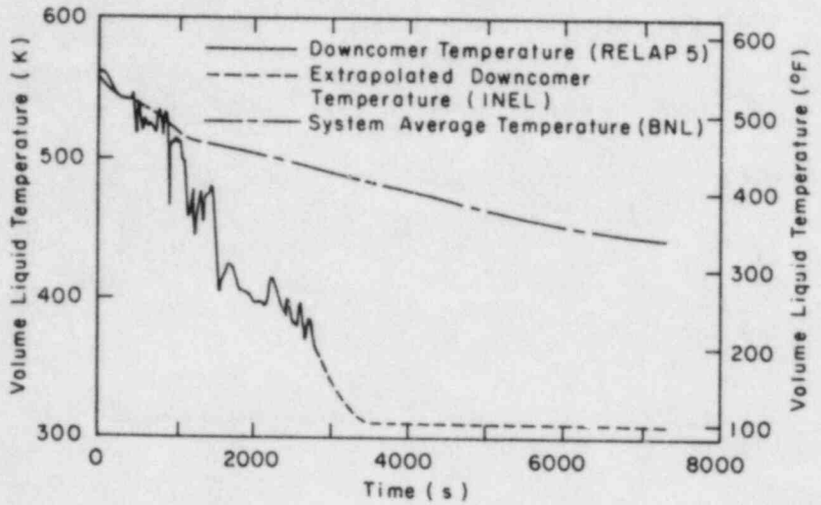

Figure 8.11 Transient 6: Liquid Temperature in the Downcomer

CAUTION: The scenario simulated contains significant conservatisms in operator actions and equipment failures.

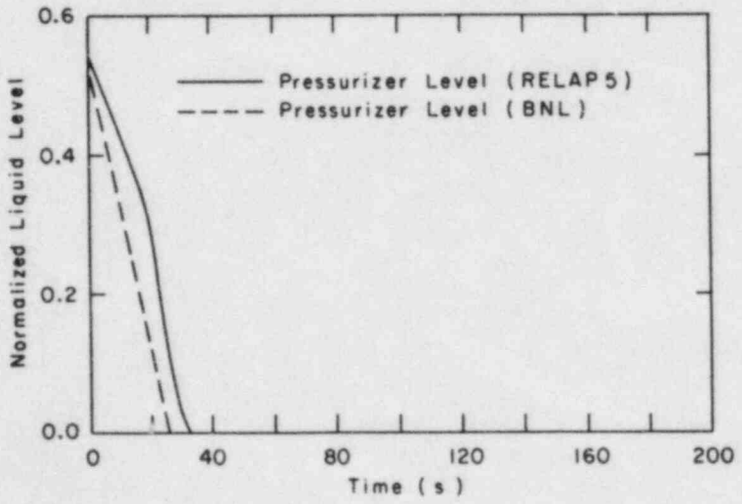

Figure 8.12 Transient 6: Normalized Pressurizer Level

CAUTION: The scenario simulated contains significant conservatisms in operator actions and equipment failures.

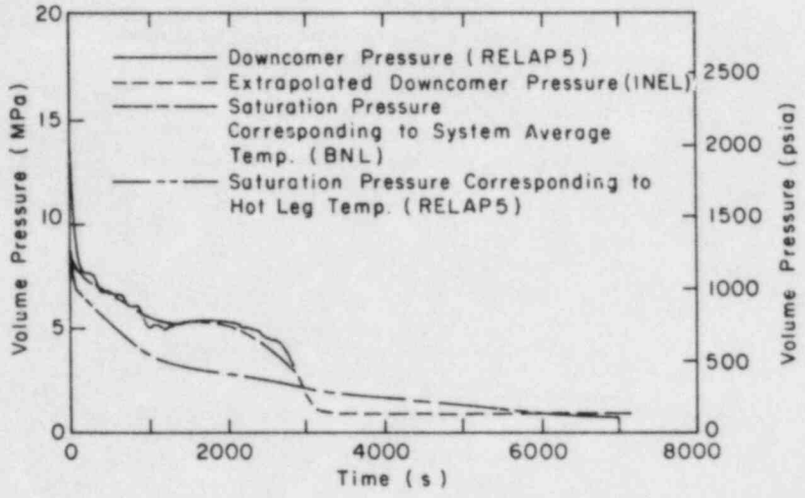

Figure 8.13 Transient 6: Downcomer Pressure

CAUTION: The scenario simulated contains significant conservatisms in operator actions and equipment failures.

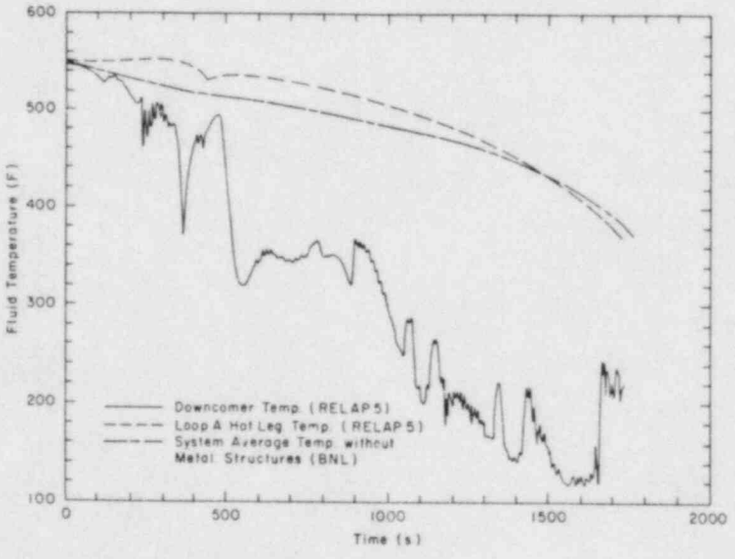

Figure 8.14 Transient 8: Downcomer and Hot Leg Liquid Temperature

CAUTION: The scenario simulated contains significant conservatisms in operator actions and equipment failures.

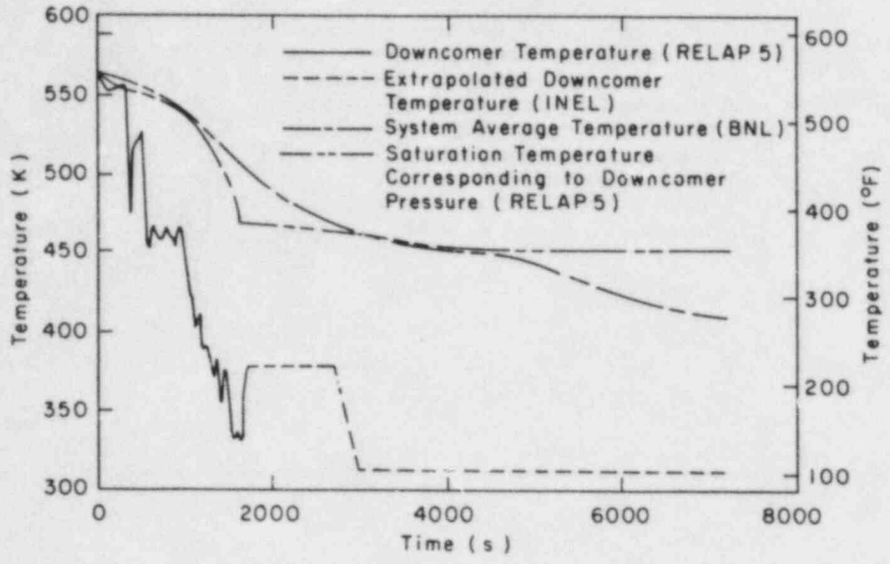

Figure 8.15 Transient 8: Liquid Temperature in the Downcomer

CAUTION: The scenario simulated contains significant conservatisms in operator actions and equipment failures.

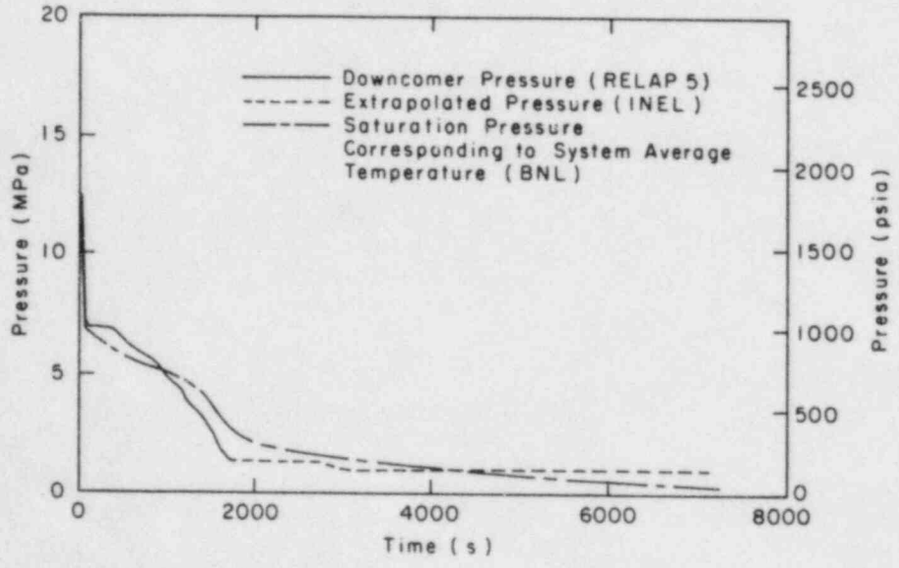

Figure 8.16 Transient 8: Downcomer Pressure

II. DIVISION OF ENGINEERING TECHNOLOGY

SUMMARY

Stress Corrosion Cracking of PWR Steam Generator Tubing

The experimental program on stress corrosion cracking (SCC) at Brookhaven National Laboratory (BNL) is aimed at the development of a quantitative model for predicting the behavior of Inconel 600 tubing in high temperature aqueous media. Empirical relationships are being established between SCC failure time, crack velocity and factors influencing cracking.

The lower temperature tests have given numerous SCC U-bend failures at 315°C in deaerated, pure water at 315°C, and now provide a continuous Arrhenius plot from 365°C to 315°C. More cracks occurred during this quarter. CERT with 0.01% carbon material was continued in secondary water ingredients. Tests at constant load were not active during this period. Computer programs remain available for handling the proposed model used for predictive purposes for Inconel 600 steam generator tubing, but the CERT data have to be improved before this can become reliable; no funding is available for this purpose now. Also verification of the model with tubes from service is due, but tubes are not yet available. Model verification with tubing from the Surry steam generator at PNL is still strongly advocated.

Probability Based Load Combinations for Design of Category I Structures

The proposed load combinations for design of concrete containments have been extended to include the effects of material strength variations. The load factors for DBA accidental pressure and safe shutdown earthquake are increased slightly, if the material strength variations are considered.

A reliability analysis method for frame structures with shear walls is being developed. In particular, the limit states for beam, column and shear wall have been defined. In addition, the global limit state for the entire structures has also been developed.

A literature review was conducted on gross errors for ordinary construction. Most serious failures or collapses occur during construction. Fundamental misconceptions regarding behavior and detailing errors appear to be the most serious source of design errors.

Identification of Age Related Failure Modes

During this quarter, the review of many nuclear power plant data bases was completed. An aging assessment of age-sensitive motor components was made to identify and characterize the associated aging and service wear effects that are likely to impair plant safety. The study also includes an evaluations of aging effects on seismic capacity of the equipment. Similar effort for the battery chargers and inventers was initiated with the LER data surce.

9. Stress Corrosion Cracking of PWR Steam Generator Tubing

(D. van Rooyen)

The objective of this program is to develop quantitative data to serve as a predictive basis for determining the useful life of Alloy 600 tubing in service.

The present experimental program addresses two specific conditions, i.e., 1) residual stress conditions where deformation occurs but is no longer active, such as when denting is stopped and 2) where plastic deformation of the metal continues.

9.1 Constant Load

No work was done in this area during this quarter.

9.2 CERT

It is essential for the completion of the program that a better distinction between the initiation and propagation stages is achieved in the CERT. These corrections are needed to improve the quantitative determination of SCC induction times and SCC rates. New data confirm an activation energy of 33 Kcal/mole for crack growth, but are still based on less reliable induction time measurements.

No complete sets of data are yet available ;for CERT in AVT, although this work is continuing.

9.3 Dents

Static dents continue in test, and are due for examination in the next quarter.

9.4 U-bends

For .01% carbon, split type tube U-bend tests are practically complete at 315°C, and some cracks have occurred at .02 and .03% carbon. Activation energy still seems to increase with increasing carbon content but less strongly in the .02-.03% carbon material. No cracks have been seen above .05% carbon at 315° or 290°C, and no carbon level has cracked at 290°C.

9.5 Future Work

Future work will be the continuation of long-term tests, and exposure in AVT. However, it is strongly recommended that work on the model, especially in crack propagation rates, be re-started to complete the quantitative relationships. These may be simplified by limited further work, and without this additional effort the work to date may lose much of its potential application. Surry or other "known" steam generator tubes are needed for model verification.

10. Probability Based Load Combinations for Design of Category I Structures

(H. Hwang, M. Reich, J. Pires, P. C. Wang,
M. Shinozuka, B. Ellingwood and S. Kao)

10.1 Load Combination Criteria for Design of Concrete Containments

The proposed load combinations for design of concrete containments reported in the previous quarter has been extended to include the effects of material strength variations. In order to include these variations, the Latin hypercube sampling technique is utilized. Given the distributions for concrete compressive strength, f_c', and steel yield strength, fy, ten pairs of f_c' and fy are selected according to the algorithm of the sampling technique. Then, each pair of f_c' and fy is used to compute limit state probabilities for representative containments and an average of ten pairs is obtained. Following the minimization procedure, for $P_{f,T} = 1.0 \times 10^{-6}$ and $a_{max} = 2a_{sse}$, the load factor for accidental pressure is 1.2 and the load factor for safe shutdown earthquake is 1.7. These values are slightly larger than those in the previous quarterly report.

10.2 Reliability Analysis of Frame Structures with Shear Walls

A reliability analysis method consistent with that for RC containment structures, was developed for plane rigid-frame structures. Structures may have shear walls in all or some of their wall openings and are subjected to horizontal in-plane earthquake ground acceleration with the Kanai-Tajimi power spectrum. As in the case of RC containment structures, the limit probability is measured in terms of the probability that, throughout the structure's lifetime, its response will reach a set of performance criteria selected to represent undesirable states of structural behavior. Such limit states were constructed for beam and column elements and for shear wall elements. For beam and column elements, limit states are associated with bending moments and shear forces, while for shear wall elements, the average shear stress within each element, which is most representative of its overall shear response, was considered for its limit state. Furthermore, a procedure to construct the global limit state in the generalized coordinate space was developed taking into consideration all the element limit states.

10.3 Design and Construction Errors

The safety checking procedures and load combinations developed so far address failures that result from unfavorable deviations in loads and strengths from the values used for design. However, approximately 75 percent of structural failures and 90 percent of total damage costs occur as a consequence of errors in conceptual planning, design, construction, and use. Such errors typically result from a misunderstanding of how a structure behaves under postulated loads, and should be avoidable within the context of state-of-the-art practice. Failures due to gross error have not been considered in the current probabilistic load combination methodologies. Recent

research has indicated that such errors are dealt with more effectively by various statistically based quality assurance and control plans. However, specific procedures that could be used to control design and construction errors are limited.

During this quarter, a literature review was conducted on gross errors for ordinary construction. The occurrence of errors is divided nearly evenly between the design and construction phases. Failures due to use or maintenance are a small percentage of the total. Most serious failures or collapses occur during construction. Relatively few failures occur from inaccurate assessments of loads and resistances. Fundamental misconceptions regarding behavior and detailing errors appear to be the most serious source of design errors.

Probabilistic modeling to include effects of gross error should include the following: (1) Changing the distribution functions of some basic variables to reflect errors; (2) Adding new variables to reflect errors, and (3) Changing the limit states or adding other limit states to reflect the presence of error.

Organization and management strategies appear to be the most effective means of dealing with the problem of gross errors in design and construction. Independent reviews, particularly at key decision points, appear to be essential. However, increasing factors of safety is not an effective strategy for dealing with gross errors.

The above review has been limited to ordinary design and construction practice. During the next quarter, extensions and applications to nuclear plant construction will be considered.

11. Identification of Age Related Failure Modes
(J. H. Taylor)

The Nuclear Regulatory Commission (NRC), Division of Engineering Technology, Electrical Engineering Branch has instituted a long-range, comprehensive research program for diagnosing and evaluating the effects of equipment aging entitled Nuclear Plant Aging Research (NPAR) program. An excellent program plan has been developed and issued by the NRC which details goals and provides an implementation strategy.

In accordance with the NRC - NPAR program plan, the following are the primary goals of the study:

1. To identify and characterize those aging and service wear effects associated with electric motors that are likely to impair plant safety.

2. To identify and recommend methods of inspection, surveillance, and condition monitoring that will be effective in detecting significant aging conditions such that proper maintenance or replacement can be implemented prior to loss of safety function.

3. To identify and recommend acceptable maintenance practices that can be undertaken to mitigate the effects of aging, and to diminish the rate and extent of degradation caused by service wear.

The objectives mentioned above will be obtained by addresing components used in nuclear power plants on an individual basis. The selection of components to be studied are made by using risk analysis, failure histories, special NRC interests, and expert judgement. The components to be adressed are electric motors, battery chargers/inverters, circuit breakers and relays.

The program will proceed through three phases for each component: review of operating data, aging assessment, and recommendation of surveillance and monitoring. As of the end of FY 1984, significant progress on electric motors has been made. The Phase I report relating to operating experience and aging-seismic assessment will be issued in the next quarter. Some highlights of the study findings are detailed below. Similar efforts on battery chargers/inverters was initiated during this period.

11.1 Electric Motors

11.1.1 Operating Data Review (M. Subudhi and E. L. Burns)

This part of the study is to achieve the first goal of the NPAR strategy. This includes an aging assessment of motor failures based on the operating data collected from the previous years of nuclear power plant reactor operation and the potential failure of age-degraded motor components in the event of seismic excitations. The data base utilized for the failure

informations consisted of the LER, IPRDS, NPRDS, NPE, and many other published documents. Since electric motors used in nulcear plants are of various sizes and constructions, the design and manufacturing details are studied for identifying the age-sensitive components such as the insulating systems. Operational stressors and environmental parameters are established, to which motors are subjected in a typical nuclear power plant. Based on the above, an aging assessment was conducted to develop the performance or functional indicators in various motor components in order to maintain the dielectric, rotational, and mechanical integrities of the equipment.

The standards and guides published by organizations such as IEEE, ANSI, NEMA, and ASTM were reviewed. Design and construction standards include those developed by ANSI and NEMA, where the material specifications are made according to ASTM standards. IEEE standards are mainly utilized for testing and maintenance purposes.

11.1.2 Aging-Seismic Correlation (M. Subudhi and J. Curreri)

Two 10HP, 480V, 60Hz induction motors were obtained from an east coast nuclear station for laboratory testing. The motors were tested in a no-load as well as loaded condition, and the dielectric parameters including current, voltage, and insulation resistance were checked before, during, and after seismic evaluations.

In addition, reports on the subject published by EPRI, SQUG and Sandia Labs were studied for evaluating the effects of aging on equipment in terms of seismic capacity.

11.2 Battery Chargers and Inverters (W. Gunther and M. Subudhi)

A preliminary review of the operating failure charactristics of the equipment was initiated with the LER data sources. Other efforts are made to obtain additional data bases for identifying the failure modes, causes and mechanisms associated with battery chargers/inverters. Trips to the manufacturing companies were made to better understand the design, manufacturing and construction of the equipment. It is expected that a comprehensive aging assessment of this component will be achieved during the next quarter.

III. DIVISION OF RISK ANALYSIS AND OPERATIONS

SUMMARY

Analysis of Human Error Data for Nuclear Power Plant Safety Related Events

Brookhaven National Laboratory has been tasked in this program to develop and apply realistic human performance data and models to help evaluate the human's role in nuclear power plant (NPP) safety. To meet this objective, the major current efforts are being placed in the following areas of investigation, namely:

- The use of Performance Shaping Factors (PSFs) and quantified expert judgment in the evaluation of human reliability - the Success Likelihood Index Method (SLIM).

- The development and testing of the Multiple Sequential Failure (MSF) Model.

- The usefulness of Probabilistic Risk Assessment (PRA) related human reliability data in resolving human factors regulatory issues.

As a result of these efforts, BNL has developed several documents which report on the findings in the above areas, namely:

- Human Error Probability Estimation Using Licensee Event Reports (NUREG/CR-3519).

- SLIM-MAUD: An Approach to Assessing Human Error Probabilities Using Structured Expert Judgment (NUREG/CR-3518).

Human Factors Aspects of Safety/Safeguards Interactions

Brookhaven National Laboratory was tasked in this program to describe potential staff interaction problems during safety-related events to prevent or mitigate those problems. In addition, the nature of these interactions was examined to identify any performance deficiencies or conflicts. The project was completed during this quarter and a NUREG/CR document will be published shortly.

Emergency Action Levels

Brookhaven National Laboratory has been tasked in this program to develop guidance for Emergency Action Levels (EALs) that can be integrated into

Emergency Operating Procedure (EOP) guidelines. From this guidance, a method will be developed that can be applied by licensees to verify that the EALs incorporated into their EOPs are usable in the control room under accident conditions. This should result in a reliable and timely basis for declaring emergencies without being too complex or burdensome to those who are trying to safely mitigate an accident. Thus far, a preliminary assessment has been made to integate EALs and EOPs based on the degradation of the fission product barrier criteria.

Protective Action Decisionmaking

In this program, BNL staff are developing a technical basis for NRC guidance on protective action decisionmaking based on an evaluation of the consequences of nuclear power plant accidents. Potential actions under consideration include sheltering, evacuation, and relocation. In the past, specific recommendations have proven to be difficult to justify because of uncertainties in potential accident sequences. Consequently, BNL will establish strategies appropriate to those sequences for which emergency planning is necessary, emphasizing credible failure modes, links to emergency action levels based on in-plant observables and containment status, and other factors such as weather.

12. Analysis of Human Error Data for Nuclear Power Plant Safety Related Events

(W. J. Luckas, Jr.)

Brookhaven National Laboratory (BNL) has been tasked in this program to develop and apply realistic human performance data and models to help quantify and qualify the human's role in nuclear power plant (NPP) safety. To meet this objective, the major current efforts are being placed in the following areas of investigation, namely:

- The use of Performance Shaping Factors (PSFs) and quantified expert judgement in the evaluation of human reliability - the Success Likelihood Index Method (SLIM).
- The development of the Multiple Sequential Failure (MSF) Model.
- The usefulness of Probabilistic Risk Assessment (PRA) related human reliability data in resolving human factors regulatory issues.

12.1 Success Likelihood Index Method (SLIM) Development
(E. A. Rosa)

The use of Performance Shaping Factors (PSFs) and quantified expert judgment using SLIM is important in the evaluation of human reliability. It should be noted that the amount of authentic quantitative human reliability data that exists is small (and is likely to remain small for the foreseeable future). It is therefore likely that subjective judgment and extrapolation will continue to play an important part. Nevertheless, present extrapolation techniques are covert, unsystematic, and rely on the knowledge of a limited number of judges. They do not systematically take into account the ways in which PSFs combine together to affect the probability of success in particular situations. Moreover, certain tasks cannot effectively be quantified using reductionist approaches. For these tasks, involving diagnosis, decision making and other cognitive activities, a holistic technique will probably be necessary.

Quantified subjective judgment has emerged from the previous analysis as being of critical importance for human reliability evaluation. SLIM is a quantified subjective judgment approach which uses PSFs as comprising any or all of the factors which combine to produce the observed likelihood of success. The basic premise of the approach is that when an expert judge (or judges) evaluate(s) the likelihood that a particula task will succeed, he or she is essentially considering the utility of the combination of PSFs in the situation of interest in either enhancing or degrading reliability. SLIM has the means of positioning a task on a subjective scale of likelihood of success, which is subsequently transformed to a probability scale. This positioning is derived by considering the judges' perceptions of the effects of the PSF in determining task reliability. NUREG/CR-2986 documents the initial appraisal of SLIM.

During the fourth quarter of FY 1984, the draft of NUREG/CR-3518 entitled "SLIM-MAUD: An Approach to Assessing Human Error Probabilities Using Structured Judgment," was finalized. The addition of Multi- Attribute Utility Decomposition (MAUD) to the basic SLIM procedure represents the incorporation of an interactive microcomputer based program into the elicitation procedures so that assessors may generate their own PSFs. The assessor generated PSFs are evaluated for theoretical consistency by the program and then converted to failure probabilities. An assessment of progress on the development of the MAUD addition to SLIM is an essential precursor to the actual field testing of the technique.

The principal objective of work in the fourth quarter was a comprehensive test of the MAUD-based implementation of SLIM. The first task accomplished in the test was a classification session whose purpose was the grouping of human actions on the basis of the PSFs influencing the actions. The remaining tasks of the test plan were operationalized and are now undergoing analysis. A NUREG/CR document will be published shortly.

12.2 Multiple Sequential Failure Model Development and Testing
(P. K. Samanta, J. N. O'Brien)

The dependence of human failure on multiple sequential action is important in the evaluation of human reliability. NUREG/CR-2211 has analyzed the nature of this dependence and has distinguished it from other types of multiple failures. Human error causes selective failure of components depending on when the failure started. Two models have been initially developed for quantifying the failure probability in a multiple sequential action. The first is very general in nature and does not require any dependent failure data. The failure probability obtained from this model is a conservative one with associated uncertainty. The uncertainty is calculated considering many possible sources such as data, coupling, and modeling. In the second model, details of the process in multiple sequential failures (MSF) are taken into account. The model increments the conditional failure probabilities by a certain amount from their lower bounds (independent failure probability). This approach provides important insights into the influence of dependence of failures on system reliability. The model can be used effectively to choose an optimum system considering the individual failure probability, dependence factor, and the amount of redundancy in a system.

During the fourth quarter of FY 1984, the small-scale psychological experiment being used to test the model was conducted. Data from it are currently being analyzed.

12.3 PRA Human Reliability Data

(J. N. O'Brien, C. M. Spettell)

An assessment of the usefulness of PRA human reliability data in resolving human factors regulatory issues facing NRC has been undertaken. In order to accomplish this, two efforts are being undertaken. First, a list of all human factors issues is being assembled and the technical research questions which must be addressed to resolve them developed. Second, all PRAs are being reviewed to illicit exactly what type of data is presented. After both of these efforts are completed, PRA data will be compared to the human factors technical questions to determine their usefulness.

During the fourth quarter of FY 1984, a taxonomy for classifying human reliability data and a method for locating these data were developed and data are being entered into a data base. A discussion paper on human factors regulatory issues was completed. This paper has been used to formalize a comprehensive set of technical research questions relevant to regulation of human factors in nuclear power plants. A systematic approach for matching human reliability data in PRAs with issues is presently being developed.

References

COMER, M. K., KOZINSKY, E. J., SECKEL, J. S., AND MILLER, D. P. (1983). "Human Reliability Data Bank for Nuclear Power Plant Operations," NUREG/CR-2744.

EMBREY, D. E. (1983). "The Use of Performance Shaping Factors and Quantified Expert Judgement in the Evaluation of Human Reliability: An Initial Appraisal," NUREG/CR-2986.

EMBREY, D. E., HUMPHREYS, P., AND ROSA, E. A. (1984). "SLIM-MAUD: An Approach to Assessing Human Error Probabilities Using Structured Judgment," NUREG/CR-3518.

HALL, R. E., FRAGOLA, J., AND LUCKAS, W. J., JR., Tech. Eds. (1981). Conference Record for NRC/BNL/IEEE Standards Workshop on Human Factors and Nuclear Safety, NUREG/CP-0035.

HALL, R. E., FRAGOLA, J., AND WREATHALL, J. (1982). "Post Event Human Decision Errors; Operator Action Tree/Time Reliability Correlation," NUREG/CR-3010.

LUCKAS, W. J., JR. AND HALL, R. E. (1981). "Initial Quantification of Human Errors Associated with Reactor Safety System Components in Licensed Nuclear Power Plants," NUREG/CR-1880.

LUCKAS, W. J., JR., LETTIERI, V., AND HALL, R. E. (1982). "Initial Quantification of Human Error Associated with Specific Instrumentation and Control system Components in Licensed Nuclear Power Plants," NUREG/CR-[illegible]16.

SAMANTA, P. K. AND MITRA, S. P. (1981). "Modeling of Multiple Sequential Failures During Testing, Maintenance, and Calibration," NUREG/CR-2211.

SAMANTA, P. K., HALL, R. E., AND SWOBODA, A. L. (1981). "Sensitivity of Risk Parameters to Human Errors in Reactor Safety Study for a PWR," NUREG/CR-1879.

SCHMALL, T. M., Ed. (1979). Conference Record for NRC/BNL/IEEE Standards Sponsored December 1979 Workshop on Human Factors and Nuclear Safety.

SPEAKER, D. M., THOMPSON, S. R., AND LUCKAS, W. J., JR. (1982). "Identification and Analysis of Human Errors Underlying Pump and Valve Related Events Reported by Nuclear Power Plant Licensees," NUREG/CR-2417.

SPEAKER, D. M., VOSKA, K. J., AND LUCKAS, W. J., JR. (1983). "Identification and Analysis of Human Error Underlying Electrical/Electronic Component Related Events Reported by Nuclear Power Plant Licensees," NUREG/CR-2987.

VOSKA, K. J. AND O'BRIEN, J. N. (1984). "Human Error Probability Estimation Using Licensing Event Reports," NUREG/CR-3519.

13. Human Factors Aspects of Safety/Safeguards Interactions

(J. N. O'Brien)

Brookhaven National Laboratory has been tasked in this program to describe potential safety/safeguards interaction problems during safety-related events and recommended actions to prevent or mitigate those problems. In addition, the nature of these interactions is to be examined to identify any performance deficiencies or conflicts.

The first step of this effort is to examine and address human factors issues which arise from consideration of impacts on the ability of personnel at nuclear power plants to effectively perform their duties as documented in NUREG-0992. Of particular interest are situations at plants which may involve conflicts in roles and missions between security measures and the other organizational units which operate the plant. This program sets out to examine the human factors aspects of these potential problems and, further, to recommend measures to prevent or mitigate any potential adverse impacts on safety.

In order to effectively address potential problems involving conflicts between security requirements and operational practices, potentially troublesome situations and human factors issues relevant to them must be identified. This involves the consideration of a wide range of situations and human factors issues. Once situations have been identified and relevant human factors issues defined, a systematic examination will reveal how potential conflicts can be prevented or mitigated.

After potentially troublesome situations and relevant human factors issues are identified, a matrix will be constructed with situations on one axis and human factors on the other. The cells in the matrix represent the basis of the analysis from which proposals will be developed to prevent or mitigate adverse effects.

The scope of the resultant report will include input from a number of individuals in the fields of operational safety, security, and human factors. However, no site visits will be conducted. Instead, the data contained in the NUREG-0992 is considered to be representative of that which would come from site visits since that is how the committee's data were generated. NUREG-0992 has been extensively analyzed and conclusions are drawn on the basis of that information and subject to review by a panel of experts in the relevant fields. No formal attempt has been made to corroborate or verify the data presented in NUREG-0992.

During the fourth quarter of FY 1984, the report was completed and submitted to NRC for review.

14. Emergency Action Levels

(W. J. Luckas, Jr.)

Brookhaven National Laboratory (BNL) has been tasked in this program to develop guidance for Emergency Action Levels (EALs) that can be integrated into Emergency Operating Procedure (EOP) guidelines. From this guidance, a method will be developed that can be applied by licensees to verify that the EALs incorporated into their EOPs are usable in the control room under accident conditions. This should result in a reliable and timely basis for declaring emergencies without being too complex or burdensome to those who are trying to safely mitigate the accident.

EALs are a plant specific, predetermined observable and/or measurable set of indications (such as a particular set of control room instrument readings having reached specific off-normal values) which are used to declare one of the Emergency Classes (Alert, Site Area Emergency, or General Emergency). A more descriptive term for EALs would be emergency declaration indicators.

After appropriate examination, an attempt is being made to utilize currently available EALs developed by utilities, such as Kansas Gas and Electric Company on their Wolf Creek Generating Station, that use the degradation of fission-product barrier approach as a starting point. The EAL guidance will be verified by testing it against the example initiating conditions listed in Appendix 1 of NUREG-0654.

During the fourth quarter of FY 1984, a preliminary assessment was made of the adaptability of the BWR Owners' Group Emergency Procedure Guidelines to integrate EALs and EOPs based on the appropriate criteria.

15. Protective Action Decisionmaking

(W. T. Pratt, A. G. Tingle, H. Ludewig,
W. R. Casey*, and A. P. Hull*)

15.1 Background

NRC regulations require that, in the case of a major nuclear power plant accident, licensees recommend protective actions to reduce radiation dose to the public. When certain emergency action levels are exceeded, the licensee recommends protective actions to State and local officials. The nature of the protective actions recommended is determined by which emergency action levels are exceeded.

In practice drills, decisions on protective action recommendations have proven to be difficult. NUREG-0654 states that if containment failure is imminent, sheltering is recommended for areas that cannot be evacuated before the plume arrives, but evacuation is recommended for other areas. The assumption in NUREG-0654 is that there would be a greater dose savings if the population were sheltered during plume passage rather than evacuated, but this assumption has not been proven. Furthermore, the recommended protective actions must be based on estimated containment failure times, which are difficult to determine.

Alternatively, other NRC publications suggest that the appropriate response would be early evacuation of everyone within a distance of about 2 or 3 miles for all events that could lead to a major release even if containment failure is imminent or a release is underway. Those at greater distances should take shelter. Further, if a release occurs, the appropriate action would be for monitoring teams to find "hot spots" (radiation dose rate exceeding about 1 R/hr) and for people to evacuate these "hot spots."

15.2 Project Objectives

The objectives of the activities to be performed in this project are to:

(1) characterize the family of potential accident sequence for which emergency planning is necessary,

(2) establish strategies appropriate to these sequences, emphasizing credible failure modes,

(3) identify those factors which would influence the implementation of these strategies,

(4) determine how these factors should be incorporated into the decisionmaking process, and

---

*BNL Safety and Environmental Protection Division

(5) develop a guidance report on the protective actions to be recommended for combinations of these factors.

15.3 Technical Approach

The technical approach is based on an evaluation of the consequences of nuclear power plant accidents as they relate to protective action decision-making. The evaluation includes a careful review of previous work (e.g. NUREG/CR-2339, NUREG-0654, NUREG/CR-2025, NUREG-0396, and reports and memoranda by the NRC staff) and its applicability to protective action decision-making. The approach is also based on a consideration of a wide range of potential accident sequences and on up-to-date assessments of containment performance. Thus the technical basis will reflect the new fission product source term information under development by the NRC/RES Accident Source Term Program Office (ASTPO). BNL staff are closely following the activities of ASTPO and, in addition, are participating in the SARP Containment Loads Working Group and in the Containment Performance Working Group. The work of these groups will be integrated into our development of protective action strategies.

The evaluation will be based in large part on results obtained from the CRAC2 computer code (Consequence of Reactor Accident Code, version 2). The output is being analyzed for a variety of release characterizations, weather sequences, and protective action strategies.

In accordance with the above, we have selected the following six facilities to represent the range of U.S. reactor and containment designs:

Zion: PWR with a large dry containment
Surry: PWR with a subatmospheric containment
Sequoyah: PWR with an ice condenser containment
Brown's Ferry: BWR with a Mark I containment
Limerick: BWR with a Mark II containment
Grand Gulf: BWR with a Mark III containment

15.4 Project Status

15.4.1 Summary of Activities

In August BNL staff gave a presentation to the NRC staff demonstrating recommended protective actions for two rather rapid accident sequences. The sequences were a bypass of containment, which produces a severe fission product release near ground level, and a containment failure induced by a hydrogen burn, which was assumed to produce an elevated release due to the heat energy contained in the plume. In both accidents only a half hour warning time is available for public response. Results from the Emergency Action Levels Project (FIN A-3271) have shown that the operator can distinguish between the sequence implying that optimum protective strategies could be applied.

The health effects of immediate concern for emergency protective actions are deaths and illnesses that occur within one year due to exposure. The CRAC 2 results for these accidents were presented in terms of individual bone marrow (T-marrow) dose versus distance from each accident. We did not consider longer term effects such as cancers and genetic disorders. This is the format used in BNL's draft report outlined below. The NRC staff suggested that the data be condensed and also recommended a writing style for the report.

Based upon the projected releases of these two severe accidents, two general strategies for protective action were developed. These strategies are primarily based on the premises that: (1) doses which are large enough to produce early injury in people (50 rem) must be avoided if at all possible and that (2) doses in excess of the PAG but less than the threshold for early injury (50 rem) should be avoided where possible and reasonable.

BNL subsequently performed additional CRAC 2 calculations to highlight the impact of alternative strategies. A draft report was prepared with the following components:

1) a general discussion of the consequences of radiation releases as a function of the cloud, ground and inhalation exposure pathways,

2) a discussion of boiling water and pressurized water reactor and containment design and the accident release characterizations pertinent to each,

3) a detailed summary of protective action strategies for accidents with severe source terms and less severe source terms.

15.4.2 Preliminary Conclusions

The results of the analyses to date have supported certain preliminary conclusions reached last quarter.

(1) In-plant conditions: BNL staff have continued evaluating specific accident sequences to determine if readily identifiable plant conditions exist which permit selection of appropriate protection action strategies. Results indicate that such links do exist and that protective action strategies can be based on in-plant observables for those accident sequences examined to this point.

(2) Warning time: BNL staff analysis of severe accidents indicates that warning times of several hours or more can be expected for the more probable accident sequences, e.g. small break LOCA or transients. Short warning times of 1 hour or less are associated only with less probable accident sequences which should be readily identified.

(3) Weather: The importance of weather in defining the consequences of a radioactive release has been convincingly reconfirmed in our analyses of different accident scenarios. The type of weather occurring at the time of a release can dramatically affect the type of protective action recommended and the size of the area for which protective action is warranted. Since weather is an observable condition, it is apparent that the recommended protective action strategies should be highly weather dependent.

(4) Plume rise: In the accident scenarios that BNL staff have evaluated, the energy of release is an important parameter affecting downwind doses. It appears that this information will also be important in selecting the appropriate strategy.

The analysis has also shown that the rate of radiation exposure from ground deposition is much slower than that from the plume. This means that a few hours are available for identifying hot spots and relocating people as opposed to the rapid movements that may be necessary for reduction of plume exposure in fast accidents.

NRC FORM 335 (11-81)

U.S. NUCLEAR REGULATORY COMMISSION

BIBLIOGRAPHIC DATA SHEET

1. REPORT NUMBER (Assigned by DDC)
NUREG/CR-2331
BNL-NUREG-51454, Vol. 4, No. 3

4. TITLE AND SUBTITLE (Add Volume No., if appropriate)
Safety Research Programs Sponsored by Office of Nuclear Regulatory Research, Quarterly Progress Report July 1 - September 30, 1984.

2. (Leave blank)

3. RECIPIENT'S ACCESSION NO.

7. AUTHOR(S)
Compiled by Allen J. Weiss

5. DATE REPORT COMPLETED
MONTH: December | YEAR: 1984

9. PERFORMING ORGANIZATION NAME AND MAILING ADDRESS (Include Zip Code)
Brookhaven National Laboratory
Department of Nuclear Energy
Upton, New York 11973

DATE REPORT ISSUED
MONTH: February | YEAR: 1985

6. (Leave blank)

8. (Leave blank)

12. SPONSORING ORGANIZATION NAME AND MAILING ADDRESS (Include Zip Code)
U. S. Nuclear Regulatory Commission
Office of Nuclear Regulatory Research
Washington, D. C. 20555

10. PROJECT/TASK/WORK UNIT NO.

11. FIN NO.
A-3014,14,16,24,41, A-3208,15, 19,26,27,57,61,66,68,70,71,75

13. TYPE OF REPORT
Quarterly

PERIOD COVERED (Inclusive dates)
July 1 - September 30

15. SUPPLEMENTARY NOTES

14. (Leave blank)

16. ABSTRACT (200 words or less)

This progress report will describe current activities and technical progress in the programs at Brookhaven National Laboratory sponsored by the Division of Accident Evaluation, Division of Engineering Technology, and Division of Risk Analysis & Operations of the U.S. Nuclear Regulatory Commission, Office of Nuclear Regulatory Research.

The projects reported are the following: High Temperature Reactor Research, SSC Development, Validation and Application, Generic Balance of Plant Modeling, Thermal-Hydraulic Reactor Safety Experiments, Development of Plant Analyzer, Code Assessment and Application (Transient and LOCA Analyses), Thermal Reactor Code Development (RAMONA-3B), Calculational Quality Assurance in Support of PTS; Stress Corrosion Cracking of PWR Steam Generator Tubing, Probability Based Load Combinations for Design of Category I Structures, Identification of Age-Related Failure Modes; Analysis of Human Error Data for Nuclear Power Plant Safety Related Events, Human Factors Aspects of Safety/Safeguards Interactions, Emergency Action Levels, and Protective Action Decision Making.

17. KEY WORDS AND DOCUMENT ANALYSIS

High Temperature Graphite Reactor
Super System Code
MINET Code
Thermal-Hydraulic Reactor Safety
Emergency Action

17a. DESCRIPTORS

Plant Analyzer
RAMONA-3B
Pressurized Thermal Shock
Stress Corrosion Cracking
Protective Action
Load Combinations
Nuclear Plant Aging
Human Error
Human Factors

17b. IDENTIFIERS/OPEN-ENDED TERMS

18. AVAILABILITY STATEMENT

19. SECURITY CLASS (This report)

21. NO. OF PAGES

20. SECURITY CLASS (This page)

22. PRICE
$

NRC FORM 335 (11-81)